Titre: Title:	Modeling of electrical arc on polluted ice surfaces
Auteur: Author:	X. Chen
Date:	2000
Type:	Mémoire ou thèse / Dissertation or Thesis
Référence: Citation:	Chen, X. (2000). Modeling of electrical arc on polluted ice surfaces [Thèse de doctorat, École Polytechnique de Montréal]. PolyPublie. https://publications.polymtl.ca/8604/

UNIVERSITÉ DE MONTRÉAL

MODELING OF ELECTRICAL ARC ON POLLUTED ICE SURFACES

XING CHEN

DÉPARTEMENT DE GÉNIE ÉLECTRIQUE

ET DE GÉNIE INFORMATIQUE

ÉCOLE POLYTECHNIQUE DE MONTRÉAL

THÈSE PRÉSENTÉE EN VUE DE L'OBTENTION

DU DIPLÔME DE PHILOSOPHIAE DOCTOR (Ph.D.)

(GÉNIE ÉLECTRIQUE)

FÉVRIER 2000

UNIVERSITÉ DE MONTRÉAL

ÉCOLE POLYTECHNIQUE DE MONTRÉAL

Cette thèse est intitulée:

MODELING OF ELECTRICAL ARC ON POLLUTED ICE SURFACES

présentée par Xing CHEN

en vue de l'obtention du diplôme: Philosophiea Doctor

a été dûment acceptée par le jury d'examen constitué de:

M. DO Xuan-Dai, Ph.D., président

M. OLIVIER Guy, Ph.D., membre et directeur de recherche

M. FARZANEH Masoud, Ph.D., membre et codirecteur de recherche

M. WERTHEIMER Michael R., Ph.D., membre

M. CHILSOM William Alexander, Ph.D., membre

ACKNOWLEDGEMENTS

The research work reported in the present thesis is carried out in the frame work of the Groupe de Recherche en Ingénierie de l'Environnement Atmosphérique (GRIEA) and the NSERC / Hydro-Quebec / UQAC Chair on Atmospheric Icing of Power Network Equipment of l'Université du Québec à Chicoutimi (QUAC) in collaboration with École Polytechnique de Montréal. I am grateful and wish to thank my co-directors, Professor Masoud Farzaneh of UQAC and Professor Guy Olivier of École Polytechnique de Montréal for their guidance and assistance throughout the course of the research. I am particularly indebted to Professor Masoud Farzaneh for his valuable support, invaluable suggestions, long discussions and understanding to the student life.

I would like to express my gratitude to Dr. Jianhui Zhang for the helpful discussions and help, to Mr. Claude D'Amours, and to Mr. Sylvain Desgagné for their technical help in various phases of this study. I wish also express my appreciation to all the other members of the GRIEA for their contributions, in one way or another, to this work.

I am grateful to the NSERC / Hydro-Quebec / UQAC Chair on Atmospheric Icing of Power Network Equipment for their financial support all during my studing.

Finally, I would like to thank my wife, Weixia, for her encouragement and support during this work.

RÉSUMÉ

L'accumulation de glace sur les lignes de transmission diminue la performance électrique pendant la période de fonte. Le contournement électrique des isolateurs recouverts de glace est une des causes importantes de panne générale d'électricité dans les régions froides.

Pour la premières fois, des études systématiques sur le développement de l'arc électrique à la surface de la glace polluée sont actuellement en cours au Laboratoire haute tension et givrage atmosphérique et à la Chaire industrielle sur le givrage atmosphérique des équipements des réseaux électriques CRSNG / HYDRO-QUÉBEC / UQAC de l'Université du Québec à Chicoutimi (UQAC). La présente thèse, étant une partie de ces études systématiques, consiste à modéliser l'arc électrique sur la surface de la glace humide et à analyser les conditions de contournement sur la surface des isolateurs recouverts de glace humide.

La majeure partie des essais expérimentaux a été effectuée sur un cylindre en verre recouvert de glace formée en régime humide, la glace la plus dangereuse en ce qui a trait à la possibilité de contournement. La glace

humide était formée dans la chambre froide au Laboratoire haute tension et givrage atmosphérique de l'UQAC.

Utilisant une caméra à grande–vitesse, un dispositif d'enregistrement des données provenant des appareils à haute tension, le développement de la décharge sur la surface de la glace était enregistré et analysé sous tension continue et sous tension alternative. Les vitesses d'arc sont mesurées dans les trois périodes de la propagation de l'arc, soit la période de démarrage, la période de développement et la période de contournement. La relation entre les rayons d'arcs et les courants d'arcs a été établie à partir des résultats expérimentaux.

La caractéristique tension–courant de l'arc a été obtenue par les essais sur le cylindre de glace. Les constantes A et n de la caractéristique de l'arc sont déterminées sous tension continue et sous tension alternative. La chute de la tension totale aux électrodes est obtenue à partir de la relation entre la tension d'arc et la longueur d'arc.

Pour le contournement sous tension alternative sur une surface de glace, comme le contournement sur une surface polluée, on a trouvé qu'il est nécessaire que la tension soit suffisante pour le réallumage de l'arc. Cette condition de développement d'arc a été déterminée expérimentalement.

La conductivité superficielle pendant le contournement a été mesurée. Des valeurs équivalentes de conductivité superficielle ont été déterminées sous tension continue et sous tension alternative.

Des facteurs influençant le contournement sur la surface de glace sont analysés. Des essais effectués ont confirmé l'influence de la conductivité de l'eau, du type de tension, de la longueur des isolateurs et de l'uniformité de la glace. Des mesures de température sont prises, pendant la fonte, sur les surfaces intérieure et extérieure ainsi qu'au centre de la masse de glace. Le courant du bloc de la glace est comparé avec les courants des surfaces intérieure et extérieure. Il est prouvé que le courant de fuite passe principalement sur les surfaces de la glace.

Basé sur les essais et selon la conception d'Obenaus relative au contournement électrique des surfaces polluées et humides en présence de zones sèches, un modèle mathématique permettant d'analyser le contournement sur une surface de glace humide a été établi. Utilisant ce modèle, la tension de contournement, le courant critique et la longueur critique d'arc sont calculés sur la surface de glace humide sous tension continue et sous tension alternative. Ce modèle a été appliqué sur les chaînes courtes et longues d'isolateurs recouverts de glace formée en régime humide. La

comparaison des résultats obtenus à l'aide du modèle avec ceux obtenus sur les courtes chaînes d'isolateurs réels se fait de façon très satisfaisante.

ABSTRACT

Ice accretion on power transmission lines can decrease the electrical insulation along the insulators. Insulator flashover as a result of ice accretion is one of the causes of power outages during ice melt.

For the first time, a research program on the modeling of electrical arc on ice surfaces has been undertaken in the High Voltage and Atmospheric Icing Laboratory and the NSERC / Hydro-Quebec / UQAC Chair on Atmospheric Icing of Power Network Equipment of the University of Quebec in Chicoutimi (UQAC). As a part of this program, the present thesis aims at the modeling and characterisation of the arc on wet-grown ice surfaces and the analysis of the flashover conditions on ice–covered insulating surfaces.

Some fundamental concepts of surface discharge, such as corona discharge, electrical arc, arc development, and mathematical model of arc on polluted surfaces, are first introduced. Then the flashover problem of ice-covered insulators and the related research activities are summarised in the literature review.

A cylindrical glass rod covered with wet-grown ice, the most dangerous type of ice associated to insulator flashover, was used in most of the experiments of the present thesis. Wet-grown ice samples were formed in the cold room of the High Voltage and Atmospheric Icing Laboratory of UQAC. By means of a high speed camera, a data acquisition system and high voltage test facilities, a series of dc and ac flashover arcs on ice surfaces were recorded and analyzed. Arc speeds in various periods of arc development, such as the arc-starting period, the arc-developing period, and the finial flashover period, were measured. The relationships between arc current and arc foot radius were obtained using regression on the test results.

The arc voltage–current characteristics under dc and ac voltages for cylindrical ice samples were determined. The arc electrode voltage drops were also obtained from the regression on the observations. Arc reignition conditions must be satisfied under ac voltage in order to complete the flashover in the same manner as polluted surfaces. The relative constants for these reignition conditions were obtained using the regression method on the test results, using an approach that was adapted from polluted-surface flashover.

The ice surface conductivity during flashover was also measured and an equivalent surface conductivity, γ_e, for both ac and dc voltage applications was defined.

Several factors influencing the flashover on ice surfaces, such as freezing water conductivity, voltage type, arcing distance, and ice surface uniformity were analyzed. The temperatures of ice surfaces and ice body were measured during the melting period. The influence of bulk ice current on the total ice current measured was estimated. It was observed that the leakage current passed principally through the ice surfaces in the cylindrical geometry.

On the basis of the above studies and following the concept of Obenaus for pollution flashover, mathematical models were established for flashovers on ice surfaces under dc and ac voltages. Using these mathematical models, the flashover voltages, critical currents, and critical arc lengths were calculated. The mathematical model was then applied to both short and long ice-covered facility insulator strings for different icing conditions. The calculated results were in good agreement with the experimental results on short insulator strings.

MODÉLISATION DE L'ARC DE CONTOURNEMENT SUR LA SURFACE DE GLACE POLLUÉE

(CONDENSE EN FRANÇAIS)

INTRODUCTION

La présence de glace à la surface des isolateurs est parfois à l'origine de perturbations graves sur les réseaux électriques. En effet, l'accumulation de glace sur les lignes électriques aériennes et les postes électriques extérieurs entraîne la dégradation de l'isolation, dans certaines circonstances. Cet affaiblissement de la tenue électrique des isolateurs peut être tel que des arcs électriques prennent naissance et se développent jusqu'à provoquer un contournement total des isolateurs, dans les cas extrêmes. La littérature mentionne certains de ces incidents.

Une revue des travaux de recherche antérieurs montre que certains auteurs ont étudié le contournement des isolateurs couverts de glace. Les résultats sont spécifiques à chaque type de glace ou de neige à une certaine température et à chaque type d'isolateur seulement, car on a toujours utilisé des isolateurs réels. Ces résultats, bien que proches de la réalité, ne nous

permettent pas d'analyser le développement de la décharge sur la surface de la glace.

OBJECTIF

Une étude systématique sur la modélisation de la décharge sur une surface de glace est actuellement en cours au Laboratoire haute tension et givrage atmosphérique et à la Chaire industrielle sur le givrage atmosphérique des équipements des réseaux électriques CRSNG / HYDRO-QUÉBEC / UQAC de l'Université du Québec à Chicoutimi (UQAC). Constituant une partie intégrante de ces travaux, la présente thèse a pour but de présenter les essais de la propagation de la décharge à la surface de la glace humide et la modélisation de l'arc de contournement électrique sur la surface de glace humide, la glace la plus dangereuse en ce qui a trait à la possibilité du contournement, en utilisant un modèle cylindrique de glace.

MÉTHODOLOGIE

La méthodologie utilisée pour atteindre les objectifs du projet comprend les points suivants :

1. Le revue des phénomènes de décharge (décharge couronne, arc électrique, modélisation d'arc électrique sur la surface polluée). L'étude bibliographique pour estimer l'état actuel des recherches.

2. L'établissement d'un modèle physique permettant la réalisation des essais au laboratoire. Des cylindres de glace humide sont utilisés dans la majeure partie de la présente thèse.

3. Utilisant une caméra à grande vitesse, un dispositif d'enregistrement des données et des appareils à haute tension, le développement de la décharge sur la surface de glace était enregistré et analysé sous tension continue et sous tension alternative. Les vitesses d'arc sont mesurées dans les trois périodes de la propagation de l'arc, soit la période de démarrage, la période de développement et la période de contournement. La relation entre les rayons de l'arcs et les courants d'arcs a été établie à partir des résultats expérimentaux.

4. L'étude des facteurs affectant le contournement, tels que la conductivité de l'eau, le type de tension, la longueur des isolateurs, la température ambiante et l'uniformité de la glace.

5. La détermination expérimentale de la conductivité superficielle de la glace pendant le contournement sous tension continue et sous tension alternative.

6. La détermination de tension–courant caractéristique de l'arc de contournement sur la surface de glace humide. Les constantes A et n de caractéristique de l'arc sont déterminées sous tensions continue et alternative. La chute de tension totale aux électrodes est obtenue à partir de la relation entre la tension d'arc et la longueur d'arc.

7. Pour le contournement en tension alternative sur la surface de la glace, la détermination des conditions de réallumage pour le développement de l'arc.

8. La proposition d'un modèle mathématique permettant d'analyser le contournement sur une surface de la glace humide basé sur les essais et selon la conception d'Obenaus.

9. L'application du modèle mathématique sur des isolateurs industriels.

CONCLUSIONS

Basé sur les essais expérimentaux sur les cylindres de glace et le modèle mathématique établi dans la présente thèse, le contournement sur une surface de glace humide sous tension continue et sous tension alternative a été analysé.

1. Les principaux processus conduisant au contournement sur une surface de glace se produisent en trois périodes, soit le démarrage d'arc, le développement d'arc et le contournement final. Des différences sont observées dans les trois périodes, soit le phénomène de développement, les courants d'arc et la vitesse d'arc.

2. Les relations entre le courant de l'arc (I en A) et le rayon de l'arc (r_0 en cm) sur une surface de glace humide peuvent être approchées par les formules suivantes :

$$r_0 = \sqrt{\frac{I}{1.67\pi}} \quad (arc\ negatif)$$

$$r_0 = \sqrt{\frac{I}{1.75\pi}} \quad (arc\ positif)$$

$$r_0 = \sqrt{\frac{I_m}{2.04\pi}} \quad (arc\ alternatif)$$

3. Les caractéristiques tension–courant de l'arc de contournement sur une surface de glace humide sont déterminées. Les chutes de la tension d'arc (E_{arc} en V/cm) et les courants d'arc (I ou I_m en A) ont pour expressions:

$$E_{arc}=213\cdot I^{-0,53} \quad \text{(arc positif) ;}$$

$$E_{arc}=169\cdot I^{-0,58} \quad \text{(arc négatif) ;}$$

$$E_{arc}=152\cdot I_m^{-0,53} \quad \text{(arc alternatif)}$$

4. Les chutes de tension cumulées aux électrodes sont déterminées à 735 V, 608 V et 953 V pour l'arc positif, l'arc négatif et l'arc alternatif respectivement.

5. Pour qu'il y ait contournement sur la surface de glace sous tension alternative, il est nécessaire que la tension soit suffisante pour réamorcer l'arc. La tension de réallumage (V_m en V) en fonction de courant d'arc (I_m en A) avec une longueur d'arc x (en cm) s'écrit ainsi :

$$V_m \geq \frac{1258x}{I_m^{0.53}}$$

La condition de réallumage peut aussi s'écrire selon la tension d'arc (V_p en V) :

$$V_p \geq \frac{449x}{I_m^{0.51}}$$

6. Les conductivités superficielles de la glace humide (γ_e) pendant le contournement sous tension continue et sous tension alternative sont déterminées. Les relations de γ_e (en μS) avec la conductivité de l'eau σ (en μS/cm) sont obtenues :

γ_e=0.061·σ+5.6 (tension positive);

γ_e=0.063·σ+5.8 (tension négative);

γ_e=0.067·σ+5.6 (tension alternative).

Les différences de γ_e sous tension positive, tension négative et tension alternative ne sont pas significatives.

7. Les résultats d'essais sur les cylindres de glace_montrent que le contournement de glace humide dépend de certains paramètres, soit la conductivité de l'eau, la nature de la tension, l'uniformité de la glace, la longueur des isolateurs, etc.

La tension de contournement (V_{ws}) diminue avec la conductivité d'eau croissante.

La tension de contournement varie également en fonction de la polarité de la tension d'essai. V_{ws} est de 6% à 9% plus faible en polarité négative qu'en polarité positive. V_{ws} est de 16% à 21% plus faible en polarité négative qu'en tension alternative. V_{ws} est de 13% à 17% plus faible en polarité positive qu'en tension alternative.

V_{ws} est influencé par l'uniformité de la glace accumulée sur le cylindre en verre. Plus la glace est uniforme, moins grande est V_{ws}.

Les essais sur les cylindres de glace humide (distance d'arc de 0,3 m à 0,92 m) confirment la linéarité de la V_{ws} en fonction de la distance d'arc.

Pendant la période de fonte, les températures de la glace et de la surface augmentent de –12°C à 0°C suivant la température ambiante.

Le courant de fuite circule à la surface de la glace. On peut négliger le courant dans le volume de la glace.

8. Le modèle mathématique permettant d'analyser le contournement sur la surface de glace humide est établi selon les études sur les cylindres de glace et la conception d'Obenaus. Utilisant ce modèle, la tension de tenue maximale, le courant critique et la longueur d'arc critique sont

calculées pour les cylindres de glace et les isolateurs industriels recouverts de glace humide.

Les calculs sur les cylindres de glace et les courtes chaînes d'isolateurs basées sur le modèle mathématique montrent que l'augmentation de la conductivité de l'eau conduit à la diminution de la tension de contournement. La longueur d'arc critique diminue de façon linéaire avec la conductivité de l'eau. Le courant critique augmente de façon linéaire avec la conductivité de l'eau.

La tension de tenue maximale, le courant critique et la longueur d'arc critique calculées varient également en fonction de la polarité de la tension. V_c est de 11% à 18% plus forte en tension alternative qu'en polarité positive. V_c est de 19% à 24% plus forte en tension alternative qu'en polarité négative.

Le courant critique calculé est environ 3 fois plus fort sous tension alternative qu'en tension continue. Le courant critique calculé est un peu plus faible en polarité négative qu'en polarité positive.

La longueur d'arc critique calculée est plus grande en tension alternative qu'en tension continue. La longueur d'arc critique calculée est un peut plus petite en polarité négative qu'en polarité positive.

Pour les distances d'arc jusqu'à 1 m, les calculs sur la glace humide confirment les linéarités de la V_c et du courant critique en fonction de la distance d'arc. Le ratio de longueur d'arc critique sur la distance d'arc augmente suivant la croissance de la distance d'arc. La comparaison des résultats obtenus sur le modèle avec ceux obtenus sur les isolateurs réels se fait de façon très satisfaisante.

Pour les longues chaînes d'isolateurs recouverts de glace, il faudrait entreprendre des recherches expérimentales pour confirmer les résultats de la présente étude.

TABLE OF CONTENTS

LIST OF TABLES

LIST OF FIGURES

LIST OF SYMBOLS

A	Arc constant
b	Exponent of ac arc reignition condition defined in Equation 7.5
b′	Exponent of ac arc reignition condition defined in Equation 7.6
DAS	Data acquisition system
dc+	Positive direct voltage
dc-	Negative direct voltage
D_m	Mean diameter of the ice cylinder.
E_{arc}	Voltage gradient of arc
E_c	Critical field strength for corona inception
ESDD	Equivalent salt deposit density
i	Instantaneous leakage current
I	Leakage current
I_c	Critical current
I_m	Peak value of ac current
k	AC arc reignition constant defined in Equation 7.5
K	Thermal diffusivity
K_1	Constant of arc foot radius defined in Equation 8.4
k′	AC arc reignition constant defined in Equation 7.6
L	Arcing distance of ice sample

n	Exponent of arc characteristic
N_{02}	Power loss per unit length after current zero
P	Power taken from the supply
r	Conductor radius
$R(x)$ or R_p	Surface resistance of the part of the ice which is not bridged by arc.
r_o	Arc foot radius
R_m	Residual arc resistance at current peak
r_p	Uniform pollution resistance per unit leakage path
U_e	Voltage drop on electrodes
UQAC	University of Quebec in Chicoutimi, Université du Québec à Chicoutimi
V_1	Applied voltage
V_2	Voltages on the measuring electrode
V_{arc}	Voltage across arc
V_c	Critical flashover voltage
V_{cx}	Minimum dc voltage to sustain the arc bridging a portion x/L of the leakage path L
V_{ice}	Voltage across the residual ice (the part of ice which was not bridged by the partial arc)
V_m	Peak values of ac voltage
V_{min}	Minimum value of applied voltage for maintaining of dc arc of x cm

V_p	Critical voltage value across the arc of x cm
V_{ws}	Withstand voltage
w	Width of ice surface
x	Length of arc
x_c	Critical arc length
σ	Freezing water conductivity
δ	Relative air density
Φ	Function to be determined experimentally
γ_e	Equivalent surface conductivity of the ice sample during flashover

CHAPTER I

INTRODUCTION

1.1 Description of the problem

In cold regions of the world, ice accumulation due to freezing rain, drizzle, in-cloud icing, icing fog, wet snow or frost causes problems to the normal operation of overhead transmission lines and their substations. Frequently, the presence of ice is accompanied by wind. These atmospheric events could sometimes lead to galloping, large-amplitude, mainly vertical motion of conductors and the consequent flashover between them. Some authors (Jones, 1993; Kiessling and Ruhnau, 1993) confirm that the excessive accumulation of ice also leads to mechanical damage to the conductors, hardware, and towers. The most serious such accident occurred in January 1998 in the areas of Montreal, eastern Ontario, and the north-eastern part of the United States. More than two million clients were out of power for a periods of several days to more than one month. The direct economic losses to Hydro-Québec were about one billion Canadian Dollars.

Another problem caused by ice accretion on high voltage insulators is the substantial decrease in electrical insulation along the insulators. Iced-insulator

flashover resulting in occasional power outages have been reported in many countries such as Canada (Drapeau, 1992; Boyer and Meale, 1988), the United States (Kawai, 1970), Japan (Matsuda, Komuro and Takasu 1991), England (Forrest, 1969), Yugoslavia (Vuckvic and Zdravkovic, 1990), China (Shu, Sun, Zhang and Gu, 1991), Norway (Fikke, Hanssen and Rolfseng, 1992), Switzerland (Meier and Niggli, 1968), etc.

Some authors (Boyer and Meale, 1988; Drapeau, 1992; Farzaneh and Kiernicki, 1995; Farzaneh and Drapeau, 1995; Farzaneh, Kiernicki and Dallaire, 1990; Farzaneh and Melo, 1990; Gorski, 1986; Chisholm and Tam, 1989) reported insulator flashover incidents caused by cold precipitation on the Hydro-Quebec and Ontario Hydro networks in Canada. The most remarkable incidents with Ontario Hydro occurred on March 9-10, 1986. The origin of the events on the Ontario-Hydro network was the accumulation of ice and short icicles on the insulators, caused by freezing rain and fog. Icicles grew at a rate of 16 mm/h (Boyer and Meale, 1988). Fifty–seven flashovers occurred in rapid succession. Twenty-seven of these flashovers were on transmission line insulators in an area just west of Toronto. This resulted in outages of most of the 500 kV transmission system in southern Ontario. Incidents that took place at the Arnaud substation on the Hydro-Quebec system on April 18, 1988, were caused by wet snow (Hydro-Quebec, 1988). A series of six flashovers resulted in a major interruption of electricity to a large part of Quebec.

Kawai (1970) and Charneski, Gaibrois and Whitney (1982) reported a certain number of insulator flashovers caused by ice accumulation on suspended and post insulators in the United States. The insulator flashovers were caused by an ice storm in a non-contaminated station in 1976. Khalifa and Morris (1968) reported power outages caused by iced insulation flashover in the west coast areas of Canada and the United States. A decrease of operating voltage from 315 kV to 280 kV was necessary to maintain service under such conditions.

Matsuda, Komuro and Takasu (1991) reported some flashover incidents caused by ice on 154 kV and 275 kV networks in Japan.

Forest (1969) presented problems related to the joint effect of ice and pollution on insulators of 400 kV lines in England.

Fikke, Hanssen and Rolfseng (1992) mentioned the destructive effect of cold precipitation and insulator contamination on the Norwegian network, caused by sea salt and man-made ions containing sulphur and nitrogen compounds.

Meier and Niggli (1968) mentioned some disturbances of grounding due to snow accumulation on a 400 kV mountain line in Switzerland.

Shu, Sun, Zhang and Gu (1991) reported flashovers on UHV lines in China caused by the joint effects of ice and pollution.

These reports confirm that the presence of atmospheric ice together with superimposed contamination sometimes leads to flashover and occasional outages.

1.2 Objective

Many of the industrial laboratories in Canada and many other countries have carried out investigations on ice accretion and its influence on the electrical performance and flashover on HV insulators. A brief history of these works is introduced in Chapter II of the present thesis.

In spite of the large number of publications on the flashover of ice-covered insulators, most of the published research has been concentrated on determining withstand voltage.

A relatively large number of investigations have made their own contribution to set up a model of the arc as it occurs on polluted insulator surfaces. The model for flashover on polluted surfaces is still a challenging point in the study of

outdoor insulation in recent years (Guan and Zhang, 1990; Sundararajan and Gorur, 1991).

However, flashover along ice-covered insulator surfaces is more complex than that of polluted surfaces. First, the type of ice formed is influenced by the freezing processes. Second, there are two discharge surfaces for ice-covered insulators: the outer ice surface and the interface of ice and insulator, compared to only one surface for polluted insulators. Flashover along the interface of ice and insulator was frequently observed in laboratory investigations. Third, the surface and bulk conductivities of ice are influenced by a number of parameters such as surrounding air temperature, freezing water conductivity, type of ice formation, and icing process.

Unfortunately, in spite of the complexity of flashover on ice surfaces and a large number of publications on the flashover performance of ice-covered insulators, only a few studies have been carried out on the fundamental aspects of the discharge.

A review of the literature shows that very few fundamental studies are available on electrical discharge on ice surfaces, and on the flashover mechanisms involved. Keeping this in mind, the present thesis aims at the modeling and

characterization of the arc on wet-grown ice surfaces, and the analysis of flashover conditions of ice–covered insulating surfaces.

1.3 Methodology

The methods used to reach the objectives are described below:

Considering the complexity of flashover on ice surfaces, an experimental procedure was set up using ice cylinders;

A high speed camera was used to analyze the arc development and to determine the arc radius and speed on ice surfaces under dc and ac conditions;

A series of tests were carried out for analyzing the factors influencing flashover, such as freezing water conductivity, arc distance, air gap length, voltage type, ice uniformity, ice temperature distribution during de-icing period, bulk ice current, etc.;

The equivalent ice surface conductivity, arc voltage-current characteristics, and arc voltage drops were obtained using linear or power regressions on the test results. The arc reignition conditions under ac voltage were also studied;

Based on the Obenaus concept for flashover on polluted surfaces, and on the experimental results as obtained in the present research, a mathematical model was developed to analyze flashover on wet-grown ice surfaces. The flashover voltages, critical currents and critical arc lengths were calculated for both positive and negative dc, and ac voltages;

The results were analysed and the mathematical model was applied on the ice samples and IEEE standard insulators strings covered with artificial ice. Good agreement between the experimental results on short string ice-covered insulators and calculated results was obtained.

CHAPTER II

THEORETICAL BASIS OF ELECTRICAL ARC AND MODELING

2.1 Introduction

The definition of the arc, in itself, is a problem since the word has been used to describe a number of electrical discharges looking more or less alike. In general, it is agreed that the arc must be defined in terms of current and voltage drop. It has been shown (Hoyaux, 1968) that many factors, such as atmospheric pressure, power sources, electrode form, have an influence on the discharge. Different kinds of discharges are defined.

Before proceeding to discuss flashover on ice surfaces, in this chapter, a brief review of electrical discharges will be presented first, with an emphasis on arc discharge, followed by the introduction of some fundamental mechanisms of arc development and modeling on polluted surfaces.

2.2 Electrical discharges

The surface flashover of ice-covered insulators, which is the main subject of the present thesis, belongs to the domain of discharges in a non-uniform field (Kuffel and Zaengl, 1984).

In non-uniform fields, various manifestations of luminous and audible discharges are observed long before flashover occurs. These discharges may be transient or steady state and are called corona discharges. Following the corona discharges, arc discharges develop and occur.

2.2.1 Corona discharge

Corona discharge is one of the causes of the power loss on transmission lines. It often leads to the deterioration of non-ceramic insulation by the combined action of discharge ions bombarding the surface, and the action of chemical compounds formed by the discharge. Corona discharge may also cause audible noise or interference in telecommunication, radio and television systems.

In a non-uniform field, various visual manifestations of locally confined ionisation and excitation processes can be viewed long before complete voltage breakdown between the electrodes occurs. Because of its importance in engineering applications, corona has been the subject of extensive studies.

Based on many measurements, an empirical relation of corona inception under ac voltage for the special case of a coaxial cylindrical geometry in air was developed by Peek (Kuffel and Zaengl, 1984):

$$\frac{E_c}{\delta} = 31.53 + \frac{9.63}{\sqrt{\delta r}} \qquad (2.1)$$

Where E_c is the critical field strength of corona inception and is in kV/cm, δ is the relative air density and r is the radius of the inner conductor and is in cm.

The polarity of the applied voltage was found to influence the visual appearance of corona. If the negative field threshold is reached, trichel pulses are observed. Hermstein zone, and pre-breakdown streamers are observed above the positive threshold field.

On a transmission conductor and under negative polarity, the corona appears as reddish glowing spots distributed along the wire. The number of spots increases with the field gradient at conductor surface. The mechanism of these pulses is of Townsend avalanche type.

Under positive voltage, the first corona mode is pulses (burst pulses and pre-onset streamers). Hermstein zone prevails in the potential range immediately above the critical potential. On transmission lines, corona appears in the form of a uniform bluish-white sheath over the entire surface.

Pre-breakdown streamers develop beyond the direct conductivity zone for higher positive voltages. The current takes on the form of a series of pulses of high amplitude. The front is extremely steep. Visually, the pre-breakdown streamer is a highly luminous arborescent spark whose foot is attached to an asperity of the cable. This phenomenon is accompanied by a sharp click. These are responsible for the radio-electric noise on high voltage lines. These discharges are in fact streamers that propagate along a photo-ionisation wave.

2.2.2 Electrical arc

The electrical arc is the last type of gas discharge. The current of electrical arc is greater than that of luminous discharge. The electrical arc is a completely ionised gas. At atmospheric pressure, this arc column has a concentration from 10^{14} to 10^{18} electron/cm^3. It is a high temperature plasma with good electrical conductivity (Hoyaux, 1968).

2.2.2.1 Type of electrical arc

The electrical arc is generally classified according to its ionised process (Kuffel and Zaengl, 1984). Considering the large densities of electrons and positive ions in the arc column, the electrical arc can not be caused by secondary electron emissions only. There are three kinds of electrical arcs according to

their ionisation mechanisms: thermionic arc, from a cathode heated by an external source; thermionic arc, from a cathode heated by the arc itself; and arc from field emissions.

In metals at room temperature, the conduction electrons do not have sufficient energy to leave the surface. If, however, the temperature of the metal is increased to some 1500-2500°K, the electrons receive energy from the violent thermal lattice vibrations: this energy is for the electrons sufficient to cross the surface barrier and leave the metal and is a function of metal type.

Very high electrostatic fields may draw electrons out of a metal surface. The field required to produce emission currents of a few microamperes is of the order of 10^7 to 10^8 V/cm. Such a field is observed on fine wires, sharp points, and submicroscopic irregularities with a quite low average applied voltage (2 to 5 kV).

At high temperatures both thermionic and field emissions will occur simultaneously.

2.2.2.2 Orders of temperature in an arc column

At atmospheric pressure the temperature of an arc is about 4000°K, and it decreases very rapidly in its radial direction (Farzaneh, 1994). Because of the large number of collisions in the arc column, the temperature of positive ions is almost equal to that of neutral molecules. There are almost no negative ions in an arc column because of the very high energy of electrons.

The electrons absorb energy from external sources, such as an applied electrical field. On the other hand, during elastic and inelastic collisions, a large fraction of their kinetic energy is converted into potential energy, causing, for example, ionisation of the struck molecule. When the temperatures of ionised gas, ions, and electrons are equal, a thermodynamic equilibrium state is reached.

2.3 Process of electrical arc development on polluted surfaces

High voltage outdoor insulators are subject to pollution by dirt and chemicals in industrial areas and near highways, and by salt deposits near the sea coast. When the insulator surface is dry, a very small capacitive current flows and the electrical voltage distribution is simply determined by the electrostatic field. In this dry condition, there is almost no decrease in the insulation strength of the

contaminated insulators. If, however, the surface becomes wet because of rain, fog, or dew, a resistive surface leakage current flows. Flashovers caused by wetted pollution layers on insulators have been reported on many transmission lines and substations.

It is generally recognised (Rizk, 1981) that pollution flashover follows the following steps: formation of a conducting layer on the insulator surface; dry band formation and partial arc development; arc propagation along the insulator surface; and finally, the flashover of the insulator.

When the resistive leakage current flows through wetted, polluted surfaces, non-uniform heating of the pollution layer occurs. This normally causes dry areas to form at narrow sections of the insulator, where the current density in the pollution layer is highest. Dry bands are formed by the extension of the dry areas and a large fraction of the applied voltage appears across these dry bands. Air breakdown occurs with the result that a quasi-stable discharge burns on the insulator surface. This discharge carries the interrupted leakage current, which has negative voltage–current characteristics. This discharge burns with its roots on electrolyte electrodes. Under certain conditions, these surface discharges can grow to produce a complete insulator flashover. The flashover is caused by the movement of the discharge roots across the wet surface in the

direction of the applied field until, eventually, the electrodes are bridged and a full arc is produced.

The mechanisms of arc development, especially in the final critical moment, is far from clear. It is generally supposed (Hampton, 1964; Claverie, 1971; Rahal, 1979) that some kind of external force is the reason of the arc propagation. The possible external forces may be static-electrical force, electromagnetic force, thermal floating force, etc. Using a discharge current of 100 mA, polluted surface resistance of 50 kΩ, and arc foot radius of 0.5 cm, Jolly (1972 and 1974) calculated the forces acting on the arc root with the following results: static-electrical force 2.8×10^{-6} N, electromagnetic force 1.6×10^{-10} N, thermal floating force 1.3×10^{-7} N. It was thought to be difficult for such small forces to produce the arc movement speed up to a few hundred m/s. So the ultimate phase of the propagation of arc was considered to be the electrical breakdown of air at the arc root. Li (1988) calculated the electrical stress ahead of the root of a propagating local arc by means of the charge simulation method and measured the dynamic potential distribution of a local arc along a polluted dielectric surface. The results show that the electric field stress at the arc root was too low to cause the dielectric breakdown of air. The temperature of the local arc was then measured by the method of relative intensities of spectral lines. The flashover was considered to be caused by the high temperature

ionisation of salt in the arc column and completed by the migration of positive and negative ions under the effects of the electrical field.

2.4 Mathematical models for polluted surface flashover

Many researchers have been working on mathematical models of pollution flashover. Although a dc flashover is similar to an ac flashover in some respects, there exist some fundamental differences, such as the process of contaminant accumulation and the existence of current and voltage zeros in ac systems. It is generally agreed (Rizk, 1981) that a separate treatment of dc and ac pollution flashover is necessary.

2.4.1 Direct current models

2.4.1.1 Obenaus' model

The first quantitative theory of flashover was proposed by Obenaus (1958). The theory models the flashover process as a discharge in series with a resistance, as shown in Figure 2.1. The discharge represents the partial flashover of the insulator surface and the resistance represents the non-bridged portion of the insulator.

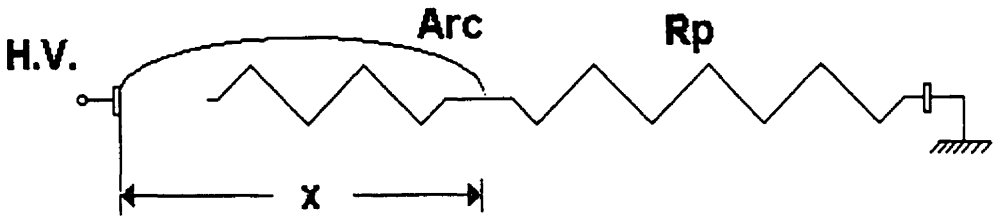

Figure 2.1 The modeling concept of Obenaus

The arc voltage V_{arc} was expressed as:

$$V_{arc} = AxI^{-n} \quad (2.2)$$

Where, A and n are the arc constants, and x is the length of the arc. According to the model, the circuit equation was then written as:

$$V = AxI^{-n} + IR_p \quad (2.3)$$

Where V (in V) and I (in A) are the values of the applied voltage and leakage current; and R_p is the surface resistance of the part of the pollution layer which is not bridged by the arc.

The critical arc length, x_c, for a fixed resistance, R_p, and applied voltage, V, can be obtained by differentiating Equation 2.3 to I and equating to zero, yielding the critical current, I_c, :

$$Ic = \frac{n}{n+1}\frac{V}{R_p} \qquad (2.4)$$

and the critical arc length, $x_{c,}$:

$$x_c = \frac{n^n}{(n+1)^{n+1}} V \frac{(\frac{V}{R_p})^n}{A} \qquad (2.5)$$

Obenaus did not develop the above equations further. But solving Equations 2.2 to 2.5, a minimum voltage for flashover, $V_{c,}$ can be expressed by:

$$V_c = \frac{n+1}{n^{\frac{n}{n+1}}} A^{\frac{1}{n+1}} x^{\frac{1}{n+1}} R_p^{\frac{n}{n+1}} \qquad (2.6)$$

2.4.1.2 Uniform pollution resistance model

Neumärker (1959) expressed the pollution layer as a uniform pollution resistance per unit leakage path as:

$$R_p = \overline{r_p}(L-x) \qquad (2.7)$$

Using the Obenaus idea, the minimum dc voltage, $V_{cx,}$ needed to sustain the arc bridging a portion, x/L, if the leakage path, L, was obtained:

$$\frac{nA}{\overline{r_p}}\left[\frac{V_{cx}}{(1+n)AL}\right]^{\frac{n+1}{n}} = \left(\frac{x}{L}\right)^{\frac{1}{n}} - \left(\frac{x}{L}\right)^{\frac{n+1}{n}} \qquad (2.8)$$

The critical voltage, V_c, was obtained by maximising the above equation:

$$V_c = LA^{\frac{1}{n+1}} r_p^{\frac{n}{n+1}} \qquad (2.9)$$

And the critical current, I_c, was expressed as:

$$I_c = \left(\frac{A}{r_p}\right)^{\frac{1}{n+1}} \qquad (2.10)$$

The critical arc length, x_c, was obtained as:

$$x_c = \frac{L}{n+1} \qquad (2.11)$$

2.4.1.3 Criteria for dc arc propagation

In pollution flashover, the arc possesses a falling voltage–current characteristic, while the series pollution layer exhibits the normal rising characteristics. Hampton (1964) established that the criterion for arc motion is:

$$E_a < E_p \qquad (2.12)$$

Where E_a is the voltage gradient in the arc and E_p is that of the pollution layer. Wilkins assumed that the discharge moves to a position where the rate of

energy expenditure is maximum. A critical current may be calculated (Wilkins, 1969), above which power increases with discharge length, and below which power decreases with discharge length. Hence, if the arc length is x, movement will occur if

$$dP/dx > 0 \qquad (2.13)$$

where P is the power taken from the supply. If the applied voltage is constant during the arc movement, Equation 2.13 reduces to (Hesketh, 1967):

$$di/dx > 0 \qquad (2.14)$$

2.4.2 Alternative current model

Under ac conditions, an arc is extinguished as the current passes through zero twice every half cycle. The arc develops only when it approaches the peak values of the applied voltage. During the remaining time, the arc reduces and recovers following the ac voltage. Arc reignition following current zero can roughly be classified into energy and dielectric breakdown (Hesketh, 1967).

2.4.2.1 Energy Reignition model

In this model, breakdown takes place when the residual arc gap is no longer able to dissipate the energy injected because of the flow of the post-zero current in a plasma that is still conducting. By describing the dynamic arc in terms of a constant power loss per unit length, the critical condition for energy breakdown was obtained (Browne, 1948):

$$U_{cr}^2 = kN_{02}R_m x \qquad (2.15)$$

Where x is the arc length, R_m is the residual arc resistance at current peak, k is the thermal diffusivity, and N_{02} is the power loss per unit length after current zero.

2.4.2.2 Dielectric reignition model

The dielectric reignition model, introduced by Rizk (1971), assumes that electrical conductance of the residual arc practically vanishes at current zero. The residual arc is treated as a hot gas having cylindrical geometry, cooled due to generalised thermal conduction, from an initial temperature of typically 3000°K (Rizk, 1971). The role of natural convection is assured to be restricted to determining the arc boundary radius.

Considering an arc in series with a uniform pollution resistance, Rizk (1981) obtained the critical voltage as:

$$\frac{V_c}{L} = \frac{xA}{Li^n} + (1 - \frac{x}{L})\overline{r_p} I_m \quad (2.16)$$

Where i and I_m are the arc current and its peak value, respectively.

Solving the above equation numerically, a relationship of the minimum flashover voltage (peak value in V) and the average pollution resistance per unit length, r_p, were obtained:

$$\frac{V_c}{L} = 23 r_p^{0.4} \quad (2.17)$$

2.4.2.3 Experimentally based arc model

Under ac conditions, the arc develops only when it approaches the peak values of the applied voltage. During the remaining time, the arc reduces and recovers following the ac voltage. In order to complete the ac flashover, arc recovery must be satisfied.

The arc reignition conditions on polluted surfaces were experimentally determined and can be expressed (Guan and Zhang, 1990) by either Equation (2.18) or Equation (2.19):

$$V_m \geq \frac{kx}{I_m^b} \quad (2.18)$$

$$V_p \geq \frac{k'x}{I_m^{b'}} \quad (2.19)$$

where, k, b, k′, and b′ are the recovery constants; V_p is the voltage across the gap of length of x cm; V_m is the applied voltage; and I_m the peak value of arc current.

Hurley and Limbourn established the minimum voltage to sustain an ac arc over a rod-rod gap of length x in series with a resistance R_p (Rizk, 1981):

$$Vc = const.x^{2/3}R_p^{1/3} \quad (2.20)$$

2.4.2.4 Dimensional analysis of flashover voltage

Dimensional analysis is a method by which information about a certain natural phenomenon is obtained, on the assumption that this phenomenon is governed by a dimensionally correct equation among certain variables. Rizk (1970) first

applied this analysis to polluted insulator flashover. The critical flashover voltages under dc and ac were expressed by the following equations respectively:

$$V_c I^n = const.\, AL \quad (2.22)$$

$$V_c I_m^{\ b} = \Phi(\frac{A}{k})kL \quad (2.23)$$

Where A and n are the arc constants; k and b are the arc recovery constants; and L is the arcing distance. The nature of function Φ needed to be determined experimentally (Rizk, 1970).

CHAPTER III

LITERATURE REVIEW ON ICE SURFACE FLASHOVER

As described in the introduction, many reports confirm that the presence of atmospheric ice on insulator strings together with superimposed contamination sometimes leads to flashover and occasional power outages.

In order to have a better understanding of the ice-covered insulator flashover processes and the present situation of the research on the subject, a literature review is carried out and reported below.

3.1 Ice accretion on insulators

Few industrial laboratories either in Canada or other countries, have carried out laboratory studies and field observation of ice accretion on HV insulators (Fikke, Hanssen and Rolfseng, 1992; Meier and Niggli, 1968; Farzaneh and Kiernicki, 1995; Farzaneh and Drapeau, 1995; Farzaneh and Melo, 1990; Gorski, 1986; Chisholm and Tam, 1989; Chisholm, Tam, Erven and Melo, 1993).

Ice build-up on post and line insulators is caused essentially by the impinging of supercooled droplets (Kuroiwa, 1958). The type of ice formation is mainly affected by air temperature, wind velocity, water droplet size, and liquid water content. Based on the studies of ice formation in nature, carried out by Kuroiwa (1958 and 1965), Imai (1953), Oguchi (1953), Phan et al. (1977), Farzaneh et al. (1994) and Su et al. (1993), depending on the atmospheric and environmental conditions, three types of ice were formed on the surfaces of energised structures: glaze, hard rime, and soft rime. If all the supercooled water droplets impinging on the impact surface are completely frozen, there is no runoff water and no icicles. In this condition, called dry-grown regime (Farzaneh, Kiernicki and Martin, 1994), both hard rime and soft rime are grown. The deposit temperature is below 0°C and is a function of a balance between the rate of heat liberation by the freezing of the droplets and the rate of heat transfer by forced convection to the environment. In contrast, if the supercooled water droplets impinging on the impact surface are not completely frozen, there is runoff water and the formation of icicles. Glaze is grown in this wet-grown regime (Farzaneh and Laforte, 1992).

In addition to atmospheric conditions, for energised insulators, electrical phenomena such as corona discharges, leakage current, water-drop elongation, and ionic wind all tend to influence the formation of ice (Phan, Allaire and Mccomber, 1977).

Glaze is transparent, with a density of about 0.9×10^6 g/m^3. Hard rime is opaque and has a density between 0.6 and 0.87×10^6 g/m^3 (Kuroiwa, 1958 and 1965; Iwai, 1953; Oguchi, 1953; Phan, Allaire and Mccomber, 1977), and soft rime is white and opaque with a density of less than 0.6×10^6 g/m^3.

Snow can sometimes be modified into a soft rime by the action of wind and welting temperatures.

The conditions favouring the formation of various types of ice in nature are summarised in Table 3.1 (Kuroiwa, 1958 and 1965).

Table 3.1

	Surrounding Air Temperature (°C)	Wind Velocity (m/s)	Water Droplet Diameter (μm)	Density (g/m^3)
Glaze	0 to -3	1 to 20	500 to 6000	(0.8 to 0.9) $\times 10^6$
Hard Rime	-3 to -15	5 to 20	5 to 20	(0.6 to 0.87) $\times 10^6$
Soft Rime	-5 to -25	5 to 20	5 to 20	$<0.6 \times 10^6$

To identify the characteristics of ice and/or snow accretion occurring naturally on high voltage transmission equipment, and evaluate their impact on electrical performance, a field observation and laboratory study program was jointly

initiated by the University of Quebec in Chicoutimi and Hydro-Quebec in 1989 (Farzaneh and Drapeau, 1995). The field observations were recorded using a video camera equipped with extended accuracy and zoom capacities. Meteorological parameters were recorded at frequent intervals. From October 1989 to April 1992, about 7 series of observations were made on various parts of the Hydro-Quebec network. Two forms of ice accretions on insulators were observed: the icicle form and the curtain form. Icicle accretions, the most common form, were observed for conditions of freezing rain accumulation ranging from a few millimeters up to 10 mm, and for air temperatures from –4°C to –1°C. Curtain accretion was observed only once and resulted from a freezing rain precipitation of 30 mm to 40 mm, at an ambient air temperature of about –1°C (Farzaneh and Drapeau, 1995).

For the purpose of the flashover tests on ice-covered insulators, various types of ice were formed on energized insulators in the climate room of the UQAC (Farzaneh and Drapeau, 1995; Farzaneh and Kiernicki, 1995). Ice was classified according to dry and wet-grown regimes. The parameters listed in Table 3.2 were selected for the insulator ice covering and flashover tests.

Table 3.2

Accumulation Regime	Air Temperature (°C)	Wind Velocity (m/s)	Water Droplet Diameter (μm)	Liquid Water Content (g/m^3)
Dry	-12	3.3	15	$6.8x10^6$
Wet	-12	3.3	80	$6.8x10^6$

Upon comparing field observations with the results of the laboratory investigation, a similarity between the ice accretions was found (Farzaneh and Drapeau, 1995). For example, in the wet-grown regime, bulk ice on the surface of the insulators and icicles around the insulator skirts were formed in the laboratory. This type of ice deposit simulated ice accretion during a freezing rain precipitation similar to that detected in the field observation (Farzaneh and Drapeau, 1995).

3.2 Flashover of ice-covered insulators

The influence of ice accretion on flashovers occurring on HV insulators has always been a challenging subject in many cold climate countries.

In Canada, Khalifa and Morris (1968) studied the influence of atmospheric ice accretion on the performance of high voltage porcelain, glass, and composite

insulator strings in 1965. Ice was formed by spraying water on vertically installed insulator strings in a cold room at temperatures ranging from –7°C to –12°C. The object of the study was to determine the leakage current, flashover voltage, as well as the influence of ice density and conductivity on the flashover performance of ice-covered insulators. Experiments under alternating voltages showed that the critical leakage current leading to flashover of ice-covered insulators is less than that of polluted insulators. The decrease in flashover voltage by ice accretion was more serious on double insulator strings than on a single string. The performance of ice-covered composite insulators was worse than that of ceramic insulator strings of the same arcing length.

Cherney (1980) studied the ac flashover performance of artificially pre-contaminated IEEE standard insulator strings and composite insulators covered with ice. Ice was formed from tap water of a conductivity 356 μS/cm in a cold room at a temperature varying from –3.5°C to –6.0°C. During the icing period, ac voltages of 145 kV and 318 kV were applied to 230 kV and 500 kV line insulator strings respectively. If there was no flashover in three hours, the voltage was considered as withstand voltage. For a string of 14 IEEE units energized at a voltage gradient of 112.4 kV/m, no flashover occurred. It was found that composite insulators had a better performance than IEEE standard insulator strings. Also, composite insulators with alternating sheds had a better performance than those with uniform sheds.

In the United States, Renner, Hill and Ratz (1971) studied the dc flashover performance of artificially ice-covered insulators. Ice was formed by spaying water on the surface of insulators in an outside test arrangement. The testing objects included glass and porcelain suspension insulator strings and a station insulator. Two voltage application methods were used. In the first method, a voltage of 400 kV was applied to the insulators and then ice accumulation continued until flashover occurred. Voltage was then cut-off immediately by a protective system. Voltage was applied again and increased until a new flashover took place. The finial applied voltage without flashover was considered as withstand voltage. In the second voltage application method, voltage was increased at a rate of 2.5 kV/s from zero until flashover. The value of applied voltage at the moment of flashover was considered as the minimum flashover voltage. The minimum flashover voltage was found to be a little higher for positive dc voltage than negative. For the vertically installed insulator string with an ice thickness less than 0.5 cm, the insulating performance was better for a single string than for a double string. But no difference was found when ice had a greater thickness. The inclined insulator string had a better flashover performance than vertical insulator string.

Schneider (1975) carried out artificial ice tests on transmission line insulators on site. Standard and anti-fog porcelain insulators, as well as composite insulators were installed vertically or in V arrangement. Ice was formed by

spraying water having a resistivity of about 35 kΩ-cm (conductivity of 29 μS/cm) at night when the ambient temperature was lower than –2.8°C. Voltage was applied during all the icing periods until flashover took place. If there was no flashover after four hours, the voltage applied was considered as the withstand voltage. It was found that the insulating performance (kV/unit) decreased with the quantity of ice accumulation. V type insulator strings had a better performance than vertical one and withstood up to 70% higher ice accumulation in that study. Composite insulator strings did not perform as well as porcelain standard insulator strings under the same icing and experimental conditions.

Charneski, Gaibrois and Whitney (1982) carried out ac flashover tests on ice-covered porcelain and composite insulators. Ice was formed in a cold room at –12°C from water with a resistivity of 5 kΩ-cm (conductivity of 200 μS/cm). During the icing period 75 kV_{ac} was applied to the insulators of an arcing distance of about 0.97 m. From a one-hour withstand test, it was found that no flashover took place at a voltage gradient of 76.7 kV/m.

Kawai (1970) carried out tests on ice-covered standard and anti-fog porcelain insulators, as well as composite insulators. Ice was formed by spraying water in a cold room, as well as on a natural site. A constant ac voltage was applied and kept until flashover occurred. It was found that the non-uniform voltage distribution along the ice-covered insulator was the reason of the strong corona

discharge near the HV and ground ends of the insulator string. The insulation performance was a non-linear function of arcing distance. The lowest flashover voltage was only 10.5 kV/unit for a porcelain insulator of 146 mm (height) x 254 mm (diameter). The maximum thickness of ice during the tests was found to be about 4 mm. Considering such a low flashover gradient after ice accumulation (71.9 kV/m) it was considered quite possible that flashovers occur on extra-high voltage transmission lines after ice accumulation.

Lee, Nellis and Brown (1975) studied the ice flashover performance on various type of insulators in vertical and horizontal positions. Ice was formed by spraying water (conductivity of 145 μS/cm at 7°C) on vertical, horizontal, and V type composite or porcelain insulators in a cold room at the air temperature varying between 0°C and –8°C. A constant ac voltage was applied 2 minutes after the ice formation until flashover took place. V type insulator strings were shown to have a better performance than vertical strings iced under similar conditions. The minimum flashover voltage of vertical insulator strings was 20% lower than that of horizontal strings iced under similar conditions. The shorter the distance between the sheds, the larger was the influence of ice accumulation.

In Japan, Watanabe (1977) compared the flashover voltages of porcelain insulators covered with ice or snow with that of contaminated insulators. Ice

was formed by spraying water having a conductivity of 100 μS/cm during the night. It was found that the effect of wet-grown ice in particular, or snow, was more significant than that of pollution in mountain areas. The flashover voltage per unit was reported to be a little lower for a long insulator string than for a short one. The design criteria of insulator strings was suggested to be 75 kV/m for ac and dc voltages and 200 kV/m for impulse voltage. The minimum flashover voltage under positive dc was found to be a little higher than under negative dc. The single insulator string had a higher flashover voltage than the double insulator strings tested.

Fujimura, Naito, Hasegawa and Kawaguchi (1979) studied the flashover performance of ice or snow covered porcelain and composite insulators. Ice was formed by spraying water in a cold room at an air temperature of –20°C. The insulator string was covered with snow brought from mountain areas and stored at –5°C. Conductivity of melting snow was 15 to 25 μS/cm. Standard suspension insulators, station insulators and composite insulators were used in the tests. After the accumulation of ice or snow, ac, dc or impulse voltage was applied to the test insulator. It was found that ac withstand voltage was 40% lower for the ice-covered insulators than that of the snow-covered, when the conductivity of melting water was between 500 to 3000 μS/cm. The dc withstand voltage of ice-covered insulators was a little lower than that of snow-covered insulators. The ac withstand voltage of snow-covered insulators was

always higher than that of polluted insulators of same equivalent salt deposit density (ESDD). The ac and dc withstand voltages of ice-covered insulators were higher than those of polluted insulators of the same ESDD. Impulse withstand voltage was found to increase linearly with the arcing distance of the insulator string.

Sugawara, et al (1990 and 1993) studied the insulation properties of atmospheric ice-covered insulators installed on high mountains and in laboratory. The surface resistances as a function of time were presented for the same two types of insulators, a string of three IEEE standard insulators and a long rod insulator. The field study was carried out at a mountain site of 1377 m altitude. The surface resistance was recorded by a print-out of digital multimeters every 5 minutes. Positive voltage (+2 kV) was applied to the sample insulators. In the laboratory study, the experiments were carried out in a cold chamber in which the minimum temperature obtainable is –30°C. The insulator surface resistances were recorded by a personal computer and a video measuring system. It was confirmed that the icing on the insulators in the field decreased the insulation resistances much more than in the laboratory experiments. It was also noted that clouds (and/or fog) decreased the insulation resistance of the insulators. A greater decrease in insulation resistance was likely to precipitate the flashover of ice-covered insulators. Laboratory studies showed that insulation resistance depended on both the kind of ice and the

shape of the insulator. Under hard rime and glaze ice accretion, the insulation resistance as a function of elapsed time during icing and de-icing had the same tendencies. This insulation resistance was found to decrease suddenly when the icicles bridged spaces between sheds during icing. Under soft rime conditions, the insulation resistance decreased much more during de-icing than during icing.

In China, Shu, Sun, Zhang and Gu (1991) studied the flashover performance of iced and polluted insulators. A pollution layer was first deposited on the insulator surface. After the pollution layer was dry, ice was formed in a cold room. On a string of 3 units of IEEE insulators, 2.3 kg of ice was accumulated. During the following ice-melting period, a water film formed on the ice surface. The maximum withstand voltage decreased with an increase of the pollution level until an ESDD of 0.09 mg/cm^2. After that level of pollution, the maximum withstand voltage remained constant. From the ESDD of 0.015 to 0.05 mg/cm^2, the maximum withstand voltage decreased 18%. From the ESDD of 0.05 to 0.1 mg/cm^2, the maximum withstand voltage decreased 13%.

Under the direction of M. Farzaneh, a systematic study of the flashover performance of ice-covered HV insulators was undertaken jointly by the UQAC and the Institut de Recherche d'Hydro-Québec (IREQ) (Farzaneh and Kiernicki, 1995; Farzaneh and Drapeau, 1995; Farzaneh, Kiernicki and Dallaire, 1990;

Farzaneh and Melo, 1990; Farzaneh, Kiernicki and Martin, 1994; Farzaneh, Kiernicki and Drapeau, 1992; Farzaneh and Kiernicki, 1997; Farzaneh, Kiernicki, Chaarani, Drapeau and Martin, 1995; Farzaneh and Laforte, 1992).

From the results of the laboratory investigation at UQAC, it was possible to discern a similarity between some of the ice accretions observed in the field and those artificially obtained in the laboratory. Within the experimental conditions, wet-grown ice deposits were formed to simulate freezing rain precipitation, as was observed in field observations. It was also found that wet-grown ice has the lowest flashover voltage for the same freezing water conductivity, compared with other types of ice.

The existence of different flashover testing methods, as those used by various researchers (Cherney, 1980; Renner, Hill and Ratz, 1971; Schneider, 1975; Lee, Nellis and Brown, 1975; Watanabe, 1977; Fujimura, Naito, Kasegawa and Kawaguchi, 1979; Sagawara, Hokari, Ando, Yoshida, Hirota and Tatokoro, 1993), makes it difficult to compare results. Two methods, based on those described in the standard IEC 507 for testing polluted insulators, were developed for testing insulators under icing conditions at UQAC (Frazaneh and Drapeau, 1995; Farzaneh and Kiernicki, 1997). Both the maximum withstand voltage method and the 50% withstand voltage method seem to be adequate and may be used for the purpose of critical flashover voltage measurements.

The main difference between these methods is the number of tests required, which is noticeably lower for the maximum withstand voltage method (Frazaneh and Drapeau, 1995; Farzaneh and Kiernicki, 1997).

The effect of several factors on the withstand voltage of a short string of several types of insulators, covered with artificial ice, were investigated at UQAC (Frazaneh and Drapeau, 1995; Farzaneh and Kiernicki, 1997). Using short strings of IEEE standard insulators from 1 to 6 units, the influences of the principal factors, such as ice uniformity, ice thickness, freezing water conductivity, and arcing distance, were investigated.

From the results, it was found (Farzaneh and Kiernicki, 1997) that the more uniform the ice distribution along an insulator string is, the lower the maximum withstand voltage is. The deviation angle of icicles, formed around the insulator sheds from a vertical axis, depended mainly on wind velocity. For example, for a given value of liquid water content, the icicles formed at wind velocities lower than 3.3 m/s are nearly vertical, resulting in a relatively uniform ice along the insulator string. By contrast, icicles formed at higher wind velocities, up to 6.4 m/s, were twisted toward the insulator string axis, resulting in a non-uniform ice accumulation along the insulator string.

The maximum withstand voltage of insulator strings covered with wet-grown ice, and with an arcing distance of less than 1 m, increased almost linearly with the arcing distance (Farzaneh and Kiernicki, 1997).

The maximum withstand voltage decreased first with the ice thickness and then stayed constant after a critical value of ice thickness. This value seems to be a function of shed or unit diameter, shed spacing, and of the type of insulator. The values of 20 mm, 25 mm, and 30 mm were respectively obtained for glass cap-and–pin (Phan and Matsuo, 1983), EPDM ((Farzaneh, Kiernicki, Chaarani, Drapeau and Martin, 1995), and porcelain post-type insulators (Farzaneh and Drapeau, 1995).

The maximum withstand voltage was found to be influenced considerably by the conductivity of the freezing water (Farzaneh and Kiernicki, 1997). For example, from 35 experimental points of insulator strings covered by uniform wet-grown ice of 20 mm thickness, it was found that the decrease in maximum withstand voltage gradient can be expressed by a power curve which follows the relation: $V_{ws}/m = 165.3 \cdot \sigma^{-0.18}$; σ being expressed in $\mu S/cm$, and V_{ws}/m, in kV/m. The effect of uniform wet ice with a thickness corresponding to 20 mm of ice and formed from freezing water with a conductivity of 80 $\mu S/cm$ is equivalent to an ESDD of about 0.13 mg/cm^2.

3.3 Modeling of electrical arc on ice surfaces

In spite of the large number of publications on the flashover of iced covered insulators, most of the published studies on the flashover performance of ice-covered insulators, have mainly concentrated on determining the withstand voltage. Generally, the pollution flashover theory is used to explain the flashover phenomena on ice surface. As described in Chapter II, it is generally recognised that the main processes of polluted insulator flashover comprise the following events: conducting layer formation; leakage current surges with associated dry-band formation; partial arc development, and final arc span across the whole insulator (Rizk ,1981).

A relatively large number of studies have made their own contribution to set up a model of the arc which occurs on polluted insulator surfaces. Many experimental investigations were carried out based on some simplified test models, such as water tanks, a thin pollution layers with the shapes of triangle, rectangle, cylinder, and disc. Rizk (1981) made a critical review of the main mathematical models for pollution flashover. The model for flashover on polluted surfaces is still a hot point in the study of outdoor insulation in recent years (Guan and Zhang, 1990; Sundararajan and Gorur, 1991).

Unfortunately, in spite of the complexity of flashover on ice surface and a large number of publications on the subject of ice-covered insulator flashover, only a few have studied the fundamental aspects of discharge. Bandel (1951), Jordan and Saint-Armand, (1976) studied corona discharge on ice needles. Phan. Allaire and Mccomber (1977) studied the evolution of corona discharge from a water drop during its transition from liquid to solid phase, and vice versa. Sato, Saito, Kaga and Akagami (1989) carried out a number of flashover tests on a plate iced by a solution of NaCl spray. The authors compared the flashover of the iced plates for various types of ice deposits. Bui, Phan, Huraux and Pissolato (1984) studied the characteristics of a dc arc between a metal electrode and an ice surface. They found that the constants of the arc do not change with ice temperature but do change with electrode polarity. This study was limited to a short air gap of 3 mm between the metal electrode and the ice surface.

A review of the literature showed that very few in-depth studies were available on electrical discharge on ice surfaces or on the mechanisms involved. Keeping this in mind, a series of studies on the modeling of electrical arc on ice surfaces were carried out in the high voltage laboratory of the UQAC since 1993 (Farzaneh, Zhang and Chen, 1994; Farzaneh, Chen and Zhang, 1996; Zhang, Farzaneh and Chen, 1995; Chen, Farzaneh and Zhang, 1995; Farzaneh, Chen and Zhang, 1996; Farzaneh, Zhang and Chen, 1997; Farzaneh, Zhang and

Chen, 1996; Chen, Farzaneh and Zhang, 1996; Farzaneh and Zhang, 1998; Zhang and Farzaneh, 1998).

At UQAC, two simplified ice samples, the triangle and cylinder ice samples, were used in the modeling of electrical arc on ice surfaces. For the triangular ice sample (280 mm, 200 mm and 15 mm in height, base and thickness), ice was formed by filling a triangular glass mould with water (Farzaneh, Zhang and Chen, 1994). The mould was then placed into a cold chamber at –12°C. Distilled water was used to form a one cm layer of ice at the bottom of the mould followed by a 5 mm ice layer using salt water with the desired conductivity. The cylindrical ice sample was formed in a climate room from supercooled droplets on the surface of a rotating glass cylinder (Farzaneh, Chen and Zhang, 1996). The inner and outer diameters of the ice sample are 890 mm and 1230 mm respectively. The lengths of the cylindrical ice samples change from 300 mm to 920 mm. This kind of ice, called wet-grown ice, is similar to the ice accumulated on insulators under natural conditions (Farzaneh and Drapeau, 1995). In order to accumulate a uniform ice thickness, the cylindrical glass tube was installed vertically and rotated at one turn per minute. The icing conditions of the cylindrical ice sample were the same as those for wet-grown ice on an insulator string and were listed in Table 3.2.

Using the triangular and cylindrical ice samples and a set of measuring equipment including a high speed camera, some principal factors for the modeling of electrical arc on ice surfaces were studied. The ice surface conductivity was analyzed during the de-icing period and during flashover (Farzaneh, Zhang and Chen, 1994; Farzaneh, Chen and Zhang, 1996, Dec.; Farzaneh, Chen and Zhang, 1996; Farzaneh, Zhang and Chen, 1997) for different types of ice under ac and dc voltages. Ice surface temperatures were measured during the de-icing period (Farzaneh, Chen and Zhang, 1996, Dec.). The electrical arc constants A and n were determined (Zhang, Farzaneh and Chen, 1995; Farzaneh, Zhang and Chen, 1997; Farzaneh, Zhang and Chen, 1996). The arc recovery condition under ac voltage was obtained (Chen, Farzaneh and Zhang, 1995; Farzaneh, Zhang and Chen, 1997). The influence of some factors, such as freezing water conductivity, ice uniformity, and ice type, on flashover voltage were studied (Farzaneh, Chen and Zhang, 1996; Chen, Farzaneh and Zhang, 1996). Using a high-speed frame camera, the propagations of ac and dc arc on ice surfaces were investigated (Farzaneh, Zhang and Chen, 1996; Farzaneh and Zhang, 1998; Zhang and Farzaneh, 1998). It was found that, for triangular ice samples, and during the dc flashover process, the arc may propagate outside or inside the ice. The propagation of arc on the ice surface can be divided into two stages. In the first stage, which covers a distance of about 45% to 60% of the total leakage distance, the velocity is relatively low, varying between 0.05 to 0.3 m/s. In the second stage,

the propagation arc velocity is about 20 to 50 m/s for an outer arc, and about only 3 to 7 m/s for an inner arc. The maximum velocities reach about 100 m/s and 50 m/s for outer and inner arcs respectively, just before flashover (Farzaneh and Zhang, 1998; Zhang and Farzaneh, 1998). The radii of both inner and outer arcs are proportional to the square root of the leakage currents. Under ac conditions and for triangular ice samples, the partial arc on ice surfaces extinguishes and reignites with the cyclical variation of applied voltage. There is a delay of about 1 ms between the variations of arc length and voltage (Farzaneh and Zhang, 1998). The arc propagation process was found to be similar to that of a dc arc. However, the maximum instant velocity of arc propagation before flashover under ac was about 4 times those under dc+ and dc- (Farzaneh, Zhang and Chen, 1996; Farzaneh and Zhang, 1998; Zhang and Farzaneh, 1998).

A mathematical model was developed to calculate the flashover voltage of ice-covered insulators based on the above experimental results (Farzaneh, Zhang and Chen, 1997; Zhang and Farzaneh, 1998). The mathematical model was applied to a short string of IEEE standard insulators and was validated with the experimental results. It was found that there is a good agreement between the flashover voltage calculated from this model and the results obtained in the laboratory (Farzaneh, Zhang and Chen, 1997, Chisholm, discussion to Farzaneh, Zhang and Chen, 1997).

CHAPTER IV

ELECTRICAL DISCHARGE PROCESS ON ICE SURFACES

4.1 Introduction

Flashover on ice surfaces is often considered to be a special type of pollution flashover. The pollution flashover process has been simulated and studied in many laboratories by using some simplified models, such as water tanks, water films, cylindrical or triangular samples covered with pollution layers, etc. (Wilkins, 1969; Claverie, 1971; Jolly, 1974; Li, 1988; Guan and Huang, 1994).

In the case of ice-covered insulators, the modeling of the arc on ice surfaces is more complicated than on polluted surfaces. As described in Chapter III, the type of ice formed is influenced by the freezing conditions such as atmospheric and environmental conditions. The surface conductivity of ice is influenced by a large number of parameters such as the surrounding air temperature (Phan and Matsuo, 1983), freezing water conductivity (Farzaneh and Drapeau, 1995), and de-icing process. All these complex intervening parameters make it difficult to establish a mathematical model based on the experimental results obtained from iced insulators.

Under actual conditions and depending on meteorological and environmental conditions, ice is accumulated either partially or wholly on the insulator string surface, forming roughly on the windward half or a complete cylinder of ice. Taking into consideration the shape and axial symmetry of the insulators, a simple cylindrical ice sample formed on a glass tube was used for this investigation.

Electrical utility experiences and many laboratory investigations have shown that, as summarized in Chapter I , flashover on ice-covered insulators occurs mainly during melting periods. During a melting period, caused by sunshine, a rise in ambient temperature, or the heating effect of leakage current, a water film was formed on the surface of the accumulated ice. The present study concentrates on electrical discharge during the melting period, because of its obvious role on insulator flashover under icing conditions.

In the present chapter the dc and ac discharge processes, using a high speed camera and a data acquisition system, were studied. A number of phenomena, as well as factors and parameters, such as discharge phenomena, arc currents, applied voltage, arc diameter and the speed of arc propagation, intervening in ice surface flashover and modeling, were studied.

4.2 Experimental conditions and procedures

As ice deposits in a wet–grown regime are more dangerous than ice grown in a dry regime (Farzaneh and Drapeau, 1995), wet-grown ice was mainly used to perform the flashover tests for the experiments carried out in this study.

In the climate room, (Figure 4.1), wet-grown ice was formed from supercooled droplets sprayed onto the surface of a glass or Plexiglass cylinder, 89 mm in diameter. This kind of ice is similar to the ice accumulated on actual insulators in natural conditions (Farzaneh and Drapeau, 1995). In order to accumulate a uniform ice thickness, the cylindrical glass tube was installed vertically and rotated at one rpm. The temperature of the climate room was maintained at -12 ± 0.2°C during ice accretion. A relatively uniform wind was obtained by using a system of eight fans placed behind a diffusing honeycomb panel. The spray system consisted of 4 air atomizing nozzles. The mean volume diameter of the supercooled droplets was 80 μm, liquid water content was 6.8 g/m^3, and wind velocity was 3.3 m/s (11 km/h), (Farzaneh and Drapeau, 1995).

The conductivity of freezing water was changed by adding sodium chloride to de-ionized water. Sodium chloride is an important contaminant in both sea coast and urban (road salting) exposure of high voltage equipment. Freezing

water conductivity was adjusted to values varying from 20 to 160 μS/cm (at 20°C) in the present study.

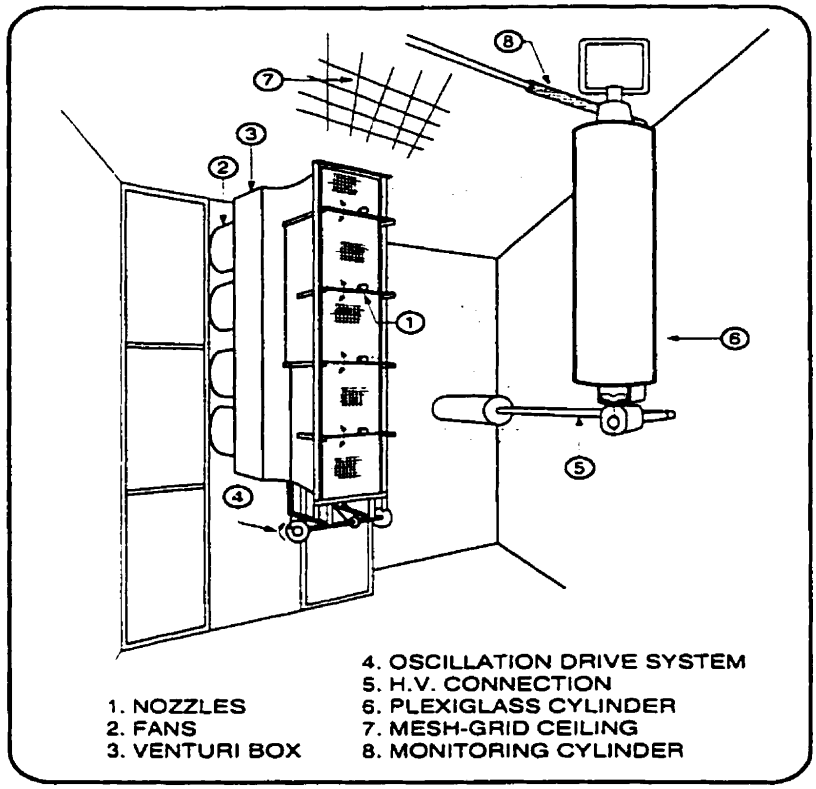

Figure 4.1 Climate room setup

Once the ice thickness reached 17 mm, accretion was stopped, the icicle cylinder was removed and a 10 mm air gap was made near the grounding electrode by cutting and removing a small part of the ice at the top of the sample, as shown in Figure 4.2. This air gap simulates the air gap formed by partial discharge on actual ice-covered insulator strings during the icing period. The flashover tests were carried out about 5 minutes after the ice sample was

placed in the climate room kept, this time, at an air temperature between 0°C and +1°C. The ice began to melt and a water film was observed on the ice surface. At this moment, ac or dc voltage was applied to the ice sample and increased at a constant rate (about 3.9 kV/s in our case) by an automatic control, until an estimated flashover voltage was reached.

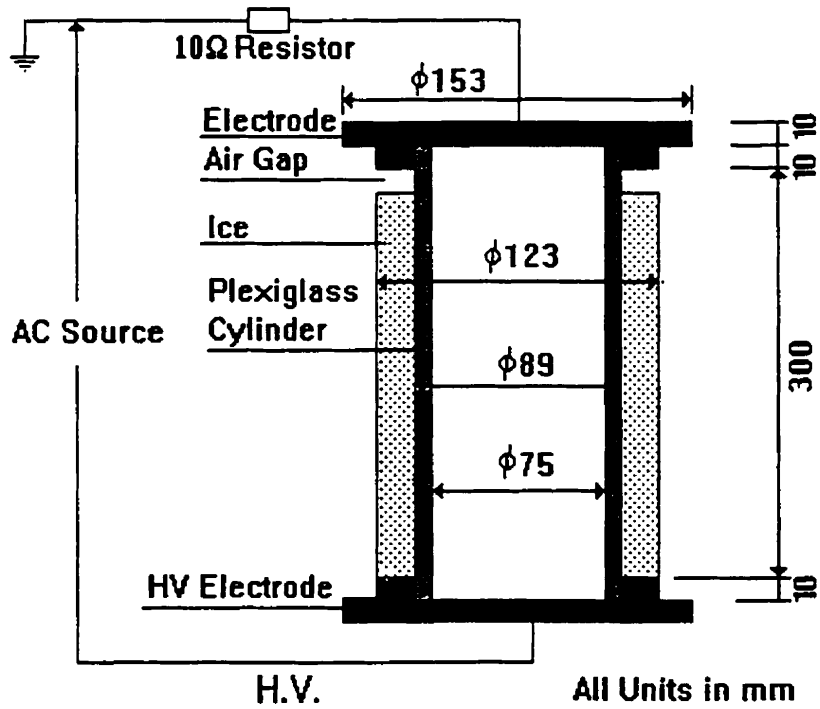

Figure 4.2 Ice sample and flashover test setup

In the ac flashover tests, high voltage was supplied by a 240 kVA, 120 kV transformer with a short-circuit impedance of about 5%. The primary coil of the transformer was connected to a 240 kVA regulator with a short-circuit

impedance of 2%. The overall short-circuit current of the H.V. system is about 28 A at the maximum operating voltage of 120 kV_{rms}. The high voltage system is shown in Figure 4.3.

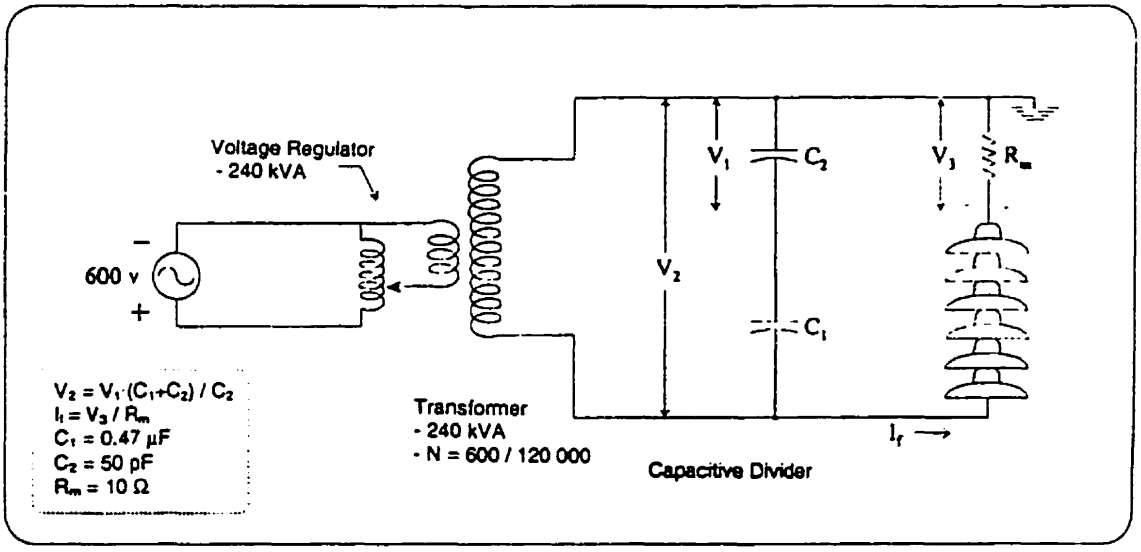

Figure 4.3 High voltage system of the H.V. laboratory of UQAC

The dc source was of the thyristor (SCR) feed-back control type, with a dynamic voltage drop of less than 5% when the load current is 0.5 A.

To record the arc development, a high speed camera (Kodak EKTAPRO EM Motion Analyzer, Model 1012) was used in the flashover tests. The highest speed of the camera is 12000 frames per second. The speeds often used in the present study were 1000 and 3000 frames per second. During the tests, the

camera was always in record condition until a flashover occurred, then the camera was stopped. The frames recorded in the last 3.2 s were transferred and saved on videotape or data file.

The applied voltage and leakage current were simultaneously recorded using a data acquisition system (DAS). This data can also be shown on the monitor connected to the high speed camera. The results obtained from these simultaneous measurements are helpful in the analysis of the behavior of arcs on ice surfaces.

4.3 Flashover process under direct voltage

Flashovers under both positive and negative direct voltages were carried out. In the present study, the electrical arc always takes place and develops from the up side (grounded side) of the ice samples, because the air gap is on this side. An electrical arc occurred when a positive voltage was applied and was defined as negative arc, while an arc corresponding to a negative voltage application was defined as positive arc.

4.3.1 Positive arc development

A series of tests on ice-covered cylinders were carried out for ice formed from freezing water of different conductivities.

Although the arc developed differently in each flashover test, some typical rules could still be obtained from a large number of tests. They are described below.

After a few minutes of voltage application, several violet arcs first appeared across the air gap. The positions of these violet arcs across the air gap were random. Under the influence of these arcs, ice near the foot of the arcs melted and the local air gap length increased. There were two possibilities for the arc development. First, only one arc established in a given position and then developed. Second, several distinct arcs started and gradually moved to other places where the air gap lengths were shorter. As the air gap became longer in several places all the violet arcs except one extinguished. The remaining arc then turned white. In this process the arc length was usually shorter than 13% to 16% of total arcing distance, and the arc current lower than 0.1 A. The arc developed very slowly on the ice surface and its speed depended on the condition of melting ice and the length of the local air gap. This process was referred to as the arc starting period.

The arc starting period can take up to 10 minutes and is mainly influenced by freezing water conductivity. The larger the conductivity, the shorter the period.

When the only existing white arc developed continually, ice surrounding the foot of the arc was destroyed. The arc became longer and brighter, the current increased and the local air gap enlarged. When the arc reached 23% to 27% of total arcing distance, it became more active and could gradually leave the surface of ice. Local ice melting was no longer the necessary condition of the arc foot development. As the arc became longer and brighter, it developed faster and the corresponding current was larger. When the arc length reached a value between 73% to 90% of total arcing distance, flashover took place suddenly. This process is referred to as the arc development period.

Figure 4.4 shows a typical positive arc development recorded by the high speed video camera at 1000 shots per second. In this example, a negative dc voltage of 36 kV was applied to an ice sample having a freezing water conductivity of $\sigma = 80$ μS/cm. The positive arc development during the period of 1.160 s just before the flashover was recorded. At t = 0 s, arc reached to about 18.7% of total arcing distance and a current of about 0.1 A. Then the arc developed slowly and became a little brighter. From t = 0 s to t = 0.9 s, arc length was about 31.3% of total arcing distance, and arc current was about 0.2 A. The average arc speed during this period was 0.04 m/s. From t = 0.9 s to t =

1.1 s, arc developed to about 56.3% of total arcing distance, and arc current was 0.22 A. The average arc speed was 0.38 m/s. From t = 1.1 s to t = 1.131 s, arc length reached about 67.5% of total arcing distance, and arc current 0.23 A. The average arc speed was 1.08 m/s. From t = 1.131 s to t = 1.140 s, arc length increased to about 72.5% of total arcing distance and the arc current increased to 0.28 A. The average arc speed was 1.667 m/s. At the moment just before flashover (t = 1.159 s), arc length reached about 85% of total arcing distance, arc current was 0.35 A. Arc speed during t = 1.158 s to t = 1.159 s was 1.974 m/s. The flashover finished during t = 1.159 s and t = 1.160 s, arc speed was higher than 45 m/s. The increases of the percentage of the positive arc length (x) to the total arcing distance (L) as a function of time are shown in Figure 4.5. Figure 4.6 shows the speeds of arc as a function of time period of this example. Figure 4.7 shows the voltage and current waveforms of this example.

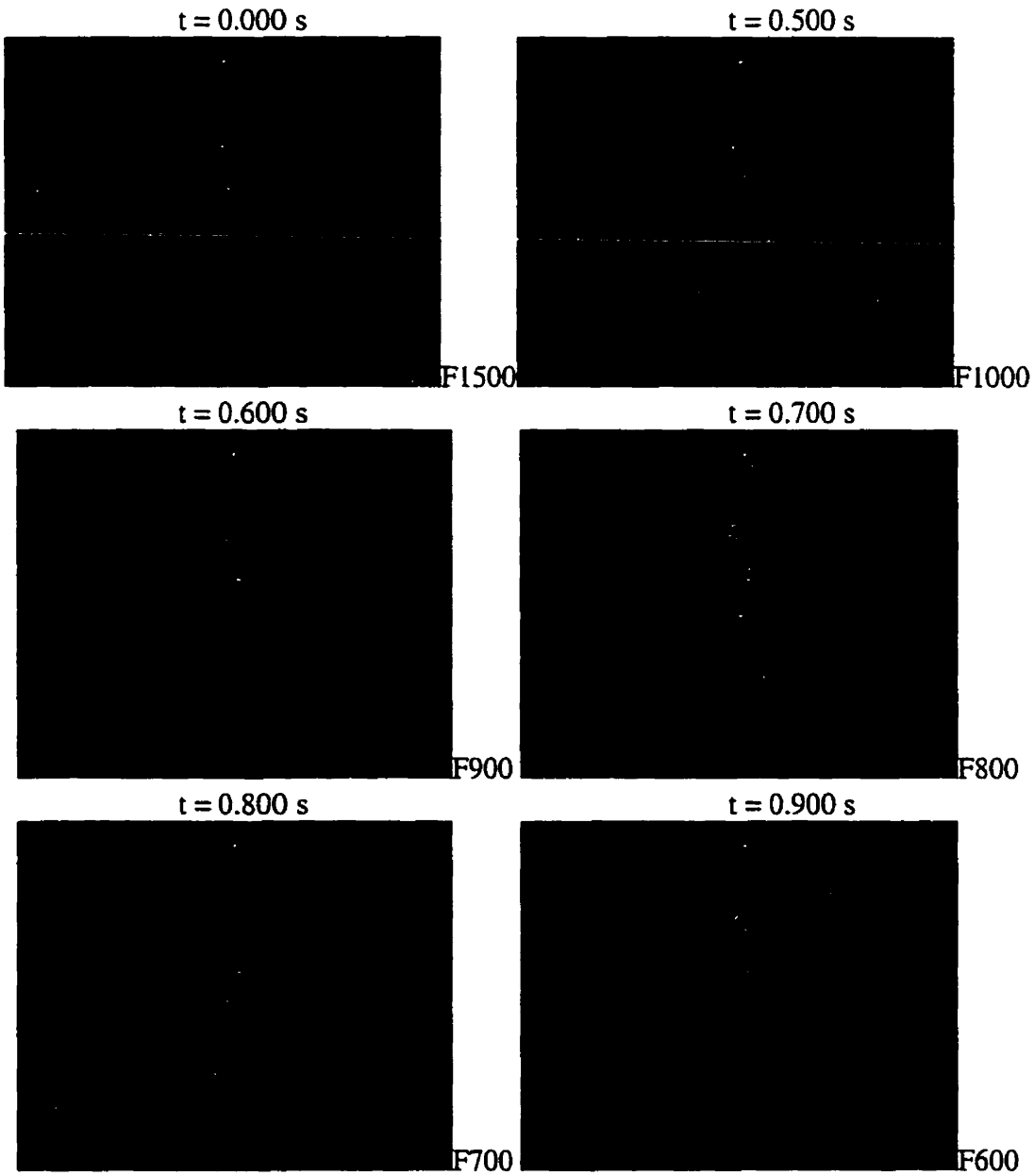

Figure 4.4 Positive arc development on ice surface

High speed camera: 1000 picture/second

negative dc voltage = 36 kV, freezing water conductivity = 80 μS/cm

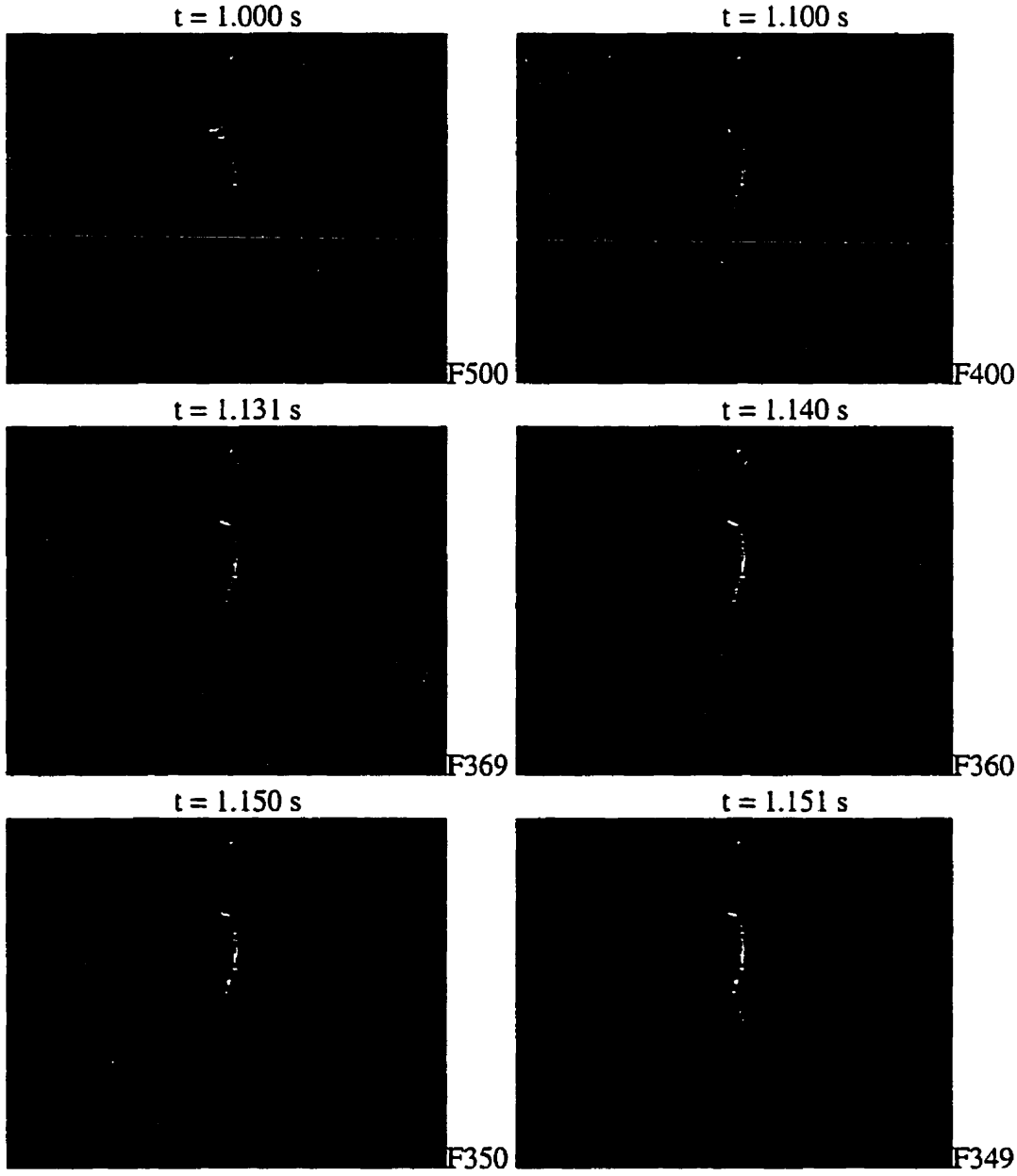

Figure 4.4 Positive arc development on ice surface (cont'd)

High speed camera: 1000 picture/second

negative dc voltage = 36 kV, freezing water conductivity = 80 μS/cm

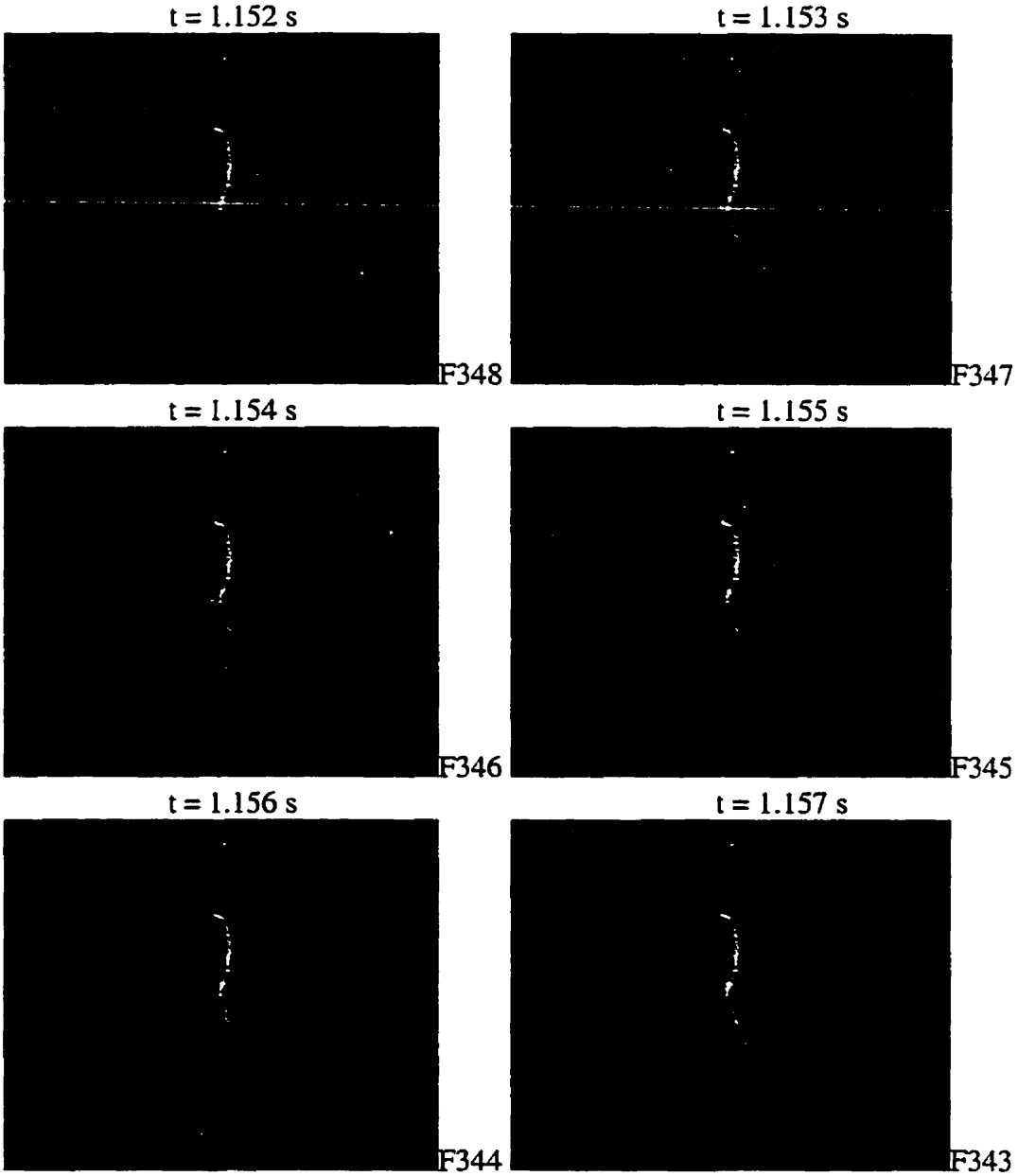

Figure 4.4 Positive arc development on ice surface (cont'd)

High speed camera: 1000 picture/second

negative dc voltage = 36 kV, freezing water conductivity = 80 μS/cm

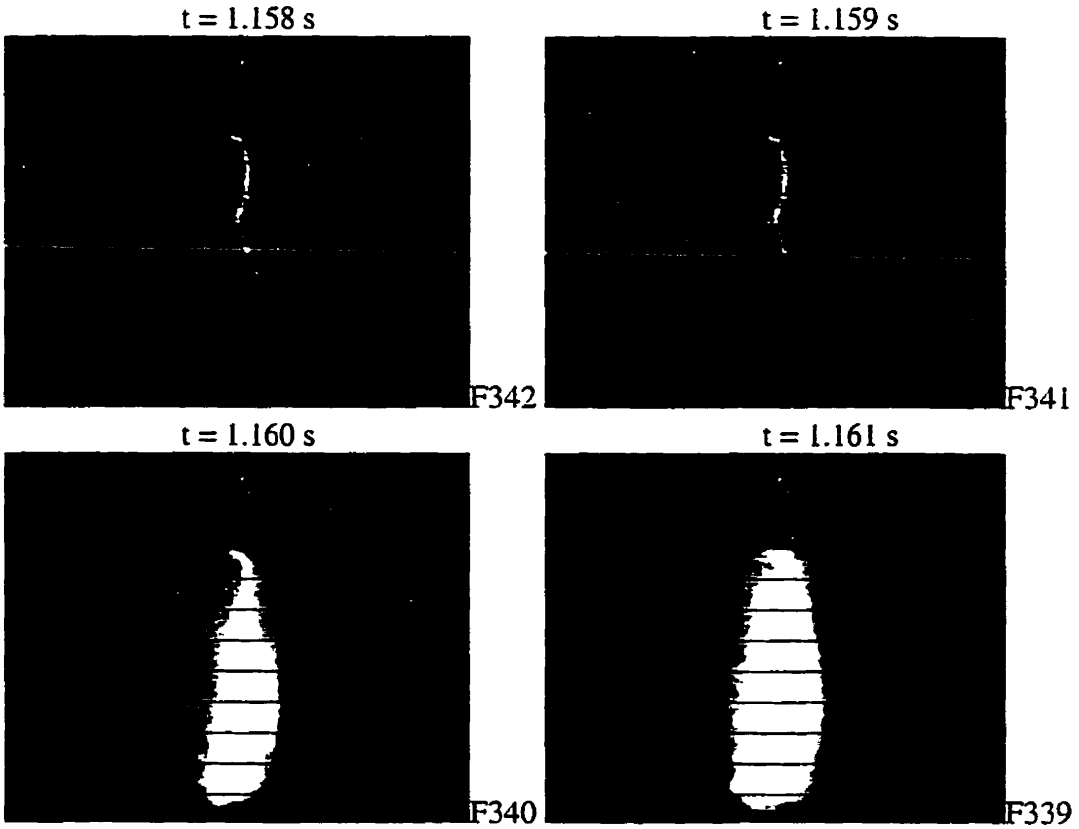

Figure 4.4 Positive arc development on ice surface (cont'd)

High speed camera: 1000 picture/second

negative dc voltage = 36 kV, freezing water conductivity = 80 μS/cm

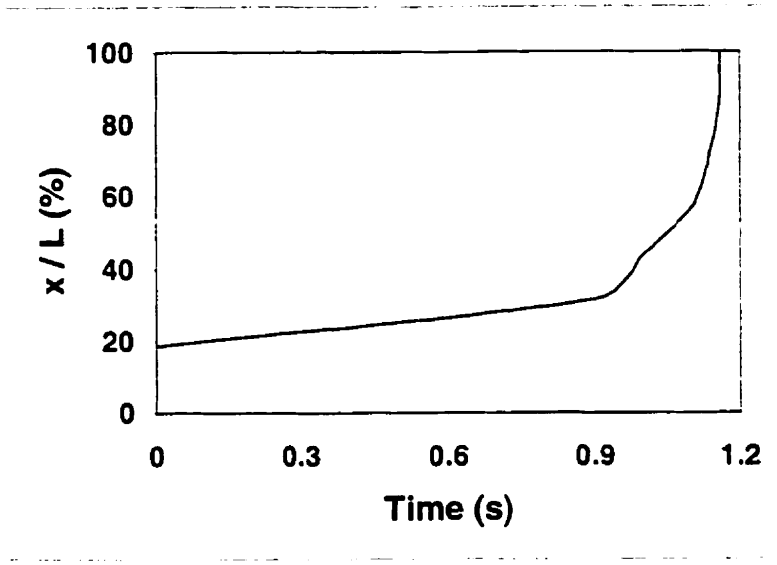

Figure 4.5 Propagation of positive arc on ice surface

σ = 80 μS/cm and V = - 36 kV

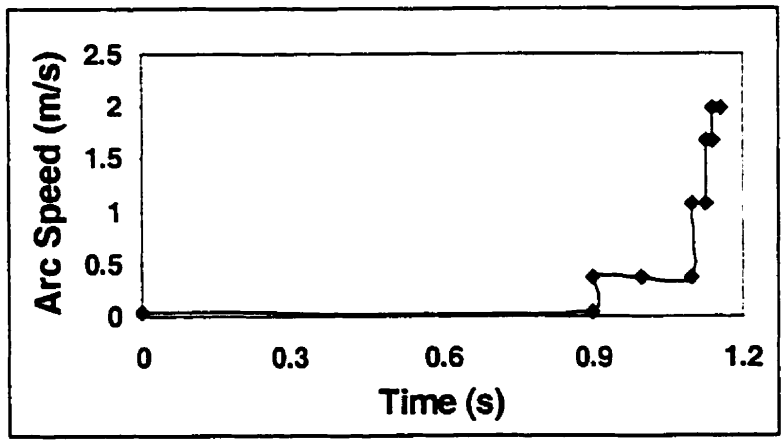

Figure 4.6 Speed of positive arc on ice surface

σ = 80 μS/cm and V = - 36 kV

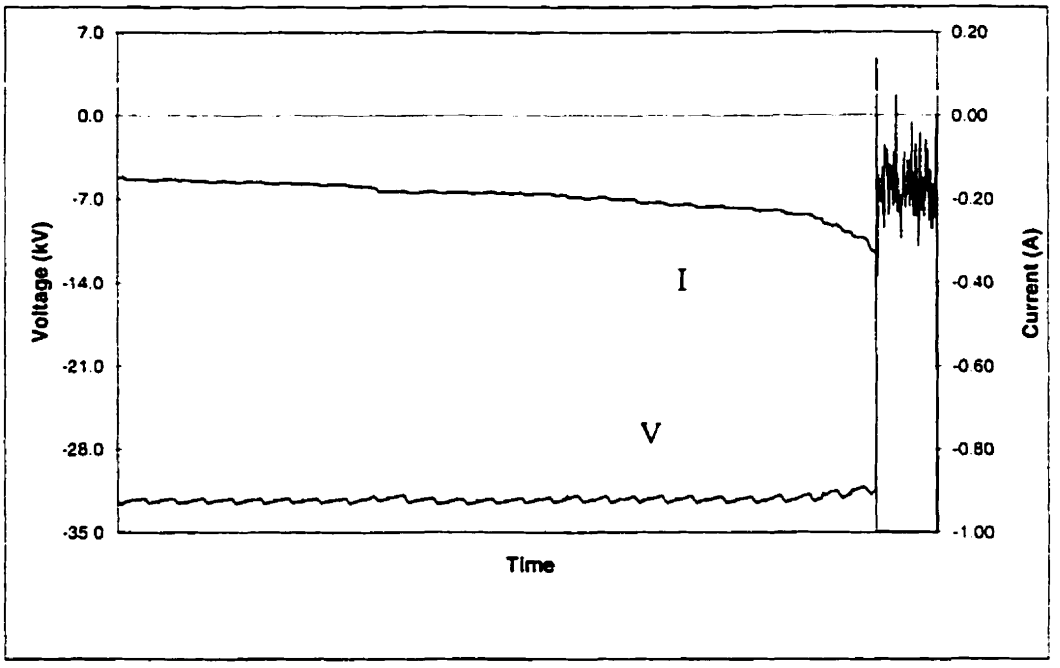

Figure 4.7 Typical negative flashover voltage and current (σ = 80 μS/cm)

From a large number of high speed camera pictures and experimental records, it is found that before the arc length reached 40% to 55% of total arcing length, the arc develops slowly and its average speed is from a few centimeters per second to about 0.1 m/s. Then, the arc develops more and more rapidly. When arc length reaches 73% to 90% of total arcing distance, flashover takes place very quickly. The average arc speed during the last two frames, just before flashover, can reach a value of about 3.1 m/s.

When arc length reaches 73% to 90% of total arcing distance, this arc leads to flashover and there is no arc distinguish observed thereafter. The value of this arc length decreases with an increase in freezing water conductivity. For conductivities ranging from 40 μS/cm to 160 μS/cm and ice samples of 0.3 m in length, this arc length is in the range of 70% to 90% of total arcing distance, and is defined as critical arc length (x_c).

The arc current corresponding to critical arc length is defined as critical current (I_c). It is found that the critical current increases slowly with an increase in freezing water conductivity. For conductivities ranging from 40 μS/cm to 160 μS/cm, the critical currents are in the range of 0.16 A to 0.28 A for the positive arcs.

The final flashover finished during two frames of the high speed camera. During the two frames the average arc speed is higher than 112 m/s.

4.3.2 Negative arc development

Negative arc development was studied in a similar way as that for positive arc. Figure 4.8 shows an example of high speed shots for negative arc development. In this example, a positive dc voltage of 36 kV was applied to an ice sample having a freezing water conductivity of σ = 80 μS/cm. The negative arc development during the period of 0.222 s just before the flashover was recorded. At t = 0 s, the arc reached a length of about 22.7% of total arcing distance, and a current of about 0.17 A. Then the arc developed slowly and became a little brighter. During t = 0 s and t = 0.100 s, arc length was about 36.3% of total arcing distance, and arc current was about 0.2 A. The average arc speed during this period was 0.41 m/s. From t = 0.100 s to t = 0.160 s, the arc developed to 45.3% of total arcing distance, and arc current was 0.24 A. The average arc speed was 0.45 m/s. From t = 0.160 s to t = 0.170 s, arc length increased to 51.7% of total arcing distance. Arc current rose to 0.25 A. The average arc speed was 1.9 m/s. During t = 0.170 s to t = 0.180 s, arc length reached 57.5% of total arcing distance, and arc current 0.26 A. The average arc speed was 1.8 m/s. From t = 0.180 s to t = 0.190 s, arc length increased to 63.7% of total arcing distance and arc current to 0.27 A. The

average arc speed was 1.8 m/s. From t = 0.190 s to t = 0.200 s, arc length kept unchanged and arc current decreased to 0.26 A. From t = 0.200 s to t = 0.210 s, arc length increased to 72.7% and arc current to 0.275 A. The average arc speed was 2.7 m/s. From t = 0.210 s to 0.215 s, the arc reached 77.3% of total arcing distance, and arc current increased to 0.28 A. The average arc speed was 2.8 m/s. During t = 0.215 s to t = 0.22 s, arc length was about 82% of total arcing distance, and arc current was 0.285 A. The average arc speed was 2.8 m/s. At the moment just before flashover (t = 0.222 s), arc length reached 85% of total arcing distance, and arc current increased to 0.31 A. The average arc speed was 4.5 m/s during t = 0.22 s to t = 0.222 s. The flashover finished during t = 0.222 s and t = 0.223 s. During this period, the average arc speed was higher than 45 m/s. The increases of the percentages of the arc length (x) to the total arcing distance (L) as a function of time are shown in Figure 4.9. Figure 4.10 shows the speed of arc as a function of time of this example. Figure 4.11 shows the voltage and current waveforms of this example.

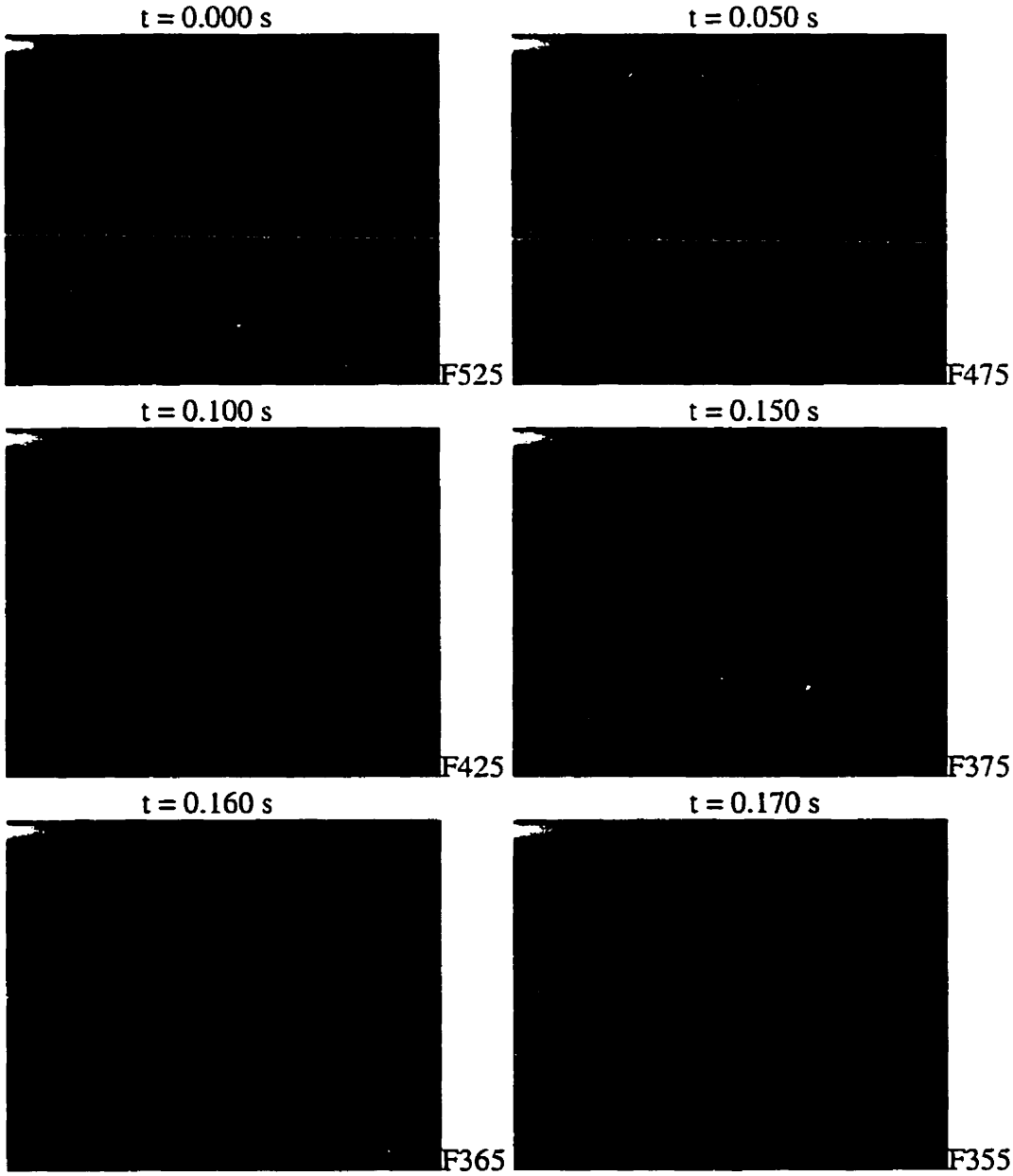

Figure 4.8 Negative arc development on ice surface

High speed camera: 1000 picture/second

positive dc voltage = 36 kV, freezing water conductivity = 80 μS/cm

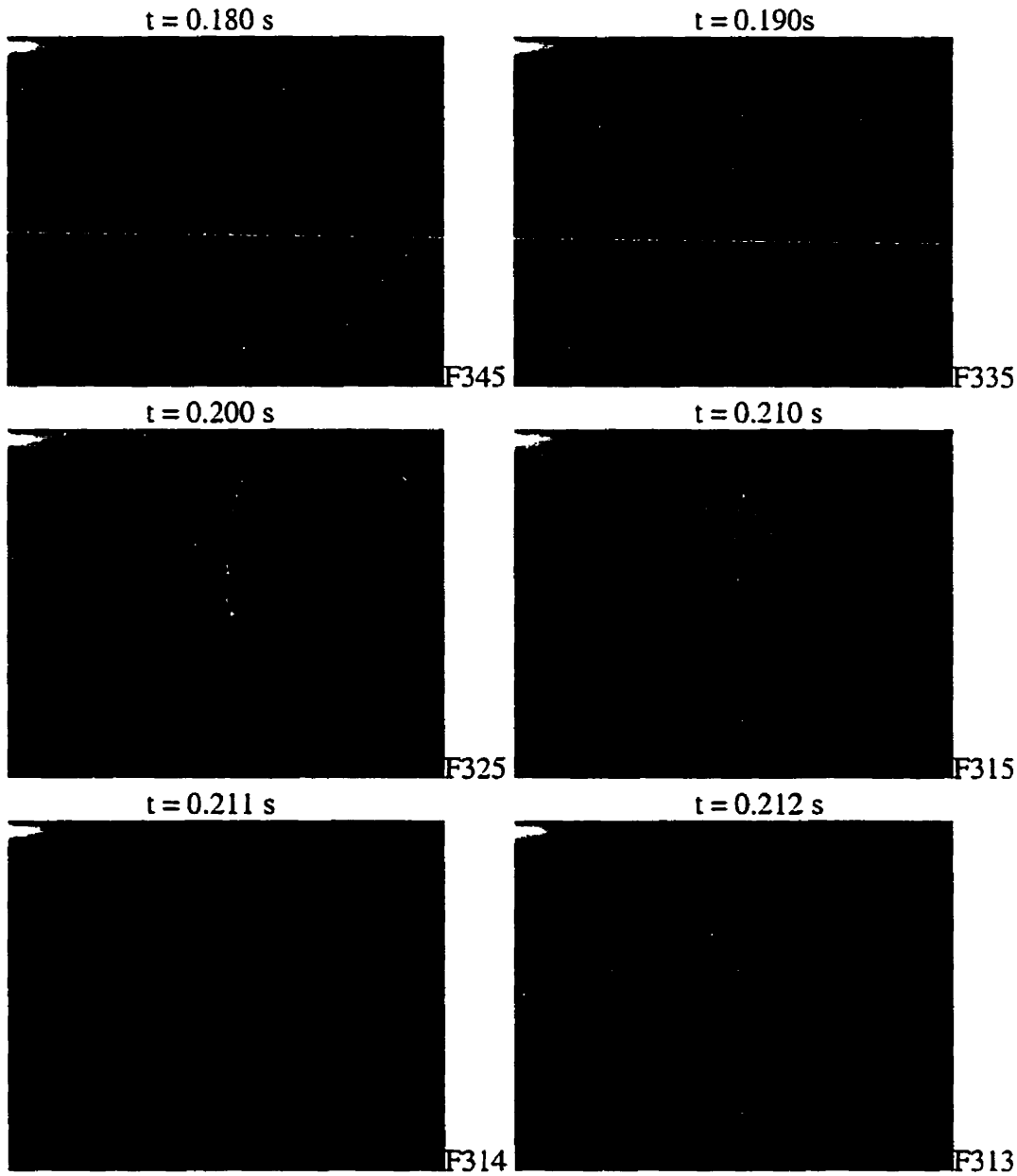

Figure 4.8 Negative arc development on ice surface

High speed camera: 1000 picture/second

positive dc voltage = 36 kV, freezing water conductivity = 80 μS/cm (cont'd)

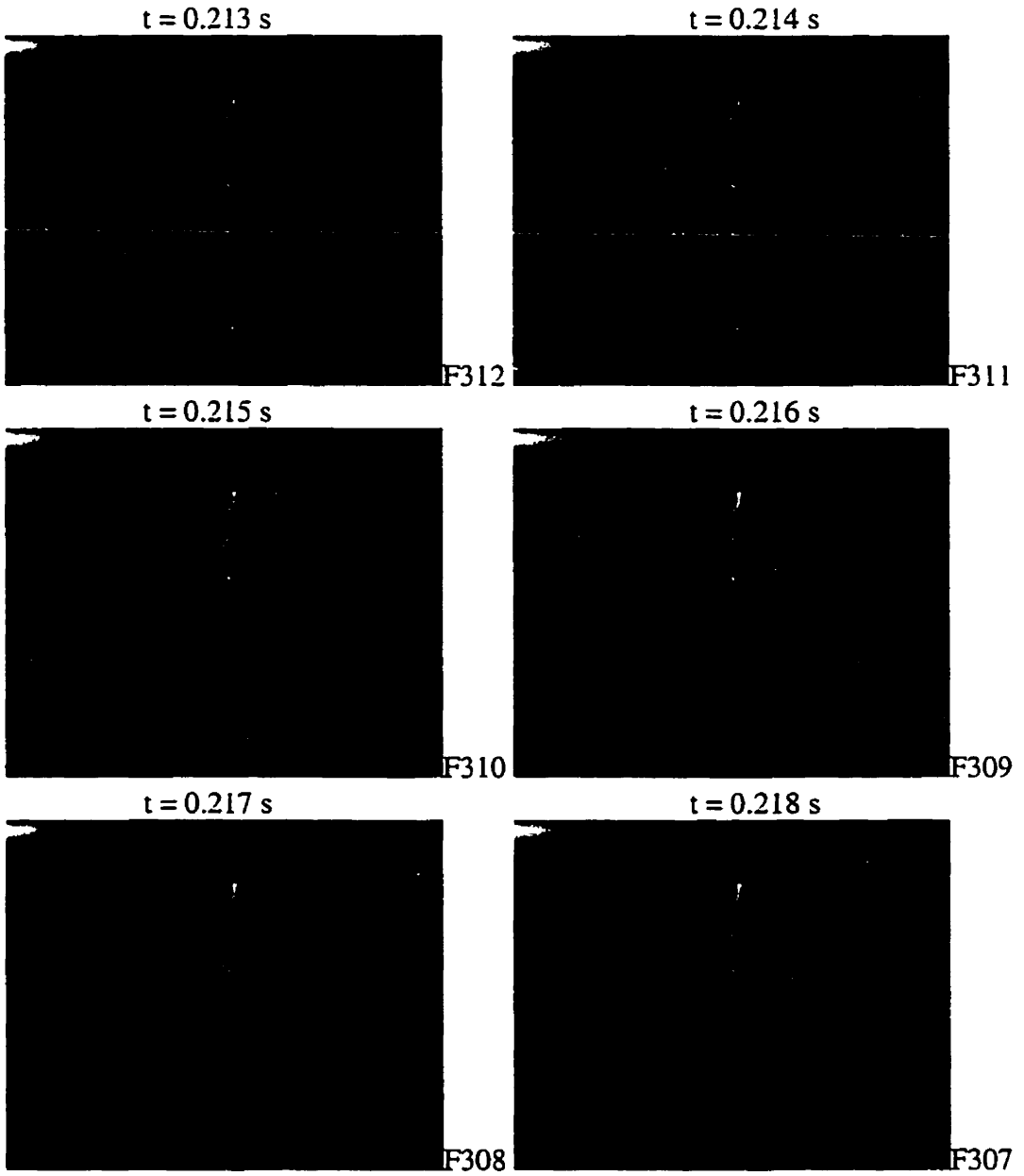

Figure 4.8 Negative arc development on ice surface (cont'd)

High speed camera: 1000 picture/second

positive dc voltage = 36 kV, freezing water conductivity = 80 μS/cm

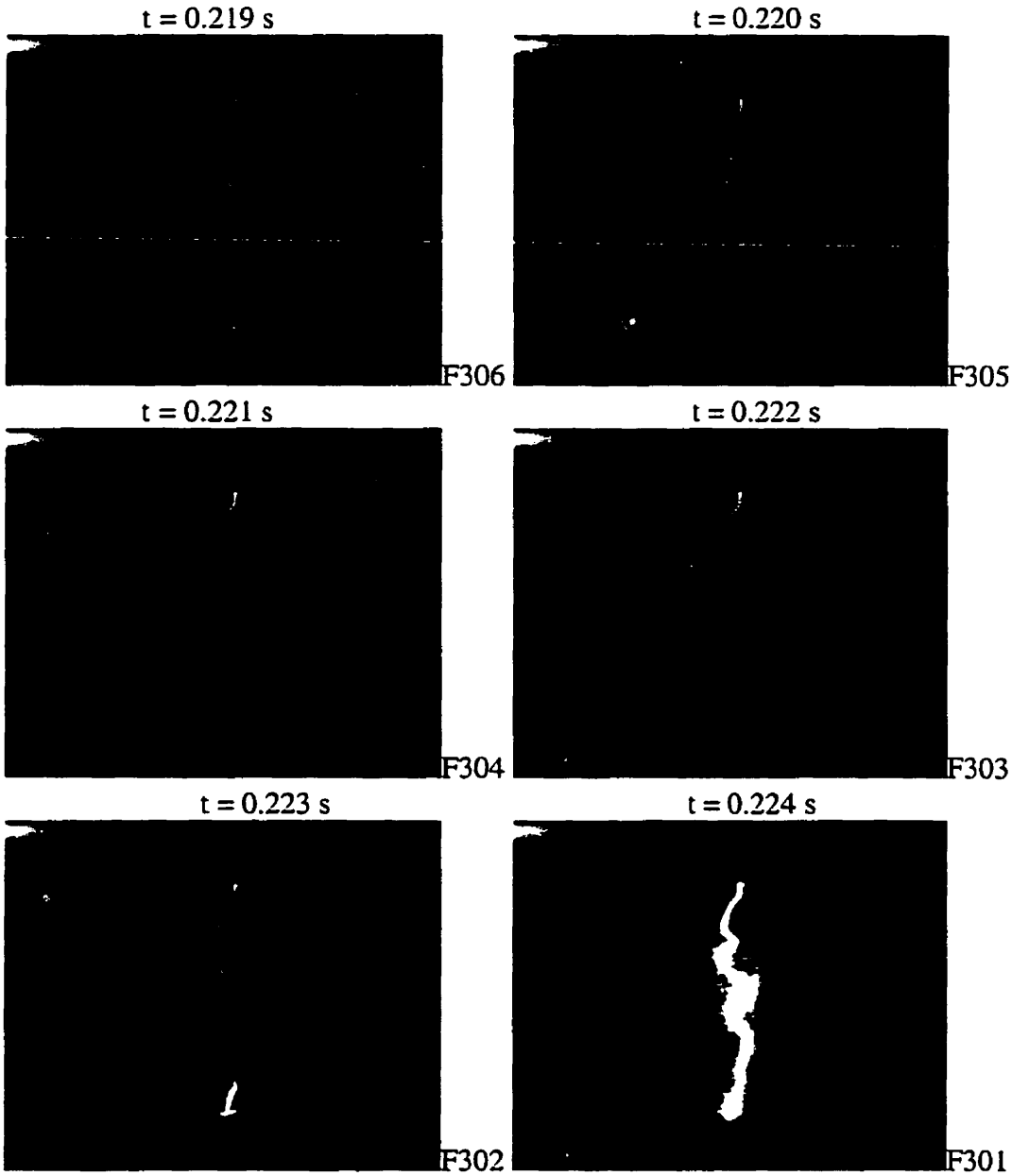

Figure 4.8 Negative arc development on ice surface (cont'd)

High speed camera: 1000 picture/second

positive dc voltage = 36 kV, freezing water conductivity = 80 μS/cm

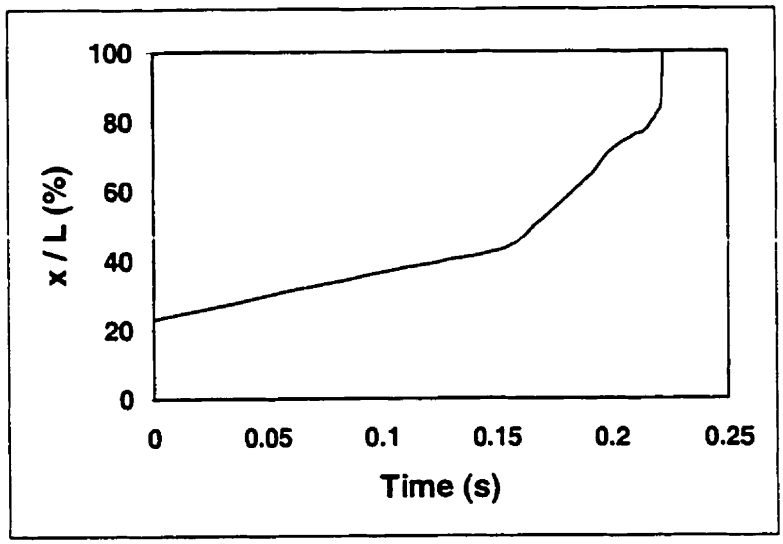

Figure 4.9 Propagation of negative arc on ice surfaces

σ = 80 μS/cm and V = 36 kV

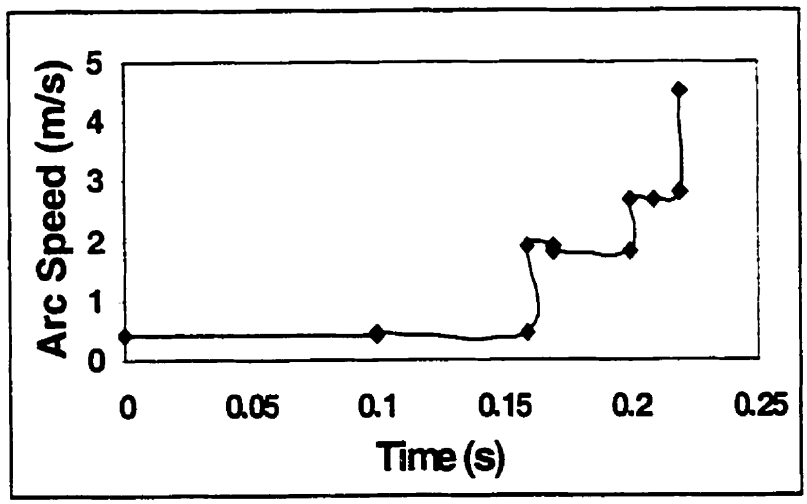

Figure 4.10 Speed of negative arc on ice surfaces

σ = 80 μS/cm and V = 36 kV

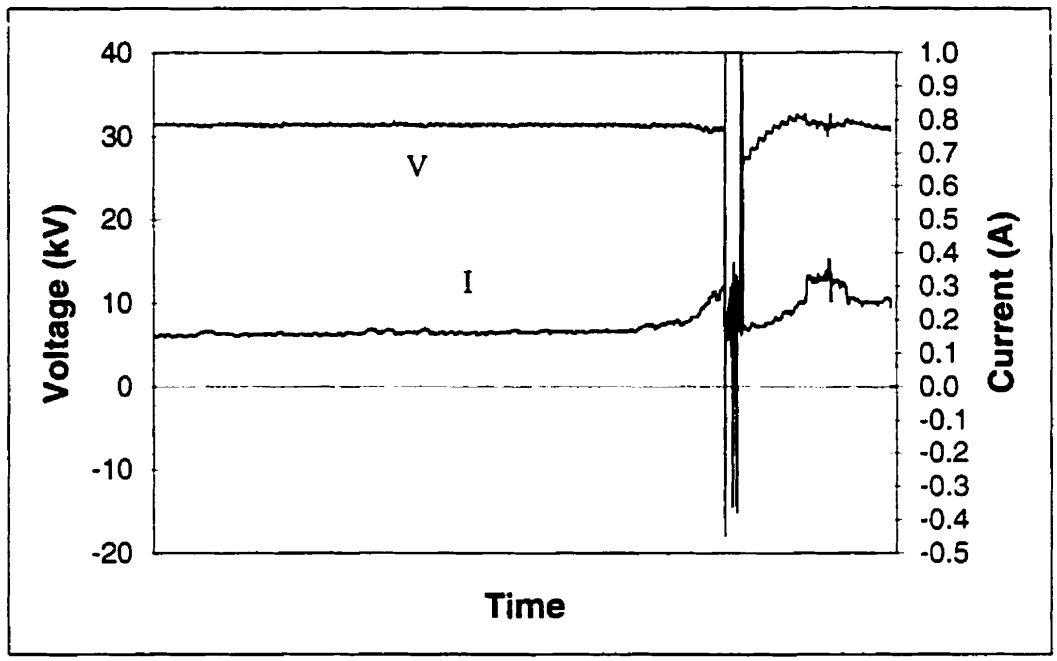

Figure 4.11 Typical positive flashover voltage and current (σ = 80 μS/cm)

Similar to the positive arc, the critical arc length of negative arc decreases with an increase in freezing water conductivity. For conductivities ranging from 40 μS/cm to 160 μS/cm, the critical arc length is in the range of 73% to 90% of total arcing distance, 30 cm in the present tests, as observed for positive arcs.

As well, similar to positive arc, the critical current of negative arc increases slowly with an increase in freezing water conductivity. For conductivities ranging from 40 μS/cm to 160 μS/cm, the critical currents are in the range of 0.18 A to 0.29 A for negative arcs, a little higher than those measured for positive arcs.

For negative arcs, before arc length reached 40% to 55% of total arcing length, the arc develops slowly and its average speed is from a few centimeters per second to about 0.5 m/s. Then, the arc develops more rapidly. Its speed can reach a value of about 4.5 m/s just before flashover occurs.

The final flashover finished during two frames of the high speed camera. During the two frames the average arc speed is higher than 135 m/s.

From a large number of high speed camera observations, similar propagation phenomena for positive and negative arcs were obtained. It was found that a negative arc developed a little more rapidly than a positive arc.

4.4 Alternative arc development

AC arc propagation was studied using a method similar to that for the dc arc.

Figure 4.10 presents a typical example of the high speed pictures of flashover on an ice sample of σ = 80 μS/cm and under an ac voltage of 36 kV_{rms}. AC arc length is found to change cyclically with the arc current. When the arc current changes from positive peak value to negative, arc length changes from maximum length to minimum and then recovers to its maximum. The maximum arc length in a cycle is expressed as x_M hereafter. Because the arc reignited and reached its new maximum length in just a quarter cycle, the instant velocity of arc is much higher than that of dc arc. In this particular example and during the one ms just before flashover, the average arc speed is 60 m/s. From a large number of test results, the maximum value of arc speed can reach 100 m/s.

AC arcs can develop only when x_M is larger than that of the former cycle. The difference between these two maximum values is the arc development length in the corresponding cycle. Figure 4.13 shows the maximum arc length, x_M, as a

function of time of this example. Figure 4.14 shows the x_M, propagation speed as a function of time of this example. Before the arc reaches 50% of the arcing distance, the x_M propagation speeds are in the range of 0.03 to 0.94 m/s. After this point, the arc develops quickly. The x_M propagation speeds can reach up to 2.5 m/s. The final flashover finished during two frames of the high speed camera. Its speed is higher than 300 m/s. Figure 4.15 shows the voltage and current waveforms of this example.

From a large number of high speed camera observations, like those of dc arc, ac arc development can also be divided into three periods; arc starting, arc development, and final flashover periods. During the arc starting period, several arcs may exist at the same time around the ice surface, and the lengths of arc can reach about 15% to 20% of total arcing distance. After this arc starting period, only one arc can exist and this arc becomes white. If the applied voltage is high enough, it can propagate slowly. The maximum arc length (x_M) propagation speed is about 0.03 to 1 m/s. When x_M reaches the critical arc length x_c , propagation speed increases suddenly to a value from 2.1 to 3 m/s. The final flashover finished during two shots of the high speed camera. During the two shorts, x_M propagation speed is higher than 300 m/s.

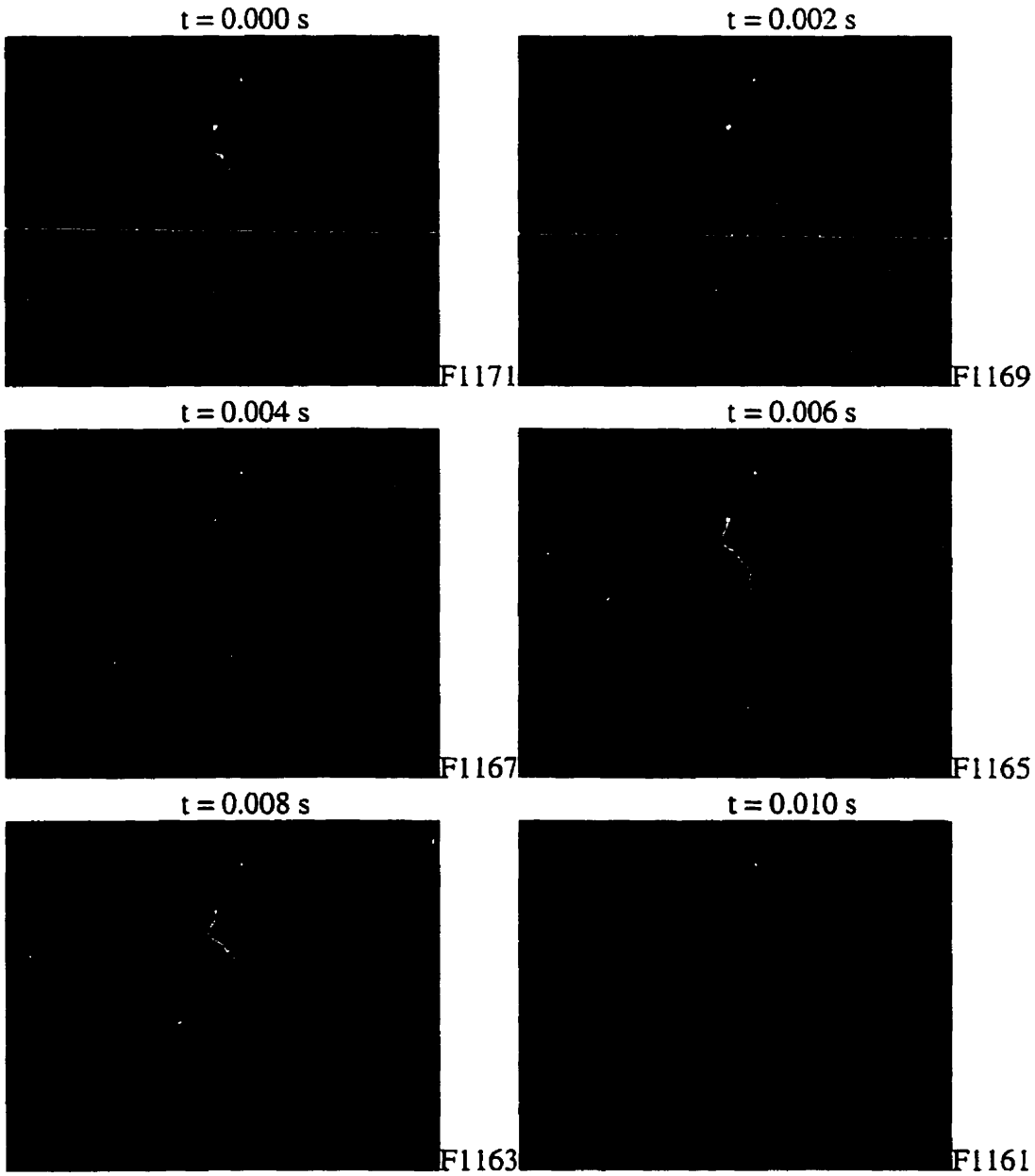

Figure 4.12 AC arc development on ice surface

High speed camera: 1000 picture/second

AC voltage = 36 kV_{rms}, freezing water conductivity = 80 μS/cm

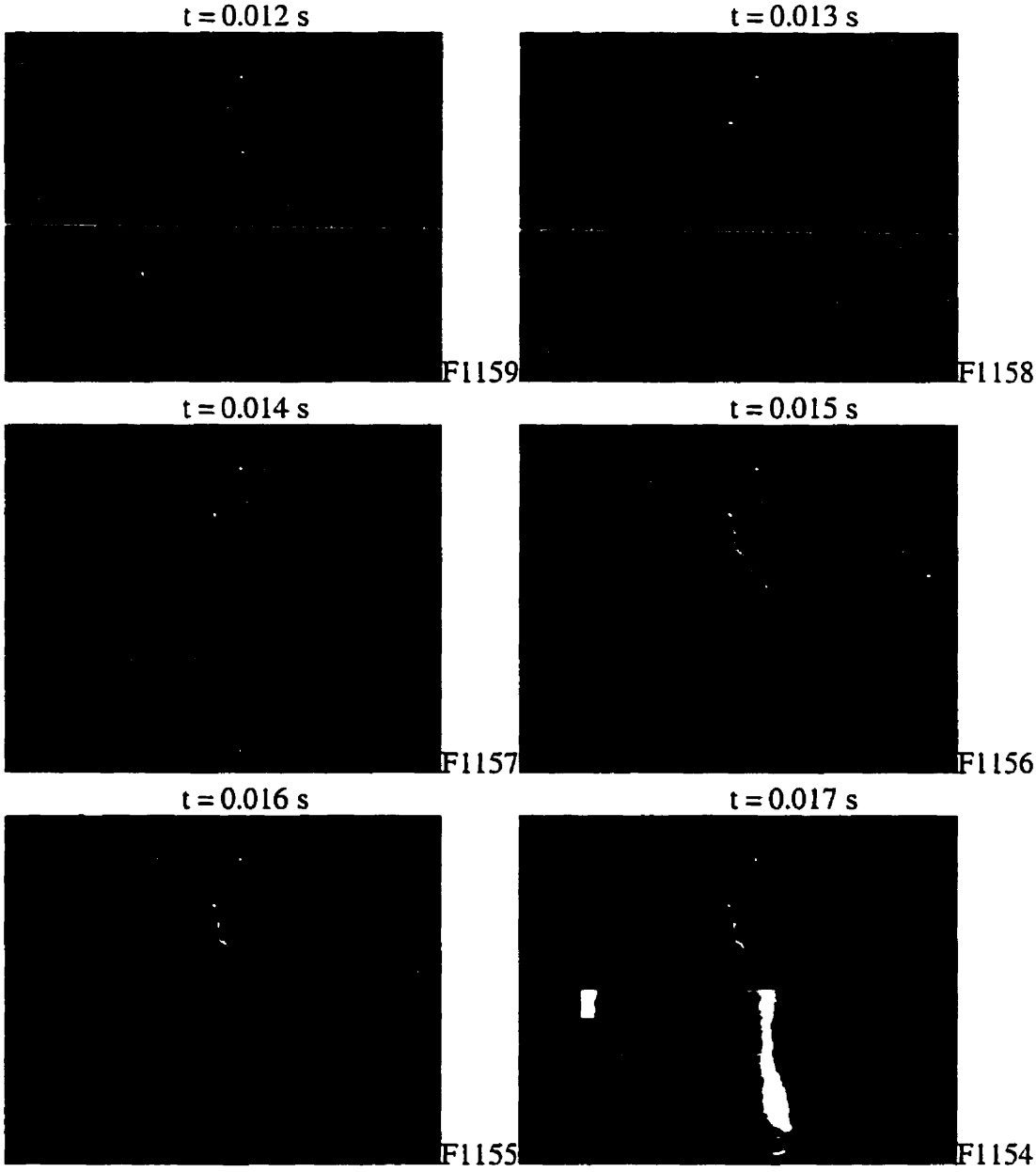

Figure 4.12 AC arc development on ice surface (cont'd)

High speed camera: 1000 picture/second

AC voltage = 36 kV_{rms}, freezing water conductivity = 80 μS/cm

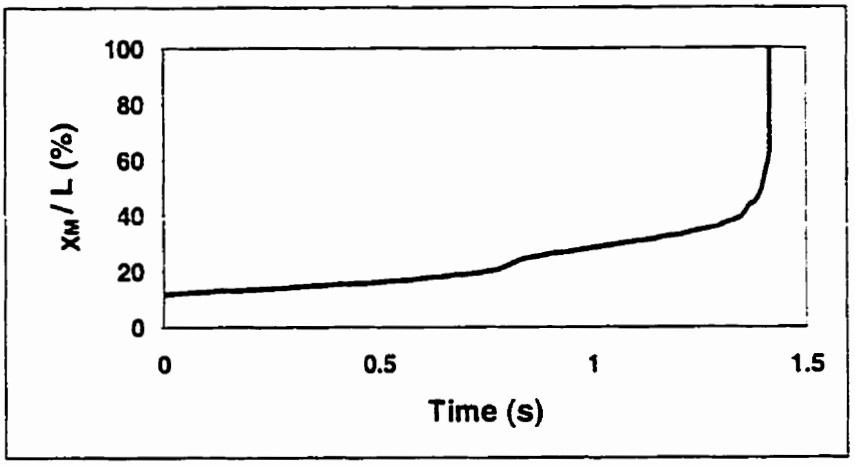

Figure 4.13 Propagation of ac arc on ice surface

σ = 80 μS/cm and V = 36 kV_{rms}

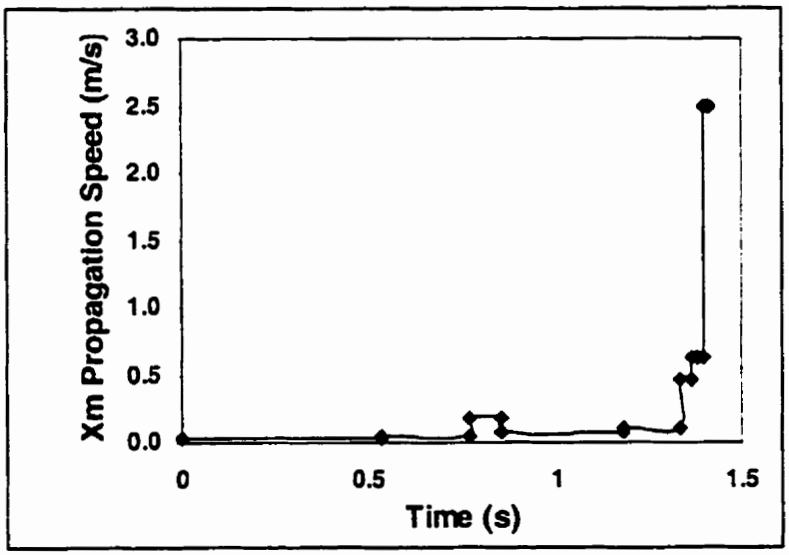

Figure 4.14 X_m Propagation speed of ac arc on ice surface

σ = 80 μS/cm and V = 36 kV_{rms}

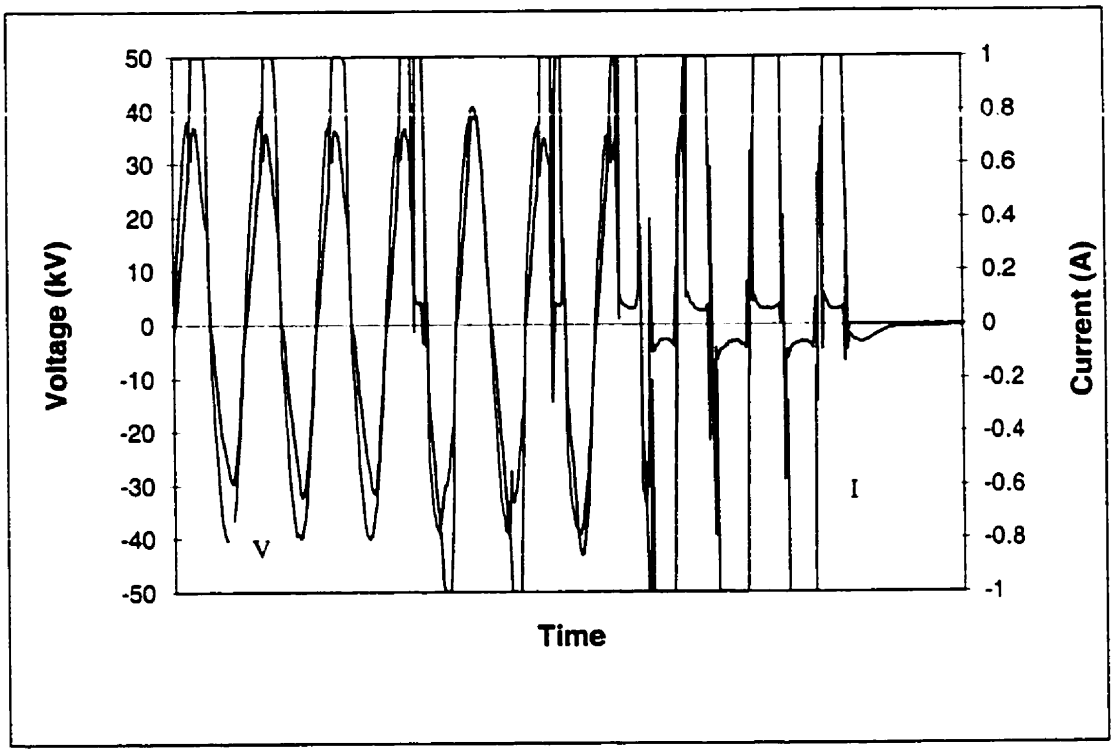

Figure 4.15 Typical ac flashover voltage and current (σ = 80 μS/cm)

In the arc starting period, arc current peak value (I_m) is found to have a value up to 0.3 A. During the arc development period, the critical arc current of ac flashover also increases with the freezing water conductivity. Its value was found to be much higher than that of dc arc. During the tests using an ice sample of 92 cm length, ac arc was sometimes found extinguished even when I_m was larger than 1 A. The critical values of I_m are in the range of 0.4 to 1 A when freezing water conductivity varies from 40 μS/cm to 160 μS/cm.

Under ac conditions the critical arc length decreases with an increase in freezing water conductivity. It is in the range of 50% to 85% of total arc distance for conductivities ranging from 40 μS/cm to 160 μS/cm.

4.5 Arc radius

Using the high speed camera, a large number of tests of arc development on ice surfaces were carried out. Figures 4.16, 4.17 and 4.18 show the relationships between arc radius, r_0, and arc current, I, for both ac and dc voltages. The arc radius can be expressed as:

$$Positive \quad arc \ : \ r_0 = \sqrt{\frac{I}{1.75\pi}} \qquad (4.1)$$

$$Negative \quad arc \ : \ r_0 = \sqrt{\frac{I}{1.67\pi}} \qquad (4.2)$$

$$AC\ arc:\ r_0 = \sqrt{\frac{I_m}{2.04\pi}} \qquad (4.3)$$

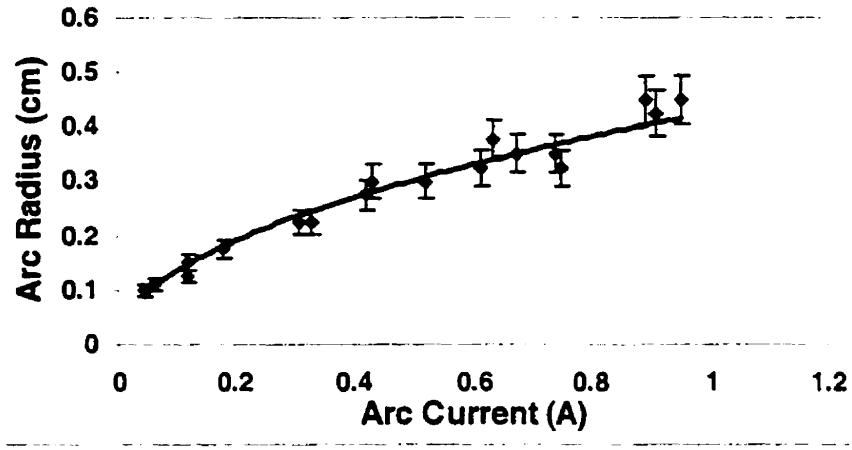

Figure 4.16 Positive arc radius as a function of arc current (10% error bars)

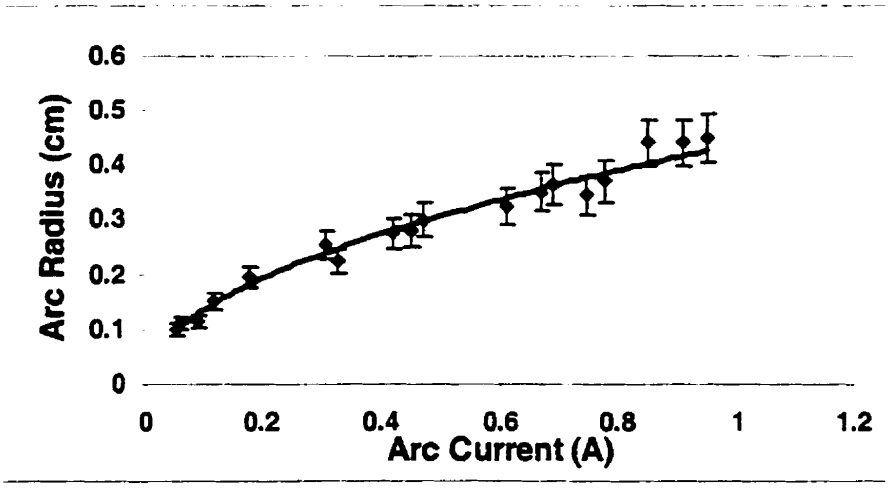

Figure 4.17 Negative arc radius as a function of arc current (10% error bars)

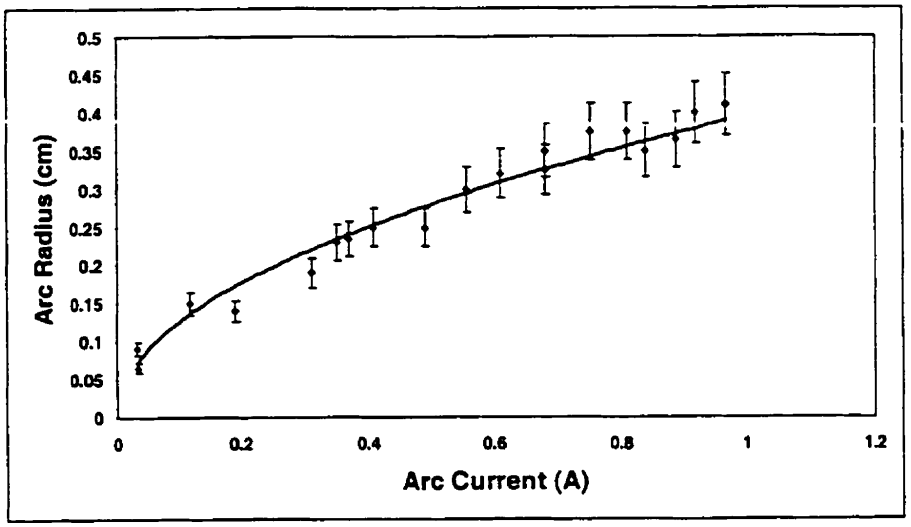

Figure 4.18 AC arc radius as a function of arc current I_m(10% error bars)

CHAPTER V

FACTORS INFLUENCING FLASHOVER ON ICE SURFACES

5.1 Introduction

As described in the literature review in Chapter III, from a relatively large number of studies already done on ice-covered insulators, ice surface flashover is a rather complicated phenomenon influenced by several factors (Farzaneh and Drapeau, 1995; Farzaneh and Kiernicki, 1997). These factors include the environmental conditions, ice type and uniformity, nature of voltage, arcing distance, etc.

To verify the effectiveness of the cylindrical ice samples for the simulation of ice covered insulator strings, a systematic study of the effects of principal factors, such as type of applied voltage, uniformity of ice, conductivity of ice, as well as the arcing distance on the maximum withstand voltage of wet–grown ice samples was undertaken in the present thesis.

The method used for the measurement of the maximum withstand voltage (V_{WS}) in this study is the same as that used in reference (Farzaneh and Drapeau, 1995) for the determination of maximum withstand voltage of ice-

covered insulators. This method was based on and developed from the method described in the standard IEC 507 which gives instructions for determining the maximum withstand voltage of contaminated insulators. V_{WS} was considered the maximum level of applied voltage at which flashover did not occur for a minimum of 3 tests out of 4, under similar icing conditions. For each withstand test, the ice sample was kept under test voltage for a period of 15 minutes.

Ice samples were formed as described in Section 4.2. The test set-up used for flashover tests is presented in Figure 4.2.

5.2 Influence of freezing water conductivity

The conductivity of freezing water was changed by adding sodium chloride to deionized water.

In the present study, freezing water conductivites are in the range of 20 to 160 μS/cm. Ice thickness was kept at 17 mm. The results of V_{WS} for ice samples as a function of freezing water conductivity are presented in Figure 5.1.

The results show that the values of maximum withstand voltage decrease with an increase in water conductivity. The variation of V_{WS} can be approximated by the power curves which follow the relation $V_{WS} = 64.2 \cdot \sigma^{-0.16}$ for wet–grown ice samples, where σ is expressed in μS/cm and V_{WS} in kV_{rms}.

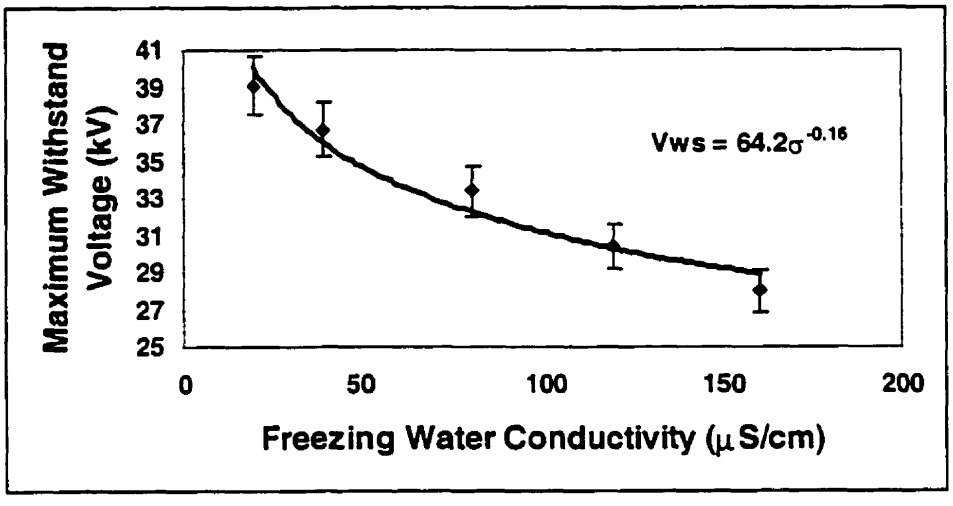

Figure 5.1 Maximum withstand voltage as a function of freezing water conductivity (4% error bars, 0.3 m ice sample)

This relationship obtained from ice samples is similar to that obtained from a short string of IEEE ice-covered insulators at the UQAC (Farzaneh and Drapeau, 1995). In the latter study, for an ice thickness of 20 mm and from 35 experimental points, the decrease in maximum withstand voltage gradient was expressed by a power curve which follows the relation $V_{WS}/m = 165.3 \cdot \sigma^{-0.18}$, where σ is expressed in μS/cm and V_{WS} in kV_{rms}.

5.3 Influence of voltage type

Flashovers under ac and dc voltages were carried out on wet-grown ice samples. Figure 5.2 presents the maximum withstand voltages in ac voltage, and positive and negative dc voltages for wet–grown ice samples. The results show that under negative dc voltage the ice sample has the lowest maximum withstand voltage. Under ac voltage the ice sample has the highest maximum withstand voltage. The V_{WS} in positive dc voltage is 6% to 9% higher than that of negative dc voltage. The V_{WS} in ac voltage is 16% to 21% higher than that of negative dc voltage.

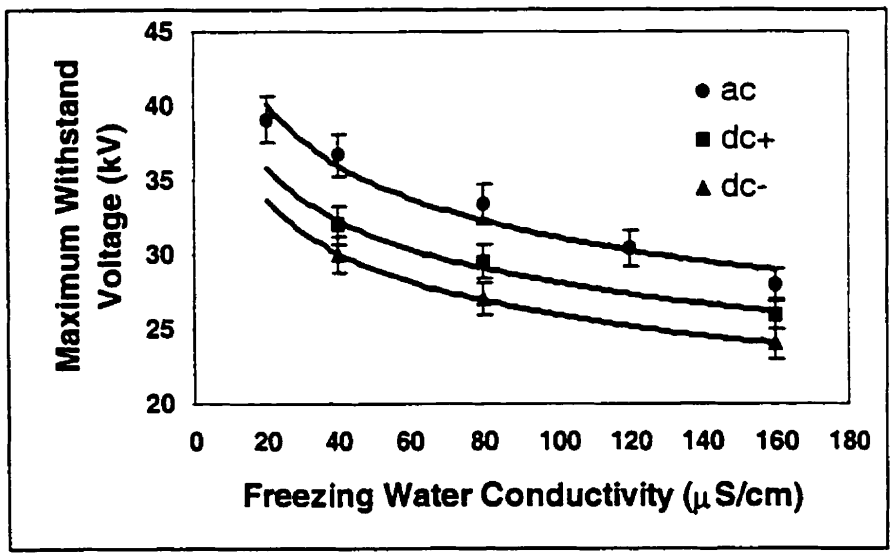

Figure 5.2 Maximum withstand voltage under ac and dc voltages (4% error bars, 0.3 m ice sample)

5.4 Influence of ice uniformity

One of the most obvious phenomena concerning ice surfaces covering energised insulators is the frequent presence of air gaps between the tips of the icicles and the HV terminal. These air gaps may be due to melting ice falling from the surface, caused either by partial arc, or by a rise in ambient temperature during or after ice accretion. In the case of suspension insulator strings, it was found that the icicles never bridged the space between the lowest insulator unit and the high voltage terminal. For a string of 3 glass insulator units, the minimum air gap between the tips of icicles hanging under the lowest insulator and the high voltage terminal was about 30 mm (Phan and Matsuo, 1983). For a post-type insulator, it was shown that such an air gap was formed at the top of the insulator near the HV terminal (Farzaneh and Drapeau, 1995). The physical aspects of wet-grown ice accretion under ac voltages on IEEE suspension and post-type insulators are presented in Figure 5.3.

Knowing that an air gap appears on the ice surface covering energised insulators, and that such an air gap is influenced by the environmental conditions, and the type and amount of ice, the study in the following paragraphs aims to determine the maximum withstand ac voltage of wet-grown ice surfaces as a function of air gap length and position (Chen, Farzaneh and Zhang, 1996).

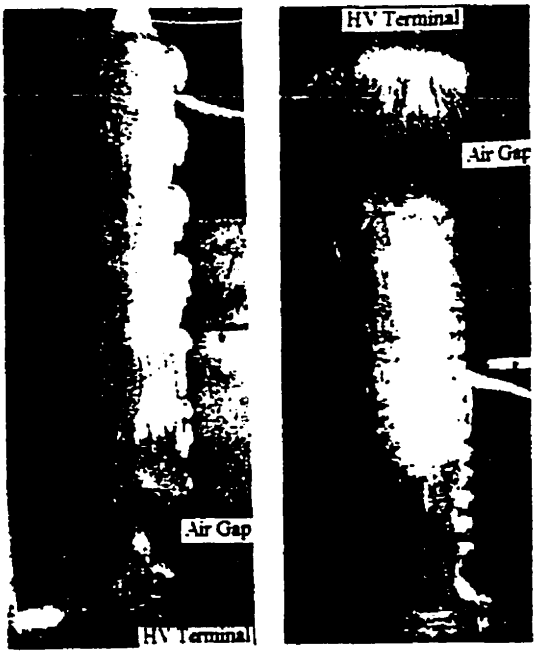

(a) IEEE (b) Post-type

Figure 5.3 Air gaps formed on IEEE suspension and post-type insulators covered with artificial ice

Once the wet-grown ice sample was formed, to a thickness of 17 mm, an air gap between 0 and 50 mm in length was made, near either the grounded or the high voltage electrodes, by removing a small section of ice, as shown in Figure 4.2. Freezing water conductivity was kept at 80 μS/cm (20°C) for each test. The maximum withstand voltages as a function of the air gap length at top end and bottom end of ice samples are shown in Figures 5.4 and 5.5 respectively.

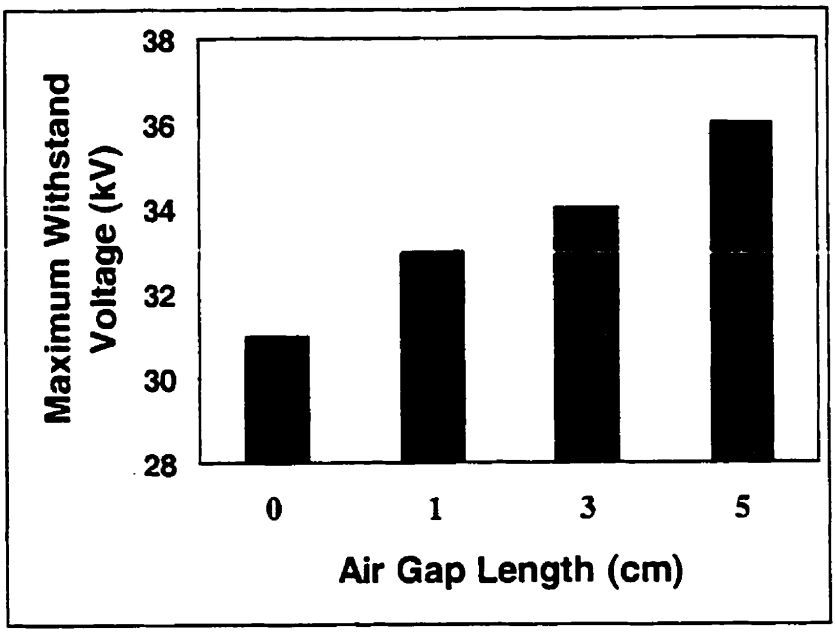

Figure 5.4 Maximum withstand voltage as a function of top end air gap length

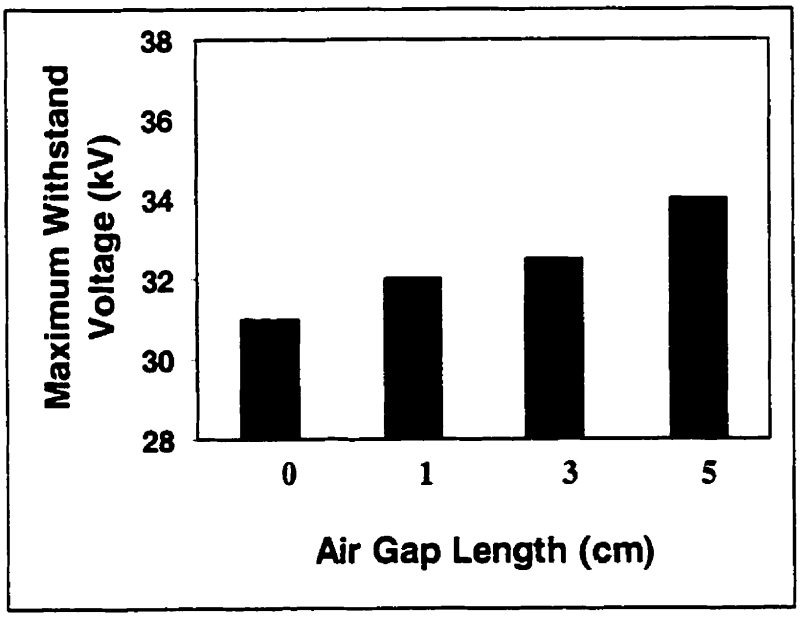

Figure 5.5 Maximum withstand voltage as a function of bottom end air gap length

It may be observed that the maximum withstand voltage increases with an increase in air gap length for both top and bottom end air gaps. It may also be noted that the influence of air gap length on V_{WS} is less pronounced for the bottom end air gaps compared with the top end. For example, with a 50 mm air gap at the bottom end of the ice sample, V_{WS} is only 9.6% higher than that without any air gap, while the difference is about 16% when the air gap is at the top end of the sample. This difference in the influence of air gap position on V_{ws} was caused by the water film formed by melting ice. In the ice sample having a bottom end air gap, the water film passed through the air gap, thus wetted the air gap. This wetted bottom end air gap means that the voltage drop across it is lower to the top end air gap where no water film passed. So the voltage was more uniformly distributed for the ice sample having air gap at the bottom end. That is the reason why bottom end air gaps have less influence than top end air gaps.

The influence of ice uniformity on maximum withstand voltage were studied using a short string of IEEE ice-covered insulators at the UQAC (Farzaneh and Kiernicki, 1997). It was found that the uniformity of ice built-up on insulators was closely related to wind velocity. For the same freezing water conductivity, the higher the wind velocity was, the larger the deviation angle of the icicles from the vertical axis, and the more non-uniform the ice. Another factor that was found to influence ice uniformity was freezing water conductivity (Farzaneh

and Drapeau, 1995). At a relatively high value of water conductivity (150 μS/cm), there was almost no ice deposited on the top sheds of the insulator (HV side). At a low conductivity of 4 μS/cm, ice distribution along the insulator was relatively uniform. The flashover tests showed that the more uniform the ice surface was, the lower the maximum withstand voltage. From the results obtained from insulator strings and ice samples, there is a coincidence for the influence of ice uniformity on maximum withstand voltage.

5.5 Influence of arcing distance

AC maximum withstand voltages were determined for wet-grown ice samples of arcing distance from 0.3 m to 0.92 m. From the results shown in Figure 5.6, it may be seen that V_{WS} increases linearly for the ice samples with the arcing distance of up to 0.92 m.

These results are in agreement with those obtained at the UQAC on short insulator strings (up to 6 units of porcelain IEEE standard insulators and 4 units of porcelain anti-fog insulators) (Farzaneh and Drapeau, 1995; Farzaneh and Kiernicki, 1997). The linear relationship between the maximum withstand voltage and the arcing distance seems to be only valid for short insulator strings. In fact, Su and Jia (1993) found that the withstand voltage gradient of insulator strings up to 5 meters in length decreased linearly with the length of

the insulator string. It may be noted that there is no certainty as to the conditions under which the tests were made.

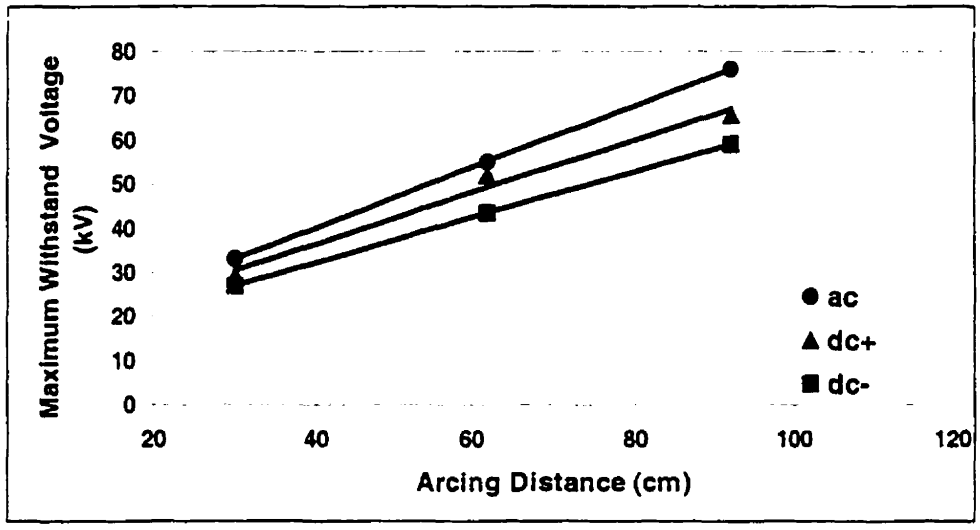

Figure 5.6 Maximum withstand voltage of ice samples as a function of arcing distance

CHAPTER VI

ICE SURFACE CONDUCTIVITY AND BULK CONDUCTIVITY

6.1 Introduction

Flashover along ice surfaces may be analyzed using the pollution discharge model, which involves the well-known Obenaus concept, as introduced in Chapter II. Under ac conditions and considering the voltage drop on the electrode, Equation 2.3 may be rewritten as:

$$V_m = AxI_m^{-n} + I_m R(x) + U_e \quad (6.1)$$

where V_m and I_m are the peak values of applied voltage and leakage current, respectively; A and n are the arc constants; x is the length of the arc; U_e is the voltage drop on the electrode; and R(x) is the residual resistance of the part of the ice layer which is not bridged by the arc. The determination of A, n, U_e, and R(x) is essential for the analysis of the discharge and arc development on the surface of ice.

In the present chapter, wet-grown ice surface conductivity is analyzed for the applications of positive dc voltage, negative dc voltage, and ac voltage.

6.2 Methods of ice surface conductivity measurements

The residual resistance R(x) is perhaps one of the most important parameters influencing flashover along ice surfaces. R(x) of the ice surface during the development of the flashover arc is influenced not only by the freezing water conductivity but also by many other factors, such as air temperature, partial arc occurring during flashover, water film formed during ice melting, etc. Therefore, in the present study, R(x) was measured specifically during the development of flashover arc instead of in a low voltage steady condition (Farzaneh, Chen and Zhang, 1996, Dec; Farzaneh, Chen and Zhang, 1996; Farzaneh, Zhang and Chen, 1997).

Once the ice sample was formed as described in Chapter IV, an air gap, one cm wide, was made near the grounding electrode by cutting out a small section of ice at the top of the sample, as shown in Figure 6.1. This air gap could simulate the air gap formed during ice accretion on actual insulators. A measuring electrode was installed at a given position on the ice sample. The sample was then placed vertically in the climate room which was adjusted to a constant temperature of 0°C. DC or ac voltage was applied and raised at a constant rate of about 3.9 kV/s. The applied voltage (V_1) and the voltages on the measuring electrode (V_2), as well as the leakage current (I) were recorded by the data acquisition system (DAS).

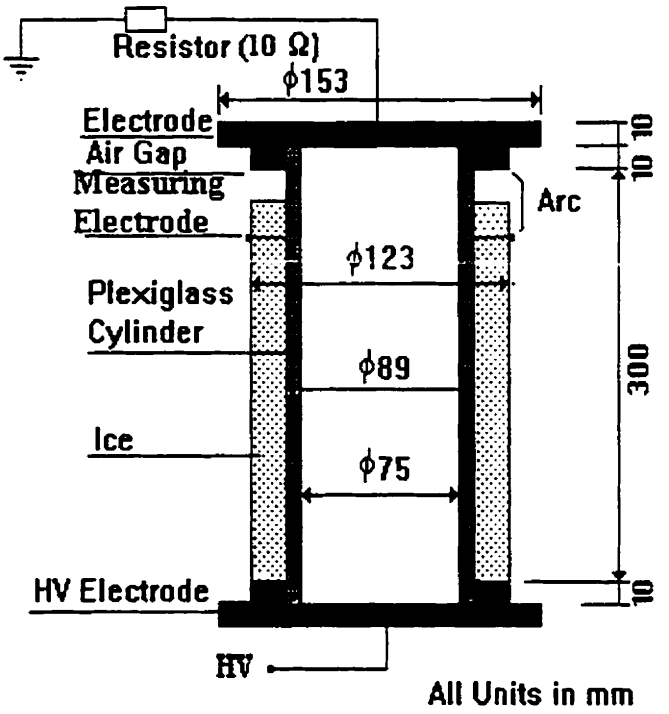

Figure 6.1 Flashover test and measuring electrode setup

The typical waveforms of V_1, V_2, and I are shown in Figure 6.2. When a partial arc reached the measuring electrode, V_2 dropped suddenly (point P) to a value equal to the voltage drop across the arc. At this specific moment, the voltage across the residual ice (the part of ice which was not bridged by the partial arc) can be obtained as follows, $V_{ice}=V_1-V_2$. Therefore, R(x) can be calculated as:

$$R(x)=\frac{V_{ice}}{I} \qquad (6.2)$$

Because the partial arc moves continuously and the position of the arc foot changes from time to time, it is difficult to distinguish the inner ice surface

current from that of the outer surface when a partial arc occurs. Therefore, an overall equivalent surface conductivity γ_e is introduced. γ_e is defined as the mean surface conductivity of the ice sample during the flashover process (Farzaneh, Chen and Zhang, 1996; Farzaneh, Zhang and Chen, 1997). For the cylindrical ice sample used in the present study, γ_e can be calculated thus:

$$\gamma_e = \frac{(L-x)}{\pi D_m R(x)} \qquad (6.3)$$

where L is the length of the ice sample, x is the arc length, and D_m is the mean diameter of the ice cylinder.

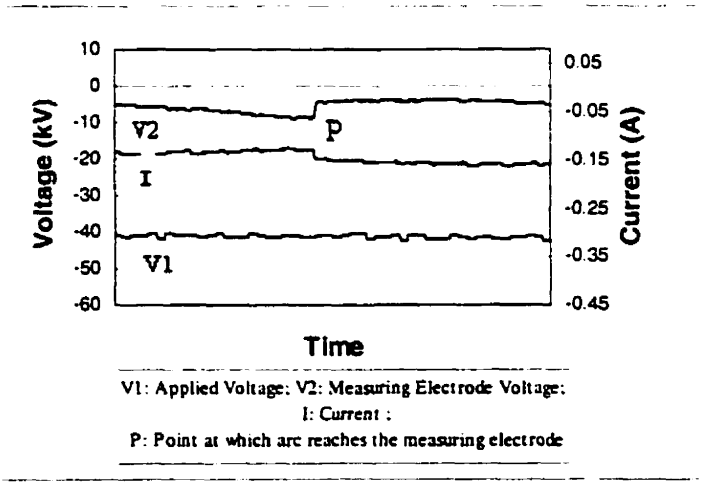

Figure 6.2 Typical waveforms

6.3 Methods of ice bulk conductivity measurements

It should be mentioned that the above measured arc current includes the ice surface currents as well as bulk ice current. To determine R(x) and γ_e as defined in Equations 6.2 and 6.3, only the ice surface currents should be used. Therefore, an estimation of the quantity of the ice bulk current is necessary in order to clarify its weight in the total arc current measured.

To estimate the current in the bulk-ice itself, the following experiments were carried out:

Using an ice sample placed between two circular copper plate electrodes, as shown in Figure 6.3, bulk-ice conductivity was measured at different air temperatures. This system was first installed in a cold chamber adjusted at −12°C, subsequently the temperature of the cold chamber was raised from −12°C to 0°C at a rate of increase of about 0.4°C/min, while the dc voltage applied to the electrodes was about 300 V.

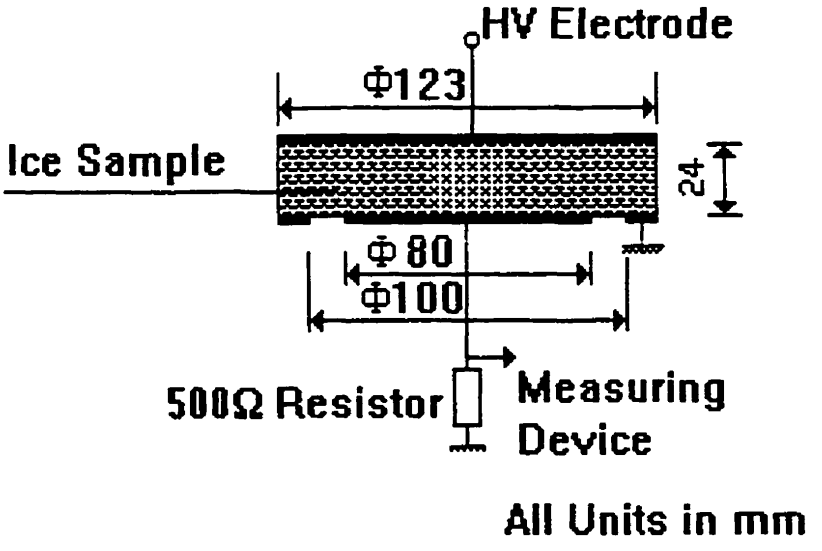

Figure 6.3 Bulk-Ice conductivity measurement circuit

The conductivity of bulk-ice was calculated from the current flowing through a 500 Ω resistor.

6.4 Ice surface and bulk temperature measurements

According to some observations and reports (Phan and Matsuo, 1983; Chisholm and Tam, 1989; Chisholm et al, 1996), flashover of ice-covered insulators usually occurs during the ice melting period. It is obvious that the presence of a water film on the ice surface is a major parameter contributing to a substantial decrease in leakage resistance, resulting in the flashover of insulators. As it was explained in references (Farzaneh and Kiernicki, 1997;

Farzaneh and Laforte, 1992), the water film on the ice surface may be caused by sunshine, a rise in air temperature, condensation, electrical discharge on the ice particles, or by leakage current at the ice surface. All these factors affect the ice temperature and melting. Thus, it is of fundamental importance to determine the variation of temperatures on the surface and bulk ice during the rise in air temperature.

The formation of a wet-grown ice sample used in the ice surface and bulk ice temperature measurements was similar to the method described in Chapter IV (Farzaneh, Chen and Zhang, 1996). Ice was formed with water having a conductivity of σ = 80 μs/cm, measured at 20°C. Three thermocouple sensors were installed at the beginning of icing, during the icing, and after the icing, respectively. In this way there are thermocouples at the interface of ice and the glass cylinder, in the middle of ice bulk, and at the outer surface of ice sample. The ice surface and bulk temperatures were measured using these thermocouples. All the temperature measurements were carried out without voltage applied to the ice samples. The air temperature of the cold chamber containing the ice sample was raised from -12°C to about 10°C at a mean rate of about 0.4°C/min. For a given air temperature, the temperatures at the three points on the ice sample were then recorded. The results are shown in Figure 6.4 (Farzaneh, Chen and Zhang, 1996).

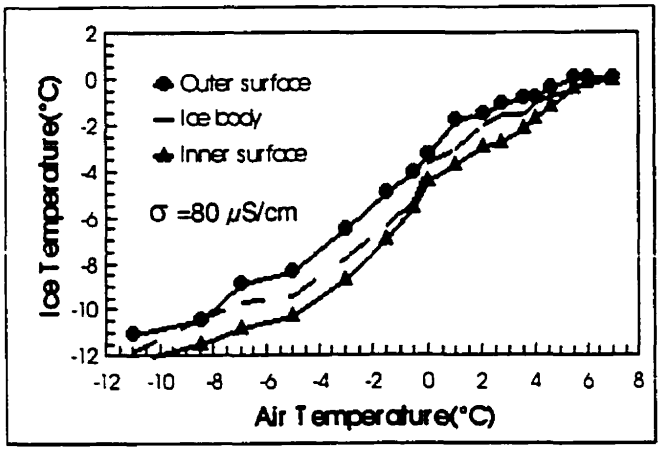

Figure 6.4 Temperatures in bulk-Ice and on outer and inner ice surfaces

It may be observed that ice temperatures increase as the air temperature rises from –12°C to 2°C. When the air temperature reaches 3°C, the temperatures of the bulk ice and inner surface approach 0°C and tend towards the saturation value of 0°C (Farzaneh, Chen and Zhang, 1996).

When the temperature at the ice surface reaches 0°C, ice starts to melt and, consequently, a water film at the surface of the ice is formed. The presence of this water film at the surface of the ice contributes to a rise in surface conductivity and leakage current, and results in flashover.

6.5 Results of ice surface conductivity measurements

A series of tests on different ice samples, made from water with various conductivities (σ). were carried out and the equivalent ice surface conductivity, γ_e, was then calculated. Figures 6.5, 6.6, and 6.7 present the results obtained for positive, negative, and ac voltage applications respectively. It may be observed that γ_e can be approximated by the following equations:

For positive voltage: $\gamma_e = 0.06 \cdot \sigma + 5.6$, (6.4)

For negative voltage: $\gamma_e = 0.06 \cdot \sigma + 5.8$, (6.5)

For ac voltage: $\gamma_e = 0.07 \cdot \sigma + 5.6$, (6.6)

γ_e being expressed in μS, and σ in μS/cm (at 20°C). It seems that there is no obvious difference for γ_e between dc and ac voltages.

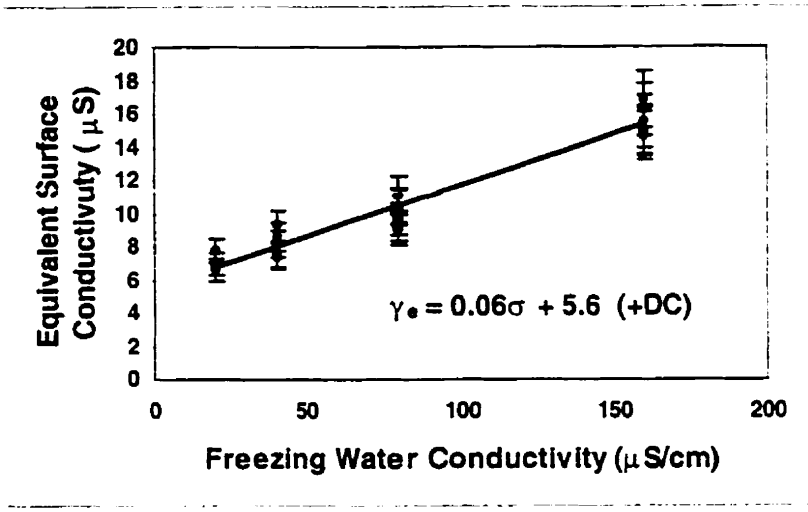

Figure 6.5 Relationship between equivalent ice surface conductivity and freezing water conductivity under positive voltage (10% error bars)

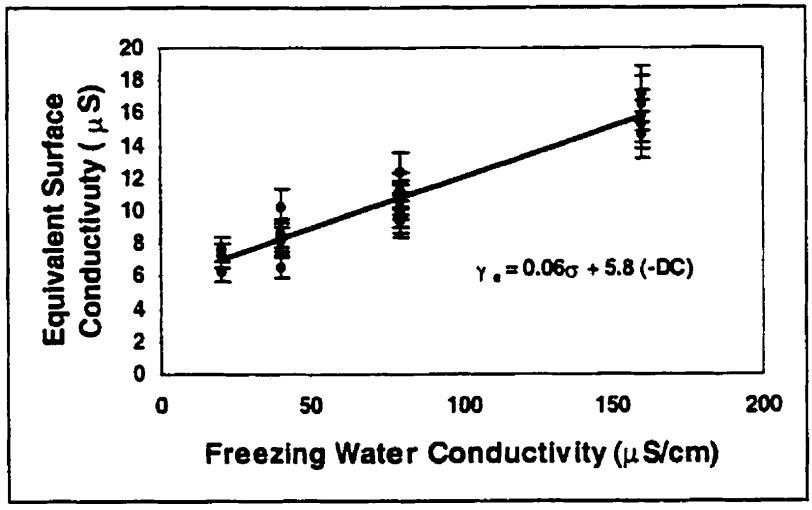

Figure 6.6 Relationship between equivalent ice surface conductivity and freezing water conductivity under negative voltage (10% error bars)

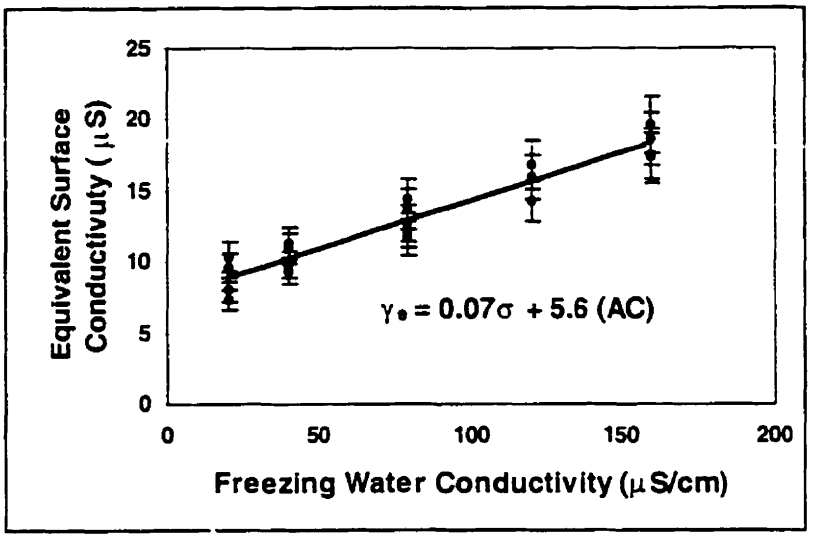

Figure 6.7 Relationship between equivalent ice surface conductivity and freezing water conductivity under ac voltage (10% error bars)

6.6 Results of bulk-ice conductivity

The results for ice samples of two values of freezing water conductivity, 30 μS/cm and 160 μS/cm, are presented in Figure 6.8.

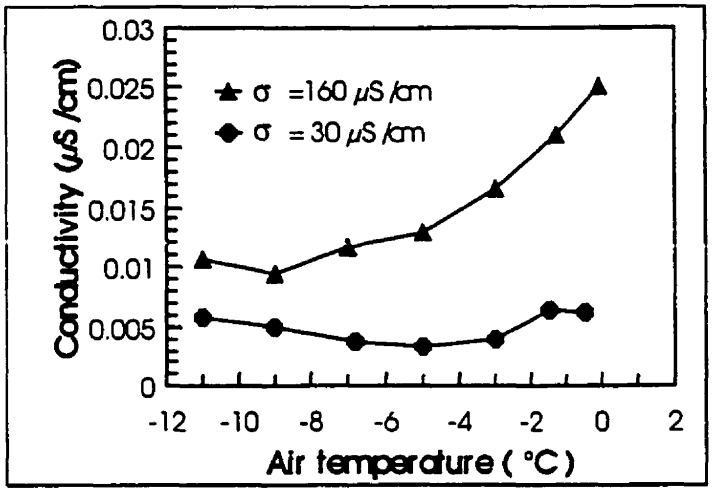

Figure 6.8 Bulk-Ice conductivity vs. air temperature

To determine and compare the intensity of the bulk-ice current and the surface current of the cylindrical ice sample, first, the bulk-ice current is calculated from the results presented in Figure 6.8. For example, at 0°C with an applied voltage of 1000 V, this maximum value of the body current was calculated at about 0.19 mA for an ice cylinder formed from freezing water of σ= 160 μS/cm. Under the same conditions, the maximum value of total surface and body current measured was 10.7 mA. In other words, the bulk-ice current represents approximately 1.8% of the maximum leakage current. According to this result the leakage current proved to flow mainly through the ice surfaces while the part flowing though the body of the ice is too insignificant to be considered. Furthermore, electrical arc during flashover on ice surface makes the difference between local ice surface temperature and bulk ice temperature larger than

those shown in Figure 6.4. Thus the bulk-ice current is more insignificant during flashover than the ice surface current. Consequently, the currents measured following the method described in Section 6.2 could be considered as surface currents.

CHAPTER VII

CHARACTERISTICS OF FLASHOVER ARC ON ICE SURFACES

7.1 Introduction

As described in Chapter IV, flashover on ice surfaces is the process of local arc development on an ice surface. The determination of local arc characteristics is of great importance for the modelling of electrical arc on ice surfaces.

On polluted surfaces, the voltage-current characteristics of local arc are normally expressed as

$$E_{arc} = \frac{V_{arc}}{x} = AI^{-n} \quad (7.1)$$

Where E_{arc} is the voltage gradient of the arc, V_{arc} is the voltage across the arc, I is the leakage current (for ac arc the peak value of the leakage current); and A and n are arc constants.

Many researchers have measured the arc constants on polluted surfaces as described in Chapter I. Various values for A and n have been summarised (Chisholm and Tam, 1989). From these studies, local arc voltage was found to

be influenced not only by the arc current, but also by other environmental conditions, such as the surrounding air humidity, air pressure, as well as the type of voltage (Rizk, 1981; Hampton, 1964; Claverie, 1971). A large difference was found between arc constants in air and in steam. It was thought that arc constants in a combined air and steam multimedia should be used in the flashover on polluted surfaces (Hampton, 1964). Voltage type was thought to have an influence on the arc constants, as well as on the electrode voltage drops (Rizk, 1981).

Arc constants for ice surfaces were not known until research at UQAC demonstrated therein. Bui et al. (Bui, Phan, Huraux and Pissolato, 1984) studied the characteristics of dc arc between a metal electrode and an ice surface with a limiting arc length of 12 mm. The characteristics of local arc on ice surfaces were measured at the high voltage laboratory of UQAC (Zhang, Farzaneh and Chen, 1995; Farzaneh, Zhang and Chen, 1997; Farzaneh, Zhang and Chen, 1996), considering the influences of environmental conditions, such as ice surface conditions and type of voltage, on local arc characteristics. In the present study, arc constants were measured directly on wet-grown ice surfaces under positive, negative, and ac voltages.

7.2 Arc constant measuring method

The wet-grown ice samples were formed using exactly the same method as that described in Section 4.2 for the flashover tests.

To determine the arc constants, a series of tests were carried out on the cylindrical ice samples. The location of the measuring electrode was adjusted to a given position, and a constant voltage was applied to the HV electrode. To change the length of the arc, a new ice sample was used and the position of the measuring electrode was readjusted to a given position corresponding to the desired arc length. The lengths of the arc were adjusted to values varying from 0.015 m to 0.15 m for an ice sample having an arcing distance of 0.3 m.

For each arc length chosen, x, the applied voltage, V_1, the voltage on the measuring electrode, V_2, and the leakage current, I, were recorded simultaneously using a Data Acquisition System (DAS).

The typical waveforms of V_1, V_2, and I under ac voltage are shown in Figure 7.1. Before the arc reaches the measuring electrode, V_2 is the sum of the local arc voltage, the electrode voltage drops and the voltage on the remaining ice surface between the foot of the arc and the measuring electrode. V_2 increases with the increase of applied voltage V_1. When the arc reaches the measuring

electrode, V_2 drops suddenly and is the sum of the voltage across the arc and the electrode voltage drops (Point P_2).

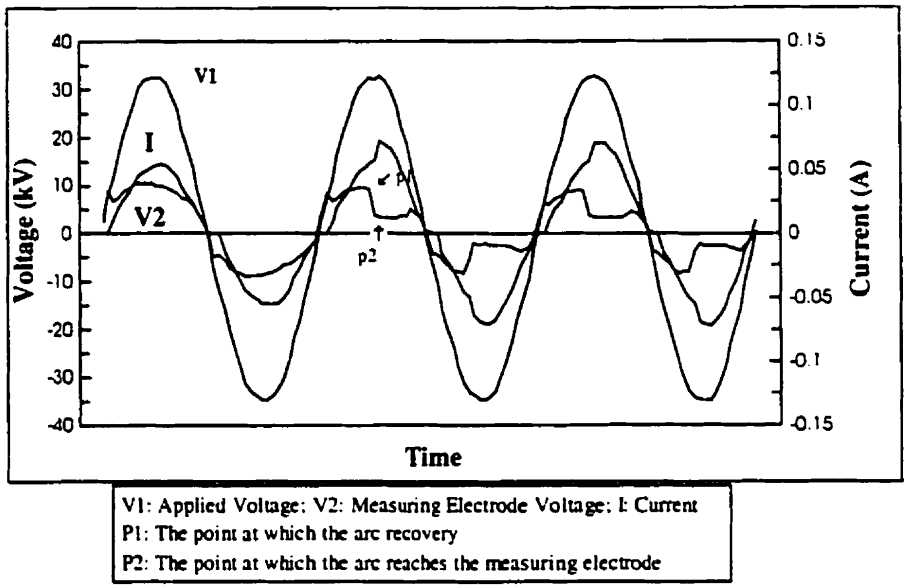

Figure 7.1 Typical waveforms

The typical waveforms of V_1, V_2, and I under dc voltage are shown in Figure 6.2.

For different ice samples, made from supercooled freezing water with various conductivities, flashover tests were carried out for different arc lengths, x. During the tests, V_1, V_2, I and x were measured. The arc constants can be obtained by using regression on the test results.

7.3 DC arc constants

As described above, the voltage, V_2, includes the electrode voltage drops. In order to determine the electrode voltage drops. a regression method is used as introduced in reference (Bui, Phan, Huraux and Pissolato, 1984). From the large quantity of measured values, different V_2 and x with the same leakage current, I, were chosen. In the present study, currents of values 0.2 A and 0.6 A were used respectively. The relationships between V_2 and I are presented in Figures 7.2 and 7.3 for negative and positive dc voltages respectively. It may be observed that there is a linear relationship between V_2 and arc length, x, with a given leakage current, I. However, when arc length x tends to 0, V_2 does not tend to 0 but to a certain value corresponding to the electrode voltage drop. The cross points of the regression curves to the Y axis correspond to the electrode voltage drops (while arc length equals zero).

The measured electrode voltage drop for positive arc is about 608 V, and is about 735 V for negative arc.

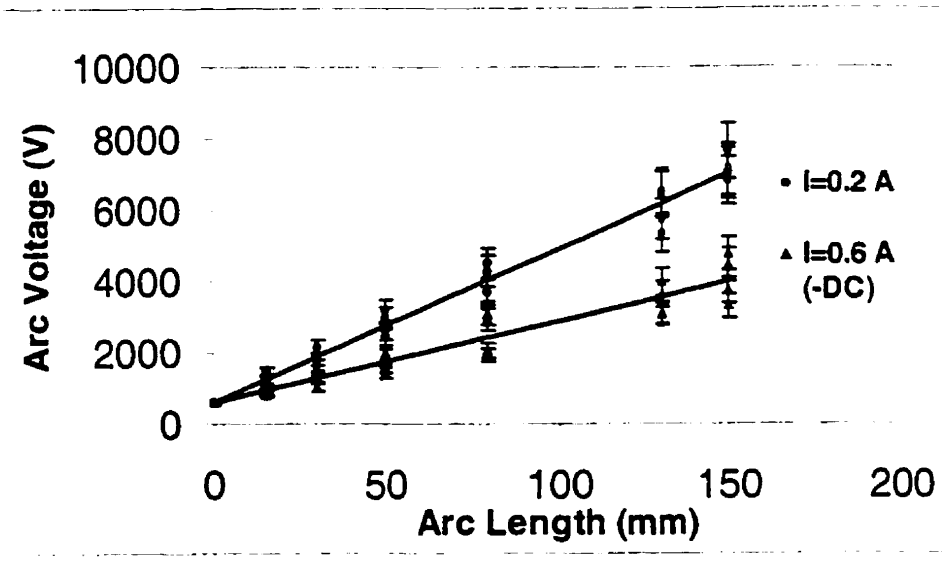

Figure 7.2 Determination of positive arc electrode voltage drops

(10% error bars)

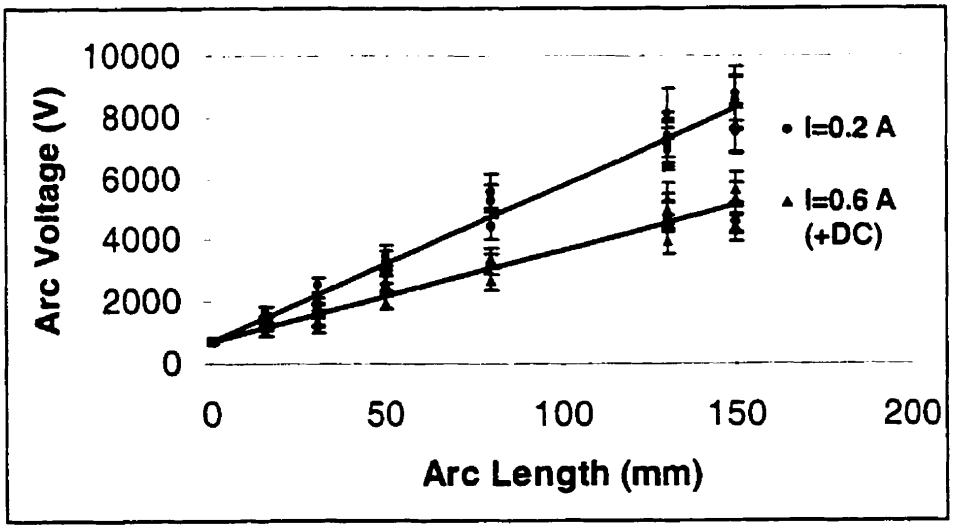

Figure 7.3 Determination of negative arc electrode voltage drops

(10% error bars)

After deducing the electrode voltage drops from V_2, the arc characteristics can be obtained, and arc constants A and n can be determined by using the regression method. The results are presented in Figures 7.4 and 7.5 for negative and positive arcs respectively.

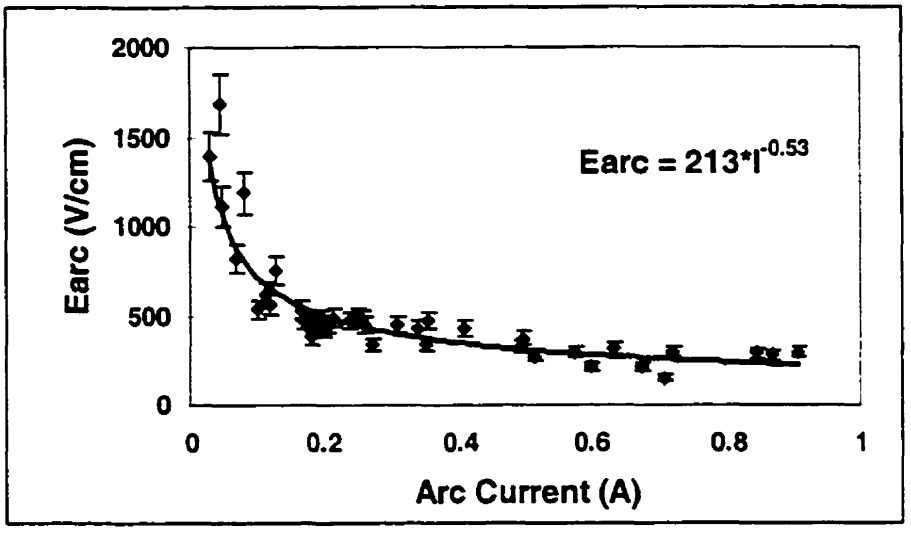

Figure 7.4 Characteristics of negative arc (10% error bars)

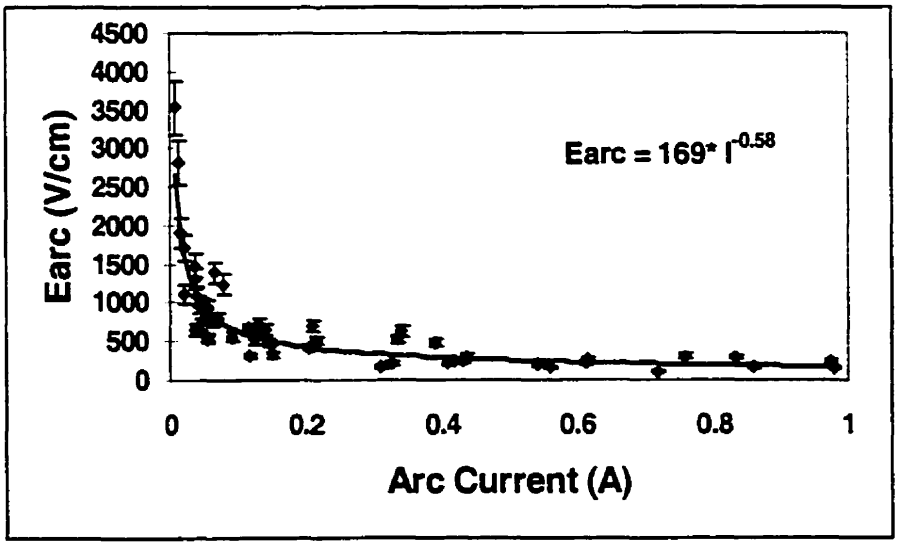

Figure 7.5 Characteristics of positive arc (10% error bars)

From Figures 7.4. and 7.5, the voltage gradient of the arc (E_{arc}) as a function of current (I) can be approximated by the following equations:

for negative arc: $E_{arc}=213 \cdot I^{-0.53}$ (7.2)

for positive arc: $E_{arc}=169 \cdot I^{-0.59}$ (7.3)

It may be noted that the obtained arc constants values on ice surface are different from those on polluted water columns which were mentioned in references (Peyregne et al, 1982; Rumeli, 1976). Rumeli quotes Hampton to give coefficients A and n of 518 and –0.273, while Peyregne et. Al . use A and n of 530 and –0.24. This is probably due to the fact that the cooling conditions and atmosphere in which the arcs burn are different between the two situations.

7.4 AC arc constants

Similar measurements were carried out to determine the ac arc constants. Using regression on the measured arc voltage drop, V_2, and the peak values of leakage current (I_m) as shown in Figure 7.1, the ac arc voltage drop was found to be about 953 V (see Figure 7.6). The voltage gradient of the arc (E_{arc}) as a function of current (I_m) can be approximated by the following equation:

for ac arc: $E_{arc}=152 \cdot I_m^{-0.52}$ (7.4)

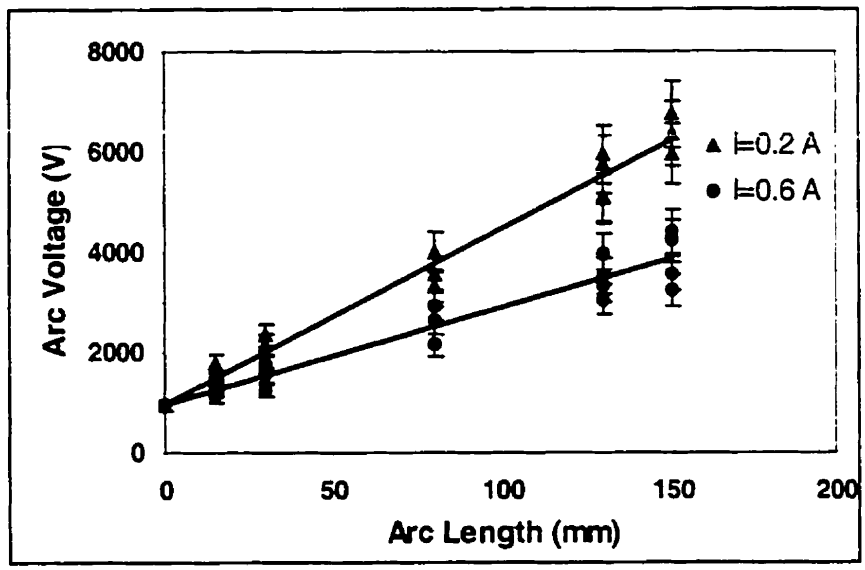

Figure 7.6 Determination of ac arc electrode drops (10% error bars)

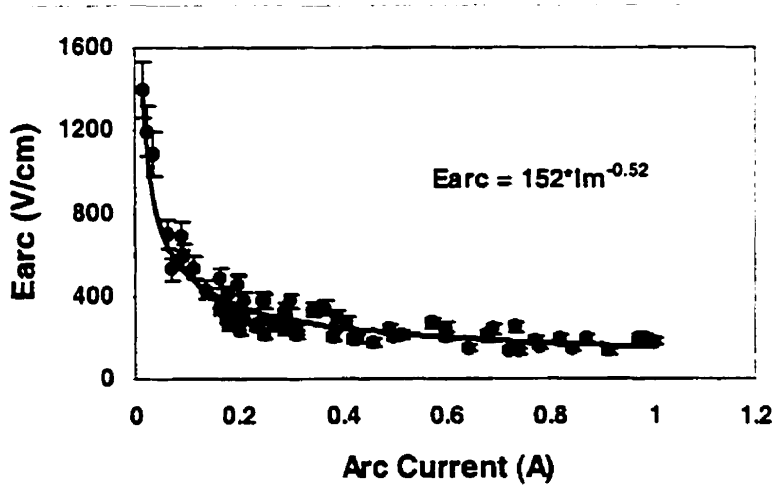

Figure 7.7 Characteristics of ac arc (10% error bars)

7.5 AC arc reignition conditions

Under ac voltage, an arc is extinguished as the current passes through zero twice every cycle. The arc develops only when it approaches the peak values of the applied voltage. During the remaining time, the arc reduces and recovers following the ac voltage. To complete the ac flashover, both the critical condition of arc stability and arc recovery must be satisfied. The former is expressed by Equation 7.1.

The arc reignition conditions on ice surfaces have been studied in our previous work (Chen, Farzaneh and Zhang, 1995; Farzaneh, Zhang and Chen, 1997). According to these studies, the reignition conditions on ice surfaces can be expressed by either Equation 7.5 or Equation 7.6

$$V_m \geq \frac{kx}{I_m^b} \quad (7.5)$$

$$V_p \geq \frac{k'x}{I_m^{b'}} \quad (7.6)$$

where, k, b, k′, and b′ are the reignition constants, V_p is the voltage across the gap of length of x cm. The general purpose of the present section is to establish the ac arc reignition conditions on a wet-grown ice surface.

The method used in the measuring of ac arc reignition conditions is similar to that described in Section 7.2 for arc constant measurement. The only difference is that for each arc length, the applied voltage, V_m, was adjusted to cause the arc recovery to occur at the peak value of applied voltage. In this way, the critical arc reignition condition is obtained.

The applied voltage, V_1, the voltage on the measuring electrode, V_2, and the leakage current, I, were recorded simultaneously using a Data Acquisition System (DAS). The typical waveforms of V_1, V_2, and I are shown in Figure 7.1. When the arc reaches the measuring electrode and the breakdown appears at the peak value of applied voltage (point P_1), the voltage V_1 at this moment corresponds to the critical values of applied voltage (V_m), necessary to cause the arc recovery for arc length x. Voltage V_2 at the moment of the breakdown (point P_1) corresponds to the critical voltage value (V_p) across the arc having a length of x.

For different ice samples, made from freezing water with various conductivities, the peak values of leakage current (I_m in A), applied voltage (V_m in V), and the corresponding voltage (V_p in V) across the arc, x cm in length, were measured. The results are shown in Figures 7.8 and 7.9. The constants k and b, corresponding to the applied voltage (Equation 7.5), or k′ and b′, corresponding to the voltage across the arc (Equation 7.6), can be obtained by applying

regression to the critical points presented in Figures 7.8 and 7.9 respectively. These constants are listed in Table 7.1.

Table 7.1

K	b	k′	b′
1258.6	0.53	449	0.51

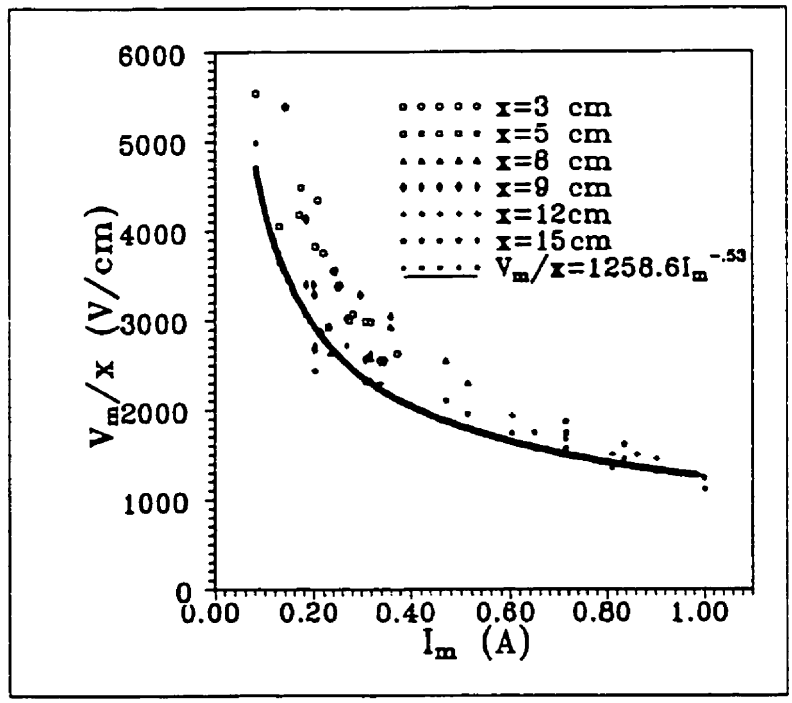

Figure 7.8 Results of reignition conditions of Equation 7.5

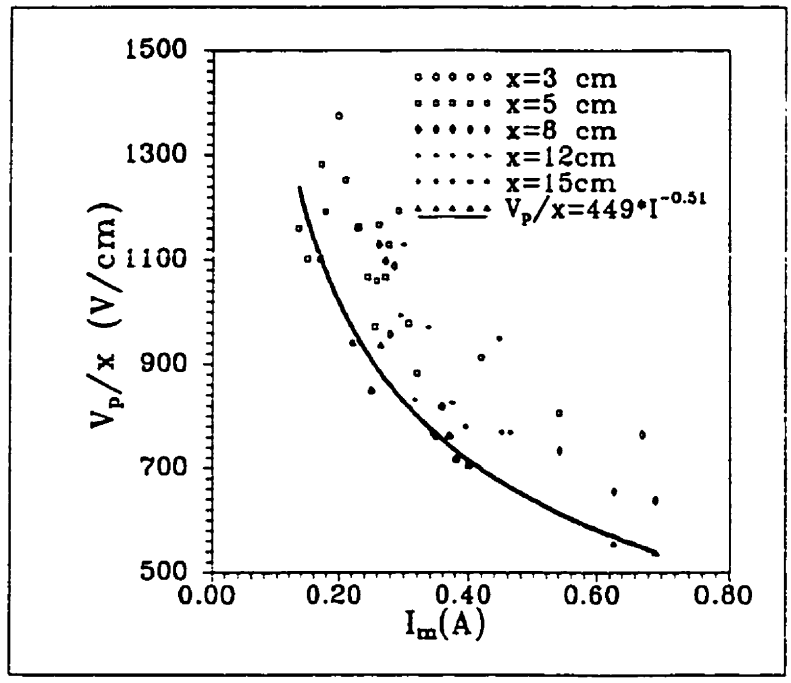

Figure 7.9 Results of reignition condition of Equation 7.6

The above results show that the reignition conditions of the arc on ice surfaces can also be expressed by Equations 7.5 and 7.6, as in the situation of polluted surfaces.

The values of constants b and b′ are close to the values of the constant n of the arc. But as previously mentioned in this chapter, the arc reignition conditions and the arc characteristics deal with two quite different aspects in the analysis of the flashover process on ice–covered insulators.

CHAPTER VIII

MODELING OF FLASHOVER ON ICE SURFACES

8.1 Introduction

In this chapter, a mathematical model is established for the modeling of flashover on ice surfaces under dc and ac voltages, based on the results obtained in the previous chapters. The flashover voltages, critical currents, and critical arc lengths are calculated for wet-grown ice samples from 0.3 m to 0.92 m in length.

8.2 DC flashover model

After the determination of the related arc constants (such as constants A and n in Chapter VII, the arc radius r_0 in Chapter IV and dc arc electrode voltage drops U_e in Chapter VI), arc reignition conditions (see Chapter VII) as well as the equivalent wet-grown ice surface conductivities (see Chapter VI), it is possible to establish a mathematical model to calculate the flashover voltage based on the Obenaus concept, as described in Chapter II. In this section, the dc flashover model is studied.

As reported in reference (Wilkins, 1969), R(x) (the residual resistance of ice layer which is not bridged by the arc, see Equation 6.1) is a function of many factors such as equivalent ice surface conductivity, γ_e, arc length(x), arc foot radius, r_0, and the arcing length, L, and width, W, of ice surface. According to Wilkins (1969) for a narrow ice strip, where the width of the ice layer is less than its length, R(x) can be expressed by :

$$R(x) = \frac{1}{\pi\gamma_e}\left[\frac{\pi(L-x)}{w} + \ln\left(\frac{w}{2\pi r_0}\right)\right] \quad (8.1)$$

and for a wide ice strip, R(x) can be expressed by

$$R(x) = \frac{1}{\pi\gamma_e}\left[\ln\frac{2L}{\pi r_0} - \ln\left(\tan\frac{\pi x}{2L}\right)\right] \quad (8.2)$$

As represented in Chapter IV, the radius, r_0, of the arc root is a function of arc current, I:

$$r_0 = \sqrt{\frac{I}{k_1\pi}} \quad (8.3)$$

In Equation 6.1, there are three variables, namely V, I, and x. For each arc length x, there exists a minimum value, V_{min}, of applied voltage (see Figure 8.1). When the voltage is lower than V_{min}, the arc can't maintain itself.

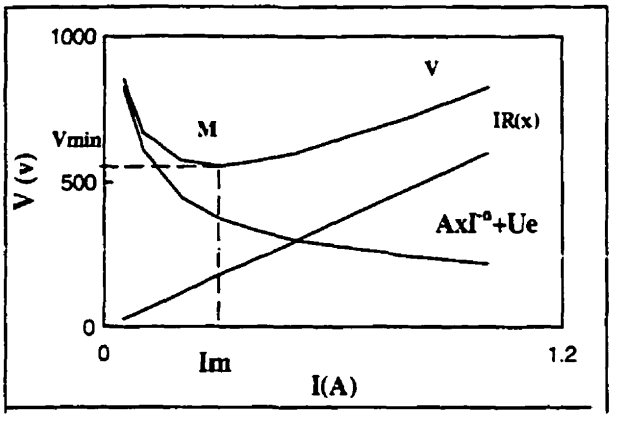

Figure 8.1 V-I relationships

The value of V_{min} for each arc length x can be obtained from Equation 6.1 using

$$\frac{dV}{dI} = 0 \quad (8.4)$$

V_{min} changes with arc length x. An instructive schematic illustration of V_{min} and arc length x is shown in Figure 8.2 (Rizk, 1971, Jan/Feb.; Alston and Zoeledziowski, 1963). Let a voltage V_s be applied to the insulator, the arc can develop to a length of x_s but no further, because the voltage required to maintain the arc exceeds V_s, if x exceeds x_s. However, if the arc length reached x'_s initially, further increase of arc would need a smaller V_{min}, so that the arc could grow to flashover. The critical arc length is x_c, which corresponds to a critical voltage, V_c, and a critical current, I_c. An arc longer than x_c leads to the completion of flashover.

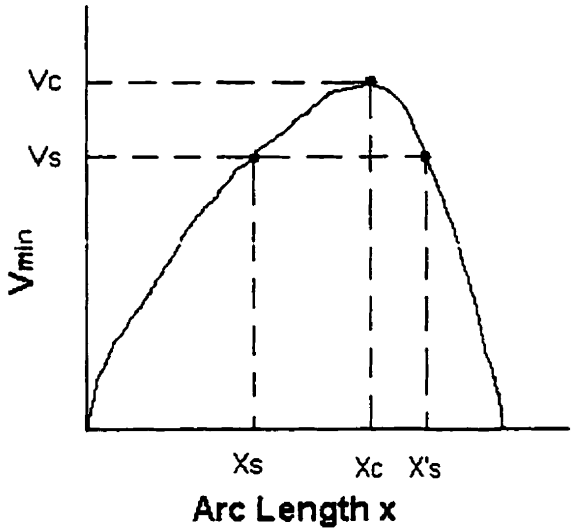

Figure 8.2 Illustration of v_{min} to arc length x

Critical arc length, x_c, may be obtained from Equation 8.5.

$$\frac{dV_{min}}{dx} = 0 \quad (8.5)$$

Using Mathcad, the flashover voltage, V_c, critical arc length, x_c, and critical current, I_c, can be obtained for ice samples under dc conditions by solving Equations 6.1 and 8.1 to 8.5.

8.3 AC flashover model

The ac flashover model can also be expressed by Equation 6.1. In this equation, V and I should be the peak values of the applied voltage and leakage current respectively.

R(x) and arc radius in ac voltage can also be represented by Equations 8.1, 8.2 or 8.3 respectively. The constants A, n, U_e, and k_1 for ac arc are obtained in Chapters VII and IV.

As described in Section 7.5, under ac conditions, arc reignition conditions must also be satisfied for the arc to continue to develop. The critical reignition condition is:

$$V_m = \frac{kx}{I_m^b} \qquad (8.6)$$

So Equation 6.1 can be rewritten as:

$$V_m = Ax\left(\frac{kx}{V_m}\right)^{\frac{-n}{b}} + U_e + R(x)\left(\frac{kx}{V_m}\right)^{\frac{1}{b}} \qquad (8.7)$$

When the constants A, n, k, b, and U_e are determined, V_m is only a function of x, as determined by Equation 8.7. When x increases from 0 to the arcing distance L, V_m will appear as a maximum value (V_c) at a critical arc length (x_c). Solving numerically Equation 8.7, V_c and x_c can be obtained. The critical current, I_c, may be determined from Equation 8.6 by

$$I_c = \left(\frac{kx_c}{V_c} \right)^{\frac{1}{b}} \quad (8.8)$$

The programs to calculate the flashover voltage, the critical arc length and critical current under dc and ac voltages are listed in Appendix I.

8.4 Applications of the model to the cylindrical ice samples

The flashover model was applied to wet–grown cylindrical ice samples of various arcing distances. The influence of freezing water conductivity, arcing distance, and the type of voltage to the flashover voltage, critical current, and critical arc distance were analyzed.

8.4.1 Calculated flashover voltage of ice samples

The flashover voltages of wet–grown ice samples were calculated using the mathematical model described in Sections 8.2 and 8.3.

Figure 8.3 presents the calculated flashover voltages under dc and ac conditions of the ice sample of 0.3 m arcing distance. It may be seen that the calculated flashover voltages decrease with an increase of freezing water conductivity.

From the calculated results, ice samples have the highest flashover voltages under ac voltage, compared with those under dc. Flashover voltages under positive dc voltages are higher than those under negative dc. AC flashover voltages are 11% to 18% higher than flashover voltages under positive voltage and 19% to 24% higher than under negative voltage. Flashover voltages under positive voltage are 5% to 10% higher than under negative voltage.

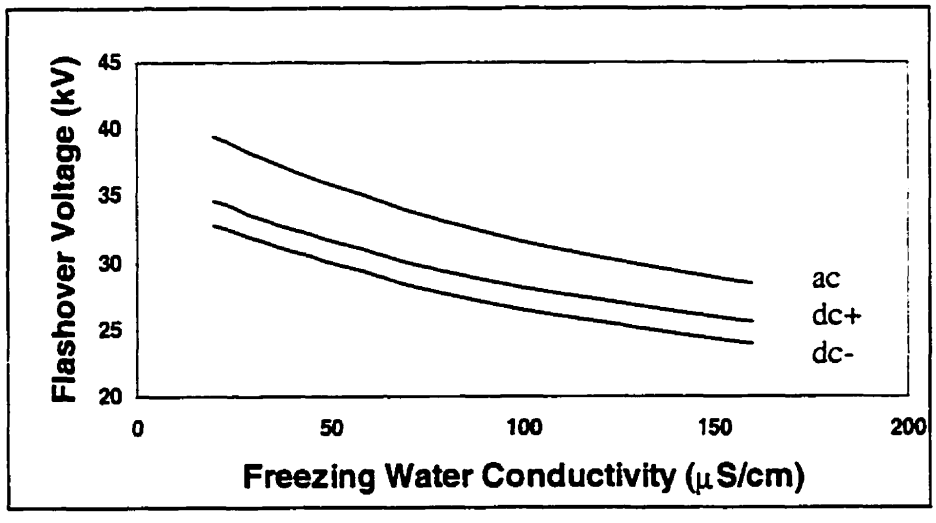

Figure 8.3 Calculated flashover voltages of ice samples (0.3 m)

8.4.2 Comparison of the results of the mathematical model with the results of experiments

A large number of flashover tests were carried out on wet–grown ice samples. The facilities and procedures were described in Chapter V. Flashover voltages were obtained for ice samples formed from different freezing water conductivities and having different arcing distances. The experimental results for an ice sample of 30 cm arcing distance, as well as the calculated results from the mathematical model, are shown in Figure 8.4, for ac and dc voltage conditions.

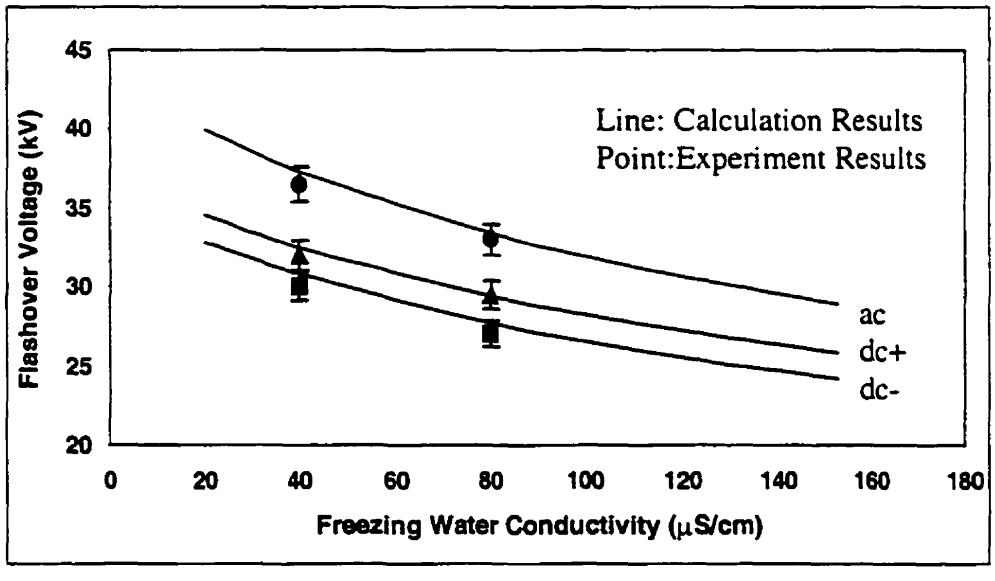

Figure 8.4 Calculated and experimental results of flashover voltages for wet-grown ice samples of 0.3 m in length (3% error bars)

From Figure 8.4, it can be seen that for the ice sample, there is good concordance between the flashover voltages calculated from the model and the results obtained in the experiments, for both dc and ac voltage applications.

8.4.3 Influence of arcing distance on flashover voltages

Similarly, the flashover voltages of ice samples having arcing distances of 0.62 m and 0.92 m were calculated. The results are shown in Figures 8.5 and 8.6.

The calculated results of flashover voltages, V_c, as a function of arcing distance, are presented in Figure 8.7. It may be seen that V_c increases linearly with the arcing distance of the ice samples, up to 0.92 m.

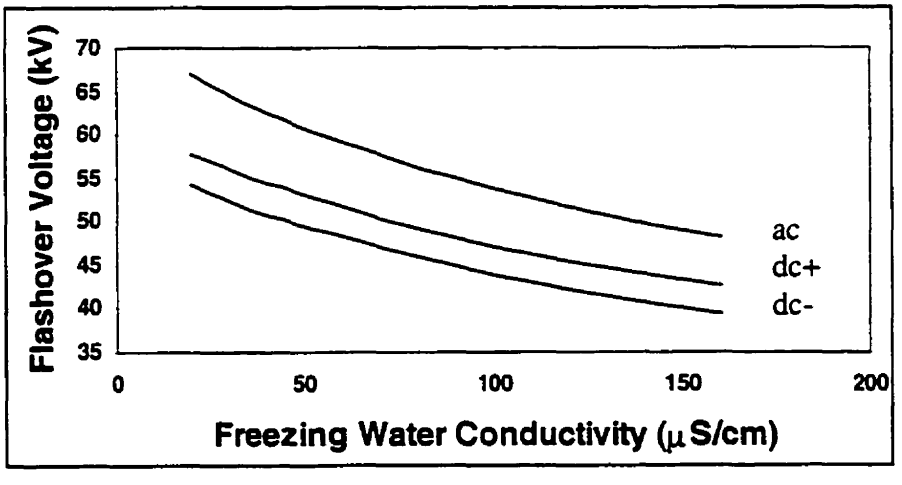

Figure 8.5 Calculated flashover voltages of ice samples (0.62 m)

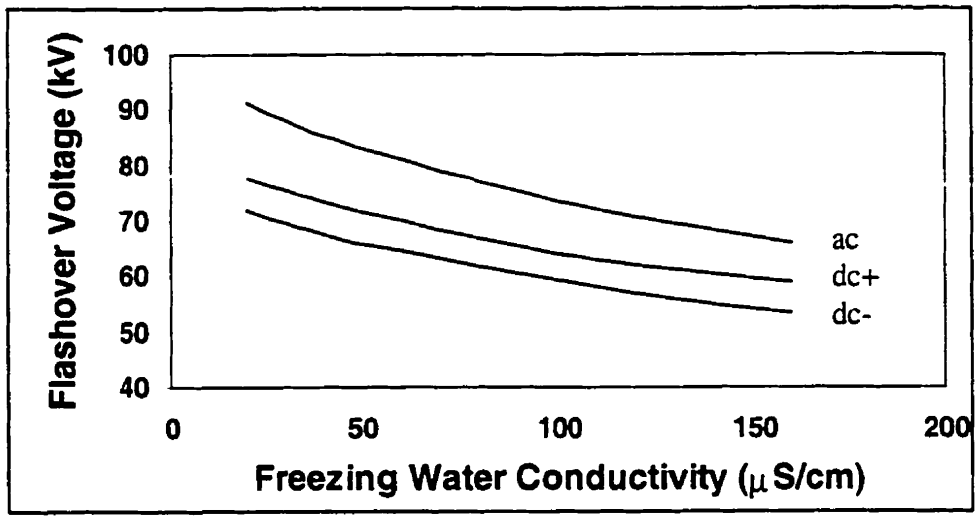

Figure 8.6 Calculated flashover voltages of ice samples (0.92 m)

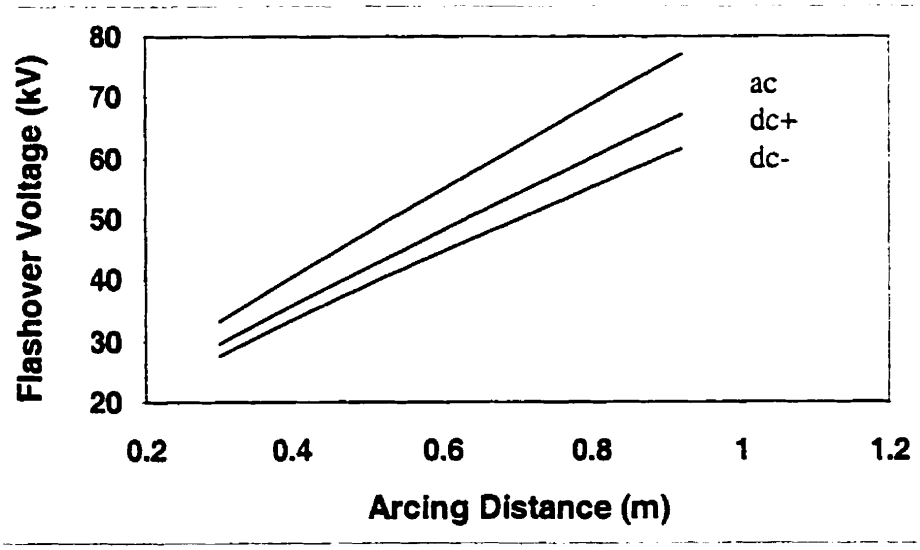

Figure 8.7 Calculated relationships between flashover voltage and arcing distance (σ=80 μS/cm)

The calculated results of the flashover voltages as a function of arcing distance of ice samples are in agreement with experimental results, as shown in Figure 8.8.

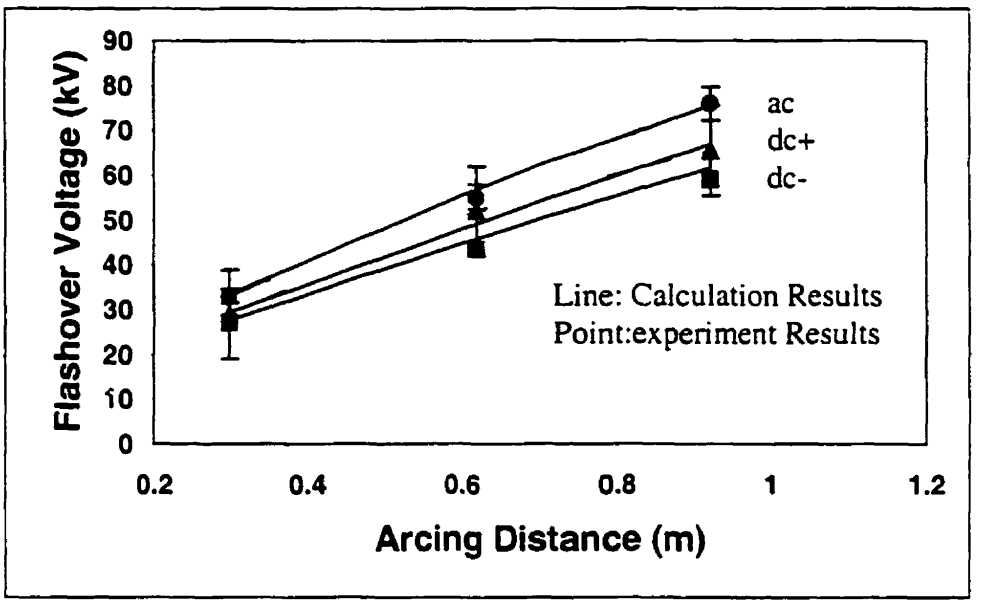

Figure 8.8 Calculated and experimental results of flashover voltages for ice samples of 0.3 m, 0.62 m and 0.92 m in length (σ=80 μS/cm, 5% error bars)

8.4.4 Calculation of critical current

Critical currents, I_c, were calculated using the mathematical model introduced in Sections 8.2 and 8.3. For an ice sample of 0.92 m, the relationships between I_c and freezing water conductivity are shown in Figure 8.9, for ac and dc voltages.

It may be observed that I_c increases with an increase in freezing water conductivity. Under ac voltage, I_c is predicted to be about 3 times that of both positive and negative dc voltages. That may be due to the fact that, under ac conditions, arc current passes zero twice in each cycle so that arc reignition conditions must be satisfied for arc development. A larger current for ac arc is needed in order to maintain and develop the arc itself. For dc conditions, I_c is predicted to be a little higher in positive voltage than in negative voltage.

The critical current, as calculated, increases with an increase in arcing distance. For example, as shown in Figure 8.10, I_c increases about 2 times when the arcing distance changes from 0.3 m to 0.92 m under ac conditions.

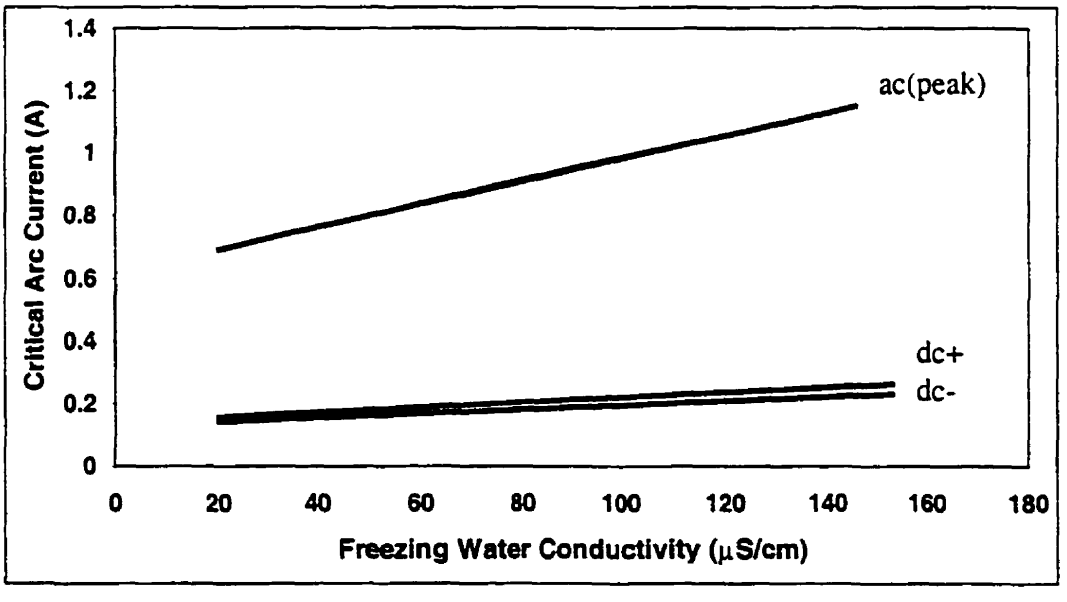

Figure 8.9 Calculated critical currents (ice sample of 0.92 m)

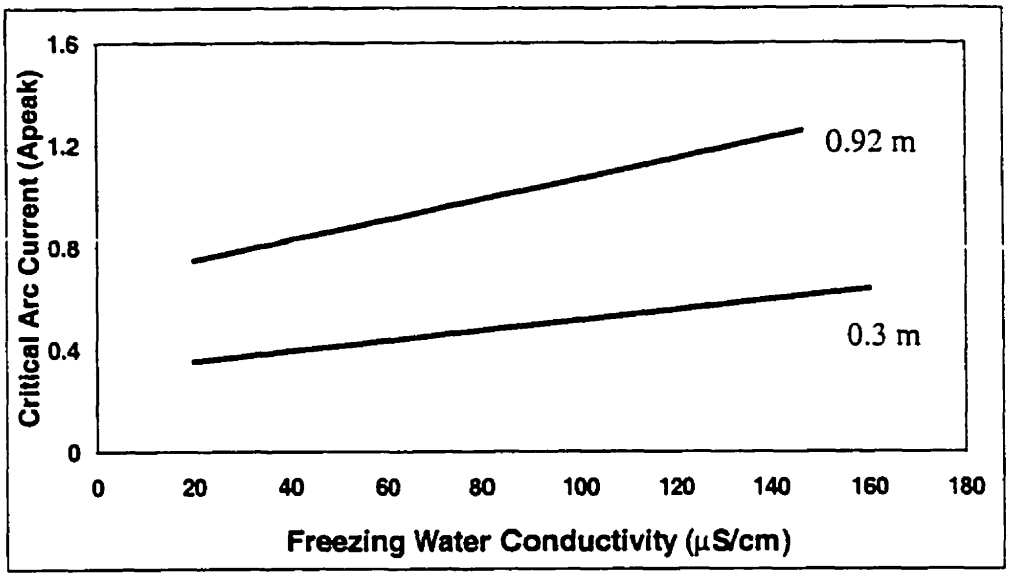

Figure 8.10 Calculated influence of arcing distance to critical currents (ac)

8.4.5 Calculation of critical arc length

Critical arc length, x_c, is also obtained from the mathematical model. For an ice sample of 0.92 m, Figure 8.11 shows the relationships between x_c (expressed as the ratio to the total arcing distance) and freezing water conductivity, for ac and dc voltages.

It may be observed from this figure that x_c decreases with an increase in freezing water conductivity. Under ac voltages, x_c is higher than those of both positive and negative dc voltages. x_c is found to be a little higher in positive voltage than in negative voltage. Under ac conditions, the critical arc length is

about 90% of the total arcing distance (in the case of 0.92 m total arcing distance). The critical positive arc length is about 87% of the total arcing distance, and the critical negative arc length is about 86% of the total arcing distance.

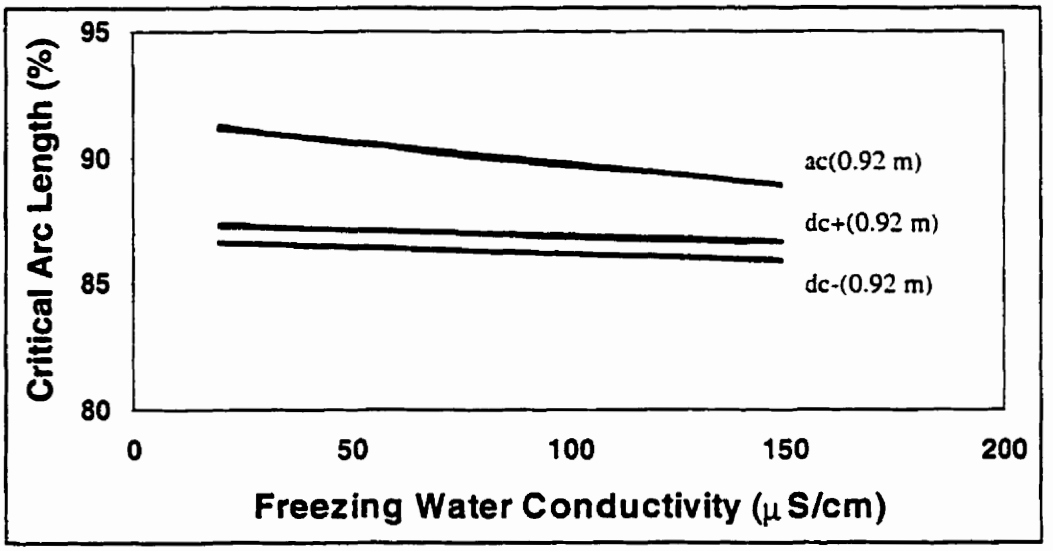

Figure 8.11 Calculated critical arc lengths

It was also found from the calculations that the ratio of the critical arc length to the total arcing distance increases with the arcing distance. For example, Figure 8.12 shows the variation of critical arc length when the arcing distance changes from 0.3 m to 0.92 m, under ac conditions. The critical arc length is about 90% of the total arcing distance when the arcing distance is 0.92 m, while the ratio is about 84% for an arcing distance of 0.3 m.

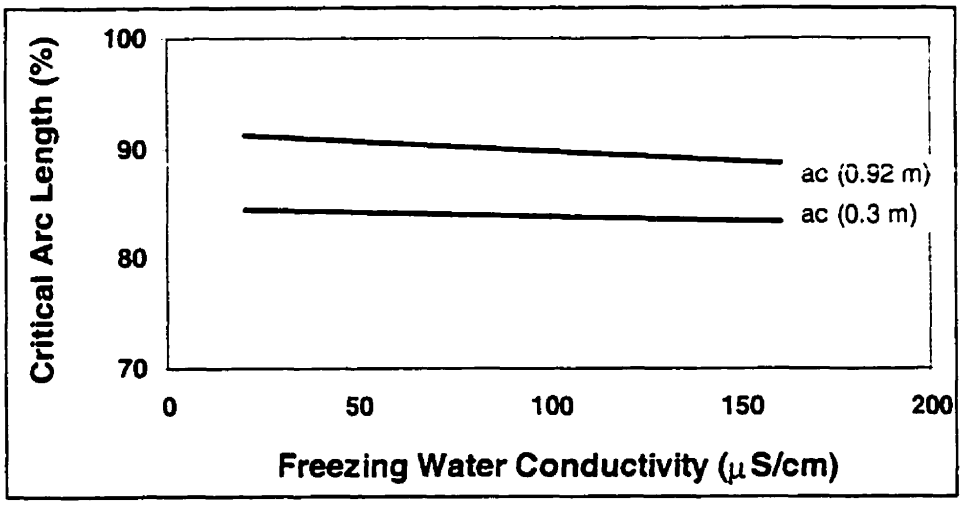

Figure 8.12 Calculated influence of arcing distance on critical arc lengths

CHAPTER IX

APPLICATIONS OF THE MATHEMATICAL MODEL TO ACTUAL INSULATOR STRINGS

9.1 Introduction

Compared to flashover of contaminated insulators, only a few researchers have studied flashover of ice-covered utility insulator strings. As a result, as introduced in Chapter II of the present thesis, the problem is far from being solved. First, the results obtained in each industrial laboratory are more or less different from each other. This may be due to the different experimental conditions, such as ice deposit processes, melting processes and measuring equipment, etc. Second, this kind of experiment is very time consuming and expensive. Ice formation on an insulator string generally needs several hours in a well equipped climate room. The time needed in an open experimental site is much longer. Third, the voltage level of the laboratory is often limited by the size of the climate room. Tests with a long ice-covered insulator string are quite difficult. Very little in-depth research has been carried out on long insulator strings. The equivalence of results obtained with short insulator strings with those of long insulator strings is also quite doubtful. This influences greatly the insulation design of EHV and UHV transmission lines in cold regions.

Keeping this in mind, it is of great importance to apply the mathematical model to the analysis of flashover of insulator strings, especially long strings. In the present chapter, first, the flashover of a short standard insulator string is analyzed using the mathematical model established in the last chapter. Then, the model is applied to a long insulator string, up to the voltage level of 735 kV (about 5 m). The results of short and long insulator strings are compared and analyzed. Finally, the future application of the mathematical model is discussed.

9.2 Application of the mathematical model to short industrial insulator strings

9.2.1 Flashover of a 5-unit IEEE standard insulators under different freezing water conductivities

As introduced in Chapter III, a mathematical model developed at UQAC was applied to a short string of IEEE standard insulators, and was validated with experimental results (Farzaneh, Zhang and Chen, 1997). IEEE standard insulators are shown in Figure 9.1. The ice on the insulator string, as shown in Figure 5.3, can be considered rectangular with length, L, and width, W. According to the experimental results of reference (Farzaneh and Drapeau, 1995) and considering an ice thickness of 20 mm, the arcing distance, L, is

equal to 0.809 m, and ice width, W, is equal to 0.462 m. For wet-grown ice, the ice surface resistance, R(x), was expressed in Equation 8.1, the equivalent wet-grown ice surface conductivity was determined by Equation 6.6. The arc constants A and n were shown in Equation 7.4. The arc radius, r_0, was obtained from Equation 4.3. The arc reignition conditions were determined in Table 7.1. Using these values and the mathematical model of Chapter VIII, the ac flashover voltage of a 5-unit IEEE standard insulator string covered with wet-grown ice was calculated.

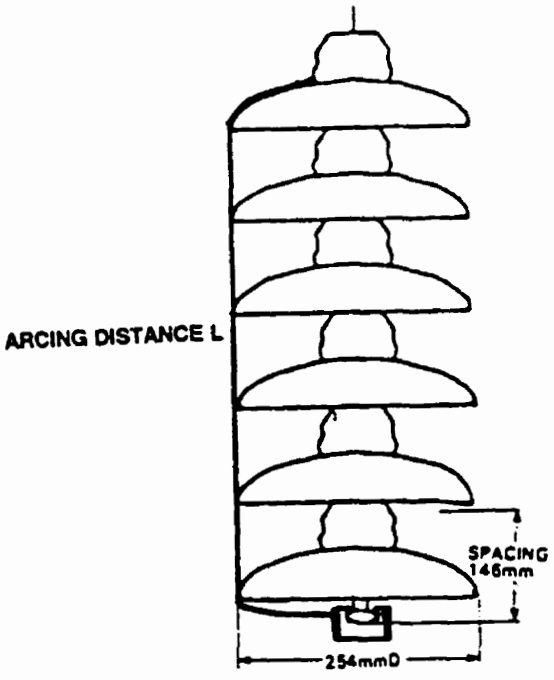

Figure 9.1 IEEE standard insulators

The calculated flashover voltages are compared with the experimental results obtained in the high voltage laboratory of UQAC. Flashover tests were carried out on a 5-unit IEEE standard insulator string covered with wet-grown ice 20 mm thick, using freezing water of different conductivities (Farzaneh and Kiernicki, 1997). The test results as well as the calculated results from the model are shown in Figure 9.2.

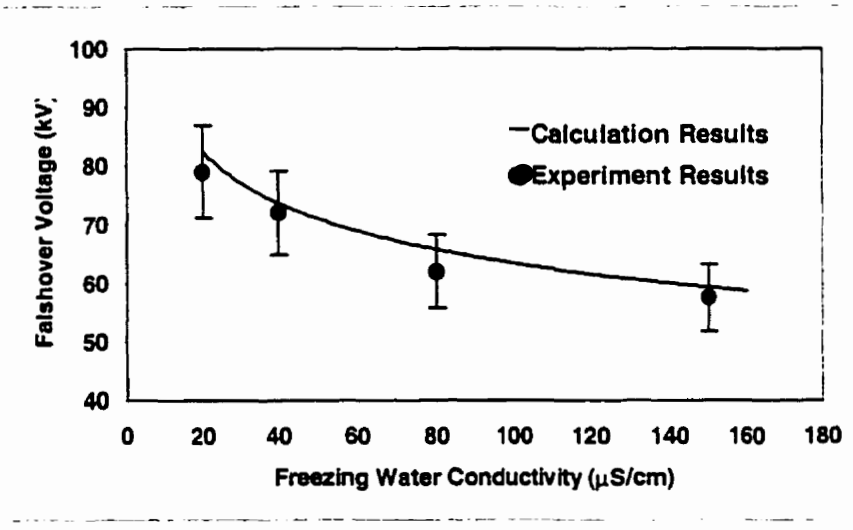

Figure 9.2 Calculated and experimental flashover voltages of a 5-unit IEEE standard insulator string (10% error bars)

Good concordance is obtained when the flashover voltages obtained from the calculations with those obtained from the tests on an IEEE standard insulator string are compared. The difference between the experimental and calculated results were less than 10% for the 5-unit IEEE standard insulator string. This

difference may first be due to geometrical simplicity of the model. In the model, the ice surface was considered to be rectangular. But ice on an actual insulator string is approximately represented by a half cylinder of ice. This difference may also be caused by the non-uniformity of ice on insulators. In the mathematical model, the ice surface was supposed to be uniform. Considering the complexity of the ice flashover problem, a mathematical model is indeed very difficult to perfect. The modeling of arc on ice surfaces has been carried out and improved continually at UQAC, as introduced in Chapter III (Farzaneh, Zhang and Chen, 1997; Zhang and Farzaneh, 1998).

9.2.2 Influence of arcing distance on the flashover voltage of short IEEE standard insulator strings

The mathematical model was then applied to IEEE insulator strings of 1 to 6 units, covered with wet-grown ice. Freezing water conductivity, σ, was kept at 80 μS/cm. The results were obtained as shown in Figure 9.3 and Table 9.1. As a comparison, the experimental results form the HV laboratory of UQAC (Farzaneh and Kiernicki, 1997) are also shown in Figure 9.3.

It can be seen that the flashover voltages obtained from the mathematical model, for 1 to 6 units of ice–covered IEEE standard insulators, increases linearly with the arcing distance of the insulator units. There is concordance

between the flashover voltages calculated from the mathematical model and the results obtained in the laboratory tests.

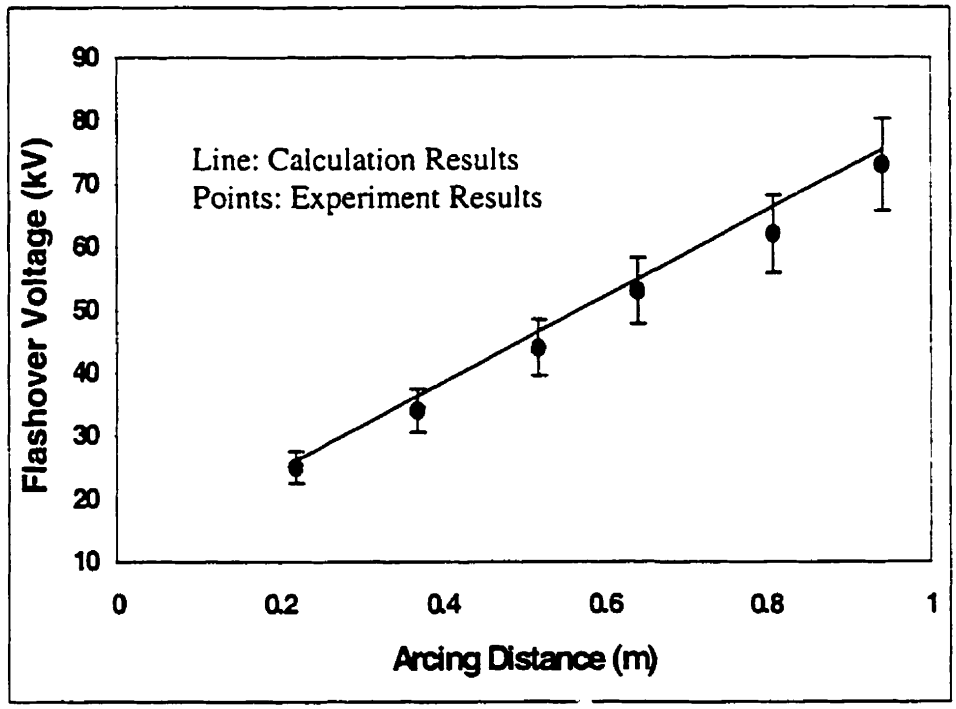

Figure 9.3 Calculated and experimental flashover voltages for IEEE standard insulators strings of 1 to 6 units (10% error bars)

The calculated results show that the average flashover gradient is about 82 kV/m for short IEEE standard insulator strings of 1 to 6 units, covered with wet-grown ice of 20 mm thick and of freezing water conductivity of 80 μS/cm.

Table 9.1

Arcing Distance L	Critical Flashover Voltage V_c	Critical Current I_c	Critical Arc Length x_c/L	Critical Arc Radius r_0
m	kV	A_{peak}	%	mm
0.22	27	0.39	82.9	2.5
0.37	39	0.52	84.3	2.9
0.52	50	0.63	85.2	3.1
0.64	58	0.71	85.7	3.3
0.809	69	0.82	86.1	3.6
0.94	77	0.89	86.5	3.7

9.3 Application of the mathematical model to long insulator strings

9.3.1 Calculation of flashover voltage of long insulator strings

As described in the introduction, flashover of ice-covered long insulator string is a necessary but difficult subject for the design the EHV and UHV transmission lines in cold regions. This has motivated the study described in this section.

In the calculation of flashover voltage of long insulator strings, ice on the insulator strings is also considered rectangular with length, L, and width, W, as described for the short insulator string in Section 9.2. The arcing distance, L, is considered to change from 1 m to 10 m. Ice width, W, is kept equal to 0.462 m and freezing water conductivity, σ is equal to 80 μS/cm. Because of the lack of experimental results for long insulator strings, the air gap length was supposed to be 10 mm, as that used in the study of short insulator strings. According to the studies in reference (Farzaneh and Kiernicki, 1997), this supposition of uniform ice formation made the calculation results a little conservative. Using the mathematical model introduced in Chapter VIII, the flashover voltage gradients of long insulator strings covered with wet-grown ice are calculated and shown in Figure 9.4 and Table 9.2.

The calculated results in Figure 9.4 and Table 9.2 show that flashover voltage increases with arcing distance for the insulators covered with wet-grown ice. With the present ice conditions, for an insulator string of 1.1 m (115 kV system), the flashover voltage is 89 kV, slightly above the nominal 66 kV line-ground voltage. When the arcing distance increases to 4.90 m (corresponding to 735 kV system) the flashover voltage increases to 308 kV, well below the nominal 424 kV line-ground voltage.

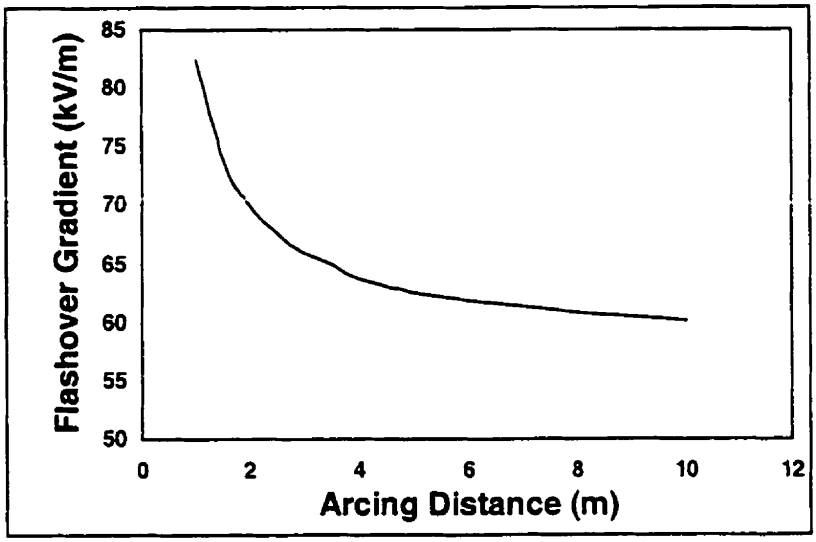

Figure 9.4 Calculated flashover gradients of long insulator strings

Table 9.2

Arcing Distance L	Critical Flashover Voltage V_c	Critical Flashover Gradient E_c	Critical Current I_c	Critical Arc Length X_c/L	Critical Arc Radius r_0
m	kV	kV/m	A_{peak}	%	mm
1.1	89	80	1.0	90.4	4.0
3	198	66	1.0	74.3	4.0
4.9	308	63	1.0	70.7	4.0
7	429	61	1.0	69.0	4.0
10	602	60	1.0	67.8	4.0

It may also be observed that flashover voltage is not a linear function of arcing distance. The flashover voltage gradient decreases with an increase in arcing distance. When the arcing distance changes from 1.1 m to 4.9 m, the flashover voltage gradient decreases from 80 kV/m to 63 kV/m. It may also be noticed that the flashover voltage gradient tends to be a constant for long arcing distance. For example, between 4.90 m and 10 m of arcing distance, the flashover voltage gradient decreases only from 63 kV/m to 60 kV/m. According to the above calculations, for the long insulator string, and the present ice conditions, the flashover voltage gradient may be finally considered to be about 60 kV/m at an ice thickness of 20 mm and a freezing water conductivity of 80 μS/cm.

9.3.2 Influence of freezing water conductivity on the flashover voltage gradient of long insulator strings

The decrease of flashover voltage gradient of ice-covered insulator strings, as shown in the above section, is of great importance to the design of transmission line and substation external insulation, especially for the EHV and UHV power projects. For power transmission projects, the conductivity of ice varies from site to site. In the present section, the influence of freezing water conductivity on the flashover voltage gradient (corresponding to insulator strings of 4.9 m and 10 m) is studied using the mathematical model. Freezing water

conductivities from 20 to 200 μS/cm were chosen for this study. The other parameters were the same as those of Section 9.3.1. The results are shown in Figure 9.5 and Table 9.3.

Table 9.3

Arcing Distance L	Freezing Water Conductivity σ	Critical Flashover Voltage V_c	Critical Flashover Gradient E_c	Critical Current I_c	Critical Arc Length x_c/L	Critical Arc Radius r_0
m	μS/cm	kV	kV/m	A_{peak}	%	mm
4.9	20	363	74	0.74	71	3.4
	40	340	70	0.83	71	3.6
	80	308	63	1.00	71	4.0
	120	284	58	1.16	71	4.3
	160	267	54	1.31	70	4.5
	200	252	52	1.45	70	4.8
10	20	708	71	0.74	68	3.4
	40	665	67	0.83	68	3.6
	80	602	60	1.00	68	4.0
	120	557	56	1.16	68	4.3
	160	523	52	1.31	68	4.5
	200	495	50	1.44	68	4.8

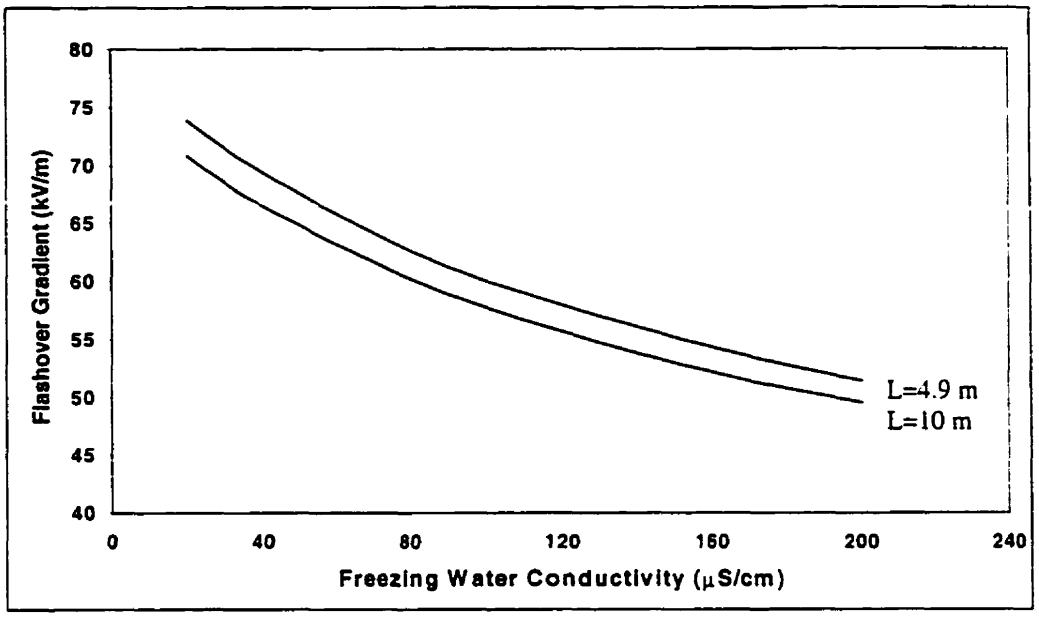

Figure 9.5 Calculated results of flashover gradient for different freezing water conductivities at an ice thickness of 20 mm

It can be seen that the flashover gradient calculated decreases with an increase in the conductivity of the spray water. For a 4.9 m insulator string, the flashover voltage gradient is only about 52 kV/m, when the freezing water conductivity is 200 μS/cm. This value is much lower than 87 kV/m, the actual nominal electrical stress of 735 kV insulator strings. These results calculated indicate that flashover is quite possible for EHV and UHV insulator strings when wet-ice melts.

It should be noted that the calculated results are validated up to about one meter (6 units of IEEE standard insulators). For longer insulator strings, the mathematical model needs to be validated by further experimental studies.

9.3.3 Discussion of the application of the mathematical model

9.3.3 1 Discussion of the flashover voltage gradient

From the above calculations, the flashover voltage gradient of long insulator strings is much lower than that of short insulator strings. This is partly in concordance with the only available experimental results on long insulator strings (Su and Jia, 1993). In the study, it was found that the withstand voltage gradient of an insulator string up to 5 m in length decreases almost linearly with the length of the insulator string. Instead of a linear decrease, the present results from the mathematical model show that the decrease can be divided into two periods for long insulator strings from 1 m to 10 m in length. For an insulator string of 1 m to 3 m, the flashover voltage gradient decreases rather rapidly, from 83 kV/m to 66 kV/m. Then the decrease stabilizes and, finally, the flashover voltage gradient remains constant at about 60 kV/m.

It is interesting to mention that the calculated results for long iced insulator strings could be compared to cold-fog test results up to 14 m leakage distance

(Chisholm, et. al. 1996). Typical flashover gradients were found as low as 20 kV per meter of leakage distance.

One of the possible reasons for the influence of insulator string length may be current distribution on the ice surface. As discussed in reference (Wilkins, 1969), current is concentrated at the foot of the arc on polluted surfaces. This is also true for arcs on ice surfaces. In the part of the ice surface that is not bridged by the arc, current becomes more and more uniformly distributed, while the distance to the arc foot increases. So for longer insulator strings, the influence of the current concentration at the foot of the arc on the total current distribution becomes less pronounced: Current distribution becomes more and more uniform, and the flashover voltage gradient finally remains constant.

In the present mathematical model, ice is considered rectangular and uniform. The studies of Farzaneh and Kiernicki (1997) show that the uniformity of ice accretion on energised insulators is influenced by many factors such as wind velocity, insulator shape, freezing water conductivity and ice thickness, etc. These factors result in a more or less non-uniform ice accumulation along the insulator string. Icicles are twisted toward the insulator string axis. The arc, during ice formation, melts a part of the ice. The experimental results in Chapter V of the present thesis, and of Farzaneh and Kiernicki (1997), show that the more uniform the ice distribution is, the lower the flashover voltage. The

influence of ice uniformity should be considered further in the mathematical model.

Non-uniform ice distribution is also caused by ice melting during the de-icing period, and flashover, especially for long insulator strings. From many observations of insulator string flashover in laboratory, damage to the ice during arc development and flashover is more serious for long ice samples and long ice-covered insulator strings.

9.3.3.2 Discussion of the critical arc length and critical current

For the example listed in Table 9.1 for a string of 1 to 6 units of IEEE standard insulators, it may be noted that the ratio of the critical arc length to total arcing distance increases a little (from 83% to 86%) with an increase in arcing distance from 0.22 m to 0.94 m. At the same time, the critical current increases from 0.40 A to 0.89 A. This tendency agrees with the experimental observations and modeling calculations of ice samples from 0.30 m to 0.92 m, in Chapters IV and VIII.

However, in the calculation results for long insulator strings, as shown in Table 9.2, the ratio of the critical arc length to total arcing distance is found to decrease from 90% to 68% when the arcing distance increases from 1.1 m to

10 m. The critical current remains constant at 1 A for a freezing water conductivity 80 μS/cm.

The different tendencies of critical arc length and critical current between short and long insulator strings may also be due to current distribution on the ice surface. As discussed in Section 9.3.3.1, for longer insulator strings, the influence of the current concentration at the foot of the arc on the total current distribution becomes less pronounced: Current distribution becomes more and more uniform. As described in Chapter VIII, for long and short insulator strings, Equations 8.1 and 8.2 are used to express ice surface resistance respectively, according to (Wilkins, 1969). Further experimental study is needed, especially for long insulator strings.

CONCLUSION

On the basis of the experimental investigations on wet-grown ice sample and the Obenaus concept, the electrical arc on ice surfaces was analysed and mathematical models were established for flashovers on ice surfaces under ac and dc voltages. From the results obtained, the following conclusions may be drawn:

1. The flashover process on ice surfaces can be defined as having three periods: the arc-starting period, the arc-developing period, and the finial flashover period. In these three periods, obvious differences were observed in the arc development phenomena, arc currents, and arc speeds.

   During the arc-starting period, several violet arcs occurred across the air gap. As the air gap became longer, one of the arcs persisted and it turned white. In this process, the arc length was usually shorter than 10% to 20% of total arcing distance, and the arc current was lower than 0.1 A for dc and 0.3 A for ac. The arc developed very slowly and its speed depended on melting ice and air gap extension.

In the arc-developing period, the arc became longer and brighter. It developed faster and the corresponding current was larger. When the arc current and the arc length reached their critical values, flashover took place rapidly.

Based on the high speed camera observations of the wet-grown ice sample 0.3 m in length, the critical currents were about 0.2 A for dc and 0.5 A for ac. The critical current increased with an increase in freezing water conductivity, especially for the ac arc. The critical arc length was from 73% to 90% of the total arcing distance for dc and 60% to 90% for ac. Before the critical point, the average arc speed was only tens of cm/s. After this point, arc developed more rapidly. Its speed can reach about 3 m/s just before flashover.

The final flashover finished during 2 frames of the high speed camera. Its speed is higher than 112 m/s. The arc current is larger than 1 A.

2. The relationships between arc current and arc foot radius were obtained using regression on the test results, and can be expressed as follows:

$$r_0 = \sqrt{\frac{I}{1.67\pi}} \quad (negative\ arc)$$

$$r_0 = \sqrt{\frac{I}{1.75\pi}} \quad (positive\ arc)$$

$$r_0 = \sqrt{\frac{I_m}{2.04\pi}} \quad (ac\ arc)$$

3. The arc characteristics were measured on a wet-grown ice cylinder. For ac and dc arcs, the following different expressions of E_{arc} (in V/cm) and I (or I_m in A) were obtained :

   $E_{arc}=213 \cdot I^{-0.53}$ (negative arc);

   $E_{arc}=169 \cdot I^{-0.58}$ (positive arc);

   $E_{arc}=152 \cdot I_m^{-0.53}$ (ac arc)

4. The electrode voltage drops under ac and dc voltages were also obtained from regression on the measured arc voltage drops. These values were 735 V, 608 V, and 953 V_{peak} for positive, negative, and ac arcs, respectively.

5. The reignition conditions for ac arcs could be expressed as an equation of the peak value of applied voltage (V_m in V), arc length (x in cm), and peak value of leakage current (I_m in A):

$$V_m \geq \frac{1258x}{I_m^{0.53}}$$

It may also be expressed as an equation of the peak value (V_p in V) across a gap of length of x cm:

$$V_p \geq \frac{449x}{I_m^{0.51}}$$

6. The ice surface conductivities during flashover were measured. The equivalent surface conductivity (γ_e in μS) for both ac and dc voltage conditions could be expressed as the function of freezing water conductivity (σ in μS/cm):

$\gamma_e=0.061\cdot\sigma+5.6$ for positive voltage;

$\gamma_e=0.063\cdot\sigma+5.8$ for negative voltage;

$\gamma_e=0.067\cdot\sigma+5.6$ for ac voltage.

The bulk ice conductivity was negligible, compared to ice surface conductivity, in the ambient temperature of –12 to 0°C, which corresponds to an ice temperature range of –12 to –3°C.

7. Many factors influencing flashover on ice surfaces were analysed by the tests on ice samples. It was found that:

   Maximum withstand voltage (V_{ws}) decreased with an increase in the freezing water conductivity;

   V_{ws} for positive dc voltage is 6% to 9% higher than that of negative dc voltage. V_{ws} for ac voltage is 16% to 21% higher than that of negative dc voltage. V_{ws} for ac voltage is 13% to 17% higher than that of positive dc voltage;

   V_{ws} increased with an increase in the length of air gaps at both the top and bottom ends of the ice surface. The influence of air gap length on V_{ws} was less pronounced for the bottom end air gaps, compared with the top end air gaps;

   V_{ws} increased linearly with arcing distance of the ice samples, up to the maximum tested length of 0.92 m;

   During the de-icing period, the temperatures of ice surfaces and the bulk ice increased as the air temperature rose from –12°C to 0°C;

The leakage current proved to flow mainly across through the ice surface, while the conduction current flowing through the body of the ice was too insignificant to be considered.

8. Mathematical models were developed for flashover on ice surfaces under ac and dc voltages based on the experiments on wet-grown ice samples. The mathematical models were applied to ice-covered facility insulator strings, under different conditions.

   For the wet-grown ice samples of 0.3 m to 0.92 m in length, the calculated flashover voltages (V_c), critical currents (I_c), and critical arc lengths (x_c) were influenced by freezing water conductivity (σ). It was found that V_c decreased with an increase in σ, following the power curves; I_c increased with σ linearly, and x_c decreased with σ linearly.

   Voltage type was found to have an influence on the calculated values for V_c, I_c, and x_c. V_c was 11% to 18% higher under ac voltage than under positive dc. V_c was 19% to 24% higher under ac voltage than under negative dc. The ratios of positive V_c and negative V_c were from 5% to 10%.

Under ac conditions, I_c was about 3 times that of I_c in both positive and negative dc voltages. For dc conditions, I_c was found to be a little higher under positive voltage.

The critical arc length was longer under ac voltage than under dc. For dc conditions, x_c was found to be a little longer under positive voltage.

The mathematical model is applied to ice-covered insulator strings.

For ice–covered IEEE standard insulator strings of 1 to 6 units (arcing distance up to 1 m), the calculated flashover voltage increases linearly with arcing distance of insulator units. The critical arc current was found to increase with arcing distance. The ratio of critical arc length to total arcing distance increased with arcing distance. There is good agreement between the calculated flashover voltage and the results obtained in the HV laboratory of UQAC.

For insulator strings longer than 1 m, further research and experimental validation of the mathematical model are needed.

REFERENCES

ALSTON, L.L. and ZOELEDZIOWSKI, S. (1963 July). Growth of Discharge on Polluted Insulation. Proc. IEEE, Vol. 110, No. 7, 1260-1266.

BANDEL, H.W. (1951). Corona from Ice Points. J. Appl. Phys., Vol. 22, 984-985.

BOYER, A.E. and MEALE, J.R. (1988 March). Insulation Flashover under Icing Conditions on the Ontario-Hydro 500 kV Transmission Line System. CEA Spring Meeting, Montreal, Canada, 20p.

BROWNE Jr., T.E. (1948). A Study of AC Arc behaviour Near Current Zero by means of Mathematical Models, AIEE Trans., Vol. 67, 141-153.

BUI, H.T., PHAN, L.C., HURAUX, C. and PISSOLATO jr., J. (1984). HVDC Flashover on the Surface of Conductive Ice. IEEE International Symposium on Electrical Insulation, Montreal, Paper 84CH1964-6, 85-88.

CHARNESKI, M.D. GAIBROIS, G.L. and WHITNEY, B.F. (1982 August). Flashover Tests of Artificially Iced Insulators. IEEE Trans. on Power App. & Syst., Vol. PAS-101, 2429-2433.

CHEN X., FARZANEH, M. and ZHANG, J. (1995 Oct.). Recovery Conditions for AC Arc on Ice Surfaces. 1995 Annual Report of Conference on Electrical Insulation and Dielectric Phenomena, Virginia Beach, Virginia, 396-399.

CHEN X., FARZANEH, M. and ZHANG, J. (1996). Factors Influencing Flashover Characteristics along Ice Surfaces. 7th International Workshop on Atmospheric Icing of Structures, Chicoutimi, Canada, 77-80.

CHERNEY, E.A. (1980 Feb.). Flashover Performance of Artificially Contaminated and Iced Long-Rod Transmission Line Insulators. IEEE Trans. on Power App. & Syst., Vol PAS-99, 46-52.

CHISHOLM, W.A. and TAM, Y.T. (1989) Outdoor Insulation Studies CIFT Conditions 1988-89 Seasons Summary. Ontario-Hydro Research Division Report, 89-217-H.

CHISHOLM, W.A. and TAM, Y.T. (1990). Outdoor Insulation Studies CIFT Conditions December 30-31, 1989 Storm Event. Ontario-Hydro Research Division Report, 90-131-H.

CHISHOLM, W.A., TAM, Y.T, ERVEN C.C. and MELO T.O. (1993). 500 kV Insulator Performance under Contamination Ice, Fog and Rising Temperature-Operating Experience and Field Studies. IEEE Power Engineering Summer Meeting, 1-8.

CHISHOLM, W.A., et al. (1996) The Cold-Fog Test, *1996 IEEE/PES winter Meeting*, January 21-25, 1996, Baltimore, MD, Paper No 96 WM 099-2 PWRD, 1-7

CLAVERIE, P. (1971). Predetermination of the Behavior of Polluted Insulators, IEEE PAS-90, 1902-1908.

CLAVERIE, P. and PORCHERON, Y. (1973). How to Choose Insulators for Polluted Areas. IEEE Trans. on Power App. & Syst., Vol. PAS-92, No.3, 1121-1131.

DRAPEAU, J.F. (1992 Avril). Impact du verglas et de la neige sur le réseau de transport d'Hydro-Québec: Analyse de la tempête du 5-6 janvier 1992 dans les

régions Manicouagan et Matapédia. Rapport scientifique, Hydro-Québec, No. IREQ-92-072,44p.

DRAPERU, J.F. and FARZANEH, M. (1993, Sept.). Ice Accumulation Characteristics on Hydro-Québec HV Insulators. 6th International Workshop on Atmospheric Icing on Structures, Budapest, Hungary, 225-230.

FAEZANEH, M. KIERNICKI, J. (1994 Sept.). Effet de la repartition de glace sur la tension de tenue maximale des isolateurs recouverts de glace humide. Rapport de l'UQAC présenté à Hydro-Québec (IREQ), 1-34.

FAEZANEH, M. KIERNICKI, J. and DALLAIRE, M.A. (1990 Sept.). AC and DC Flashover Performance of Ice-Covered Insulators during a De-Icing Period. 5th International Workshop on Atmospheric Icing of Structures, Tokyo, Japan, Paper No. B-48, 1-4.

FARZANEH, M. (1991 August). Effect of Ice Thickness and Voltage Polarity on the Flashover Voltage on Ice Covered High Voltage Insulators. Proceedings of 7th International Symposium on HV Engineering, Dresden, Germany, Vol. 4, Paper 43.10, 203-206.

FARZANEH, M. (1994). Ingénierie de la haute tension, Notes de cours.

FARZANEH, M. and DRAPEAU, J.F. (1995 April). AC Flashover Performance of Insulators Covered with Artificial Ice. IEEE Trans. on Power Delivery, Vol. 10, No.2, 1038-1051.

FARZANEH, M. and KIERNICKI, J. (1997 Oct.). Flashover Performance of IEEE Standard Insulators under Ice Conditions, IEEE Trans. on Power Delivery, Vol. 12, No. 4, 1602-1613.

FARZANEH, M. and KIERNICKI, J. (1995 March/April). Flashover Problem Caused by Ice Build-up on Insulators. IEEE Electrical Insulation Magazine, Vol. 11, No. 2, 5-17.

FARZANEH, M. and LAFORTE, J.L. (1992 Dec.). Effect of Voltage Polarity on Icicles Grown on Line Insulators. International Journal of Offshore and Polar Engineering, Vol. 2, No. 4, 298-302.

FARZANEH, M. and MELO, O.T. (1990). Properties and Effect of Freezing Rain and Winter Fog on Outline Insulators. Cold Regions Science and Technology, Vol. 19, 33-46.

FARZANEH, M. and ZHANG, J. (1998). Behavior of DC Arc on Ice Surfaces. Proceedings of 8th International Workshop on Atmospheric Icing of Structures. Iceland, 1998.

FARZANEH, M. and ZHANG, J. (1998). Propagation of AC Arc on Ice Surfaces. Paper Submit to IEEE EI-98, Washington DC, USA.

FARZANEH, M., CHEN X. and ZHANG, J. (1996 Dec.). A Study of Surface Conductivity and Flashover Voltage of Ice Samples Formed under Various Freezing Conditions. International Journal of Offshore and Polar Engineering, Vol. 6, No. 4, 298-303.

FARZANEH, M., CHEN X. and ZHANG, J. (1996). The Influence of Applied Voltage on the Surface Conductivity of Atmospheric Ice Deposited on Insulating Surfaces. Conference Record of the 1996 IEEE International Symposium on Electrical Insulation, Montreal, 275-278.

FARZANEH, M., DALLAIRE, M.A., BEN-DALLAH, M. (1986 Dec.). Essais de tenue électrique en courant continu sur les isolateurs précontaminés et recouverts de glace. Rapport pour Hydro-Québec, Dirrection d'Inégnierie de lignes, Contrat No. H0924306, 1-22.

FARZANEH, M., DALLAIRE, M.A., MELO, O.T. and BOYER, A.E. (1989 August/Sept.). Interception of Supercooled Droplets by Energized Line Insulators. Proceedings of 6th International Symposium on HV Engineering, New Orleans, Paper 42.26. 1-4.

FARZANEH, M., KIERNICKI, J. and DRAPEAU, J.F. (1992). Ice Accretion on Energized Line Insulators. International Journal of Offshore and Polar Engineering, Vol. 2, No 3, (ISSN 1053-5381).

FARZANEH, M., KIERNICKI, J. and MARTIN, R. (1994). A Laboratory Investigation of the Flashover Performance of Outdoor Insulators Covered with Ice," Proceedings of the 4th International Conference on Properties and Applications of Dielectric Materials, Brisbane, Australia.

FARZANEH, M., KIERNICKI, J., CHAARANI, R., DRAPEAU, J.F. and MARTIN, R. (1995 Aug./Sept.). Influence of Wet-Grown Ice on the AC Flashover Performance of Ice-Covered Insulators. Proceedings of the 9th International Symposium on High Voltage Engineering, Graz, Austria, Paper No. 3176, 1-4.

FARZANEH, M., ZHANG, J., CHEN X. (1994). A Laboratory Study of Leakage Current and Surface Conductivity of Ice Samples. 1994 Annual Report of

Conference on Electrical Insulation and Dielectric Phenomena, Arlington, Texas, 631-638.

FARZANEH, M., ZHANG, J., CHEN X. (1996). DC Characteristics of Local Arc on Ice Surfaces. Atmospheric Research, 46, 1998, 49-56.

FARZANEH, M., ZHANG, J., CHEN X. (1997). Modelling of the AC Arc Discharge on Ice Surfaces. IEEE Trans. on Power Delivery, Vol. 12, No. 1, 1997, 325-338.

FIKKE, S.M., HANSSEN, J.E. and ROLFSENG, L. (1992 May). Long Range Transported Pollutants and Conductivity of Atmospheric Ice on Insulators. IEEE/PES Summer Meeting, Seatttle, Washington, USA, 1-9.

FORREST, J.S.(1969). The Performance of High Voltage Insulators in Polluted Atmospheres. Conference Paper IEEE Winter Meeting, New York, 1969.

FUJIMURA, T., NAITO, K., HASEGAWA,Y. and KAWAGUCHI, T.K. (1979). "Performance of Insulators Covered with Snow or Ice," IEEE Trans. on Power App. & Syst., Vol. PAS-98, pp. 1621-1631.

GORSKI, R.A.(1986). Meteorological Summary-March 10. 1986- Multiple Outages on the Southern Ontario (Central Region) 500 kV System. Ontario-Hydro, Met. Report, No. 80604-1, 1-40.

GUAN, Z. and HUANG, C. (1994 July). Discharge Performance of Different Models at Low Pressure Air. Proceedings of the 4th International Conference on Properties and Applications of Dielectric Materials, Brisbane, Australia, Paper 5102.

GUAN, Z. and ZHANG, R. (1990). Calculation of DC and AC Flashover Voltage of Polluted Insulators. IEEE Trans. On Electrical Insulation, Vol. 25, No. 4, 723-729.

HAMPTON, B.F. (1964 July). Flashover Mechanism of Polluted Insulation. Proc. IEE, Vol. 11, No. 5, 985-990.

HESKETH, S. (1967 AVRIL). General Criterion for the Prediction of Pollution Flashover, Proc. IEE, Vol. 114, 531-532.

HOYAUX, M.F. (1968). Arc Physics. Springer-Verlag New York Inc.

Hydro-Quebec. (1988). Analysis of the Hydro-Quebec System Blackout on April 1988. Official Hydro-Quebec Report, Montreal, 1988.

IMAI, I. (1953). Studies on Ice Accretion. Research on Snow and Ice. No. 1. 35-44.

JOLLY, D.C. (1972). Contamination flashover, Part I: Theoretical Aspects, IEEE PAS-91, 2437-2442.

JOLLY, D.C. et al. (1974). Dynamic Theory of Discharge Growth over Contaminated Insulator Surfaces. IEEE Conf. Paper, No. C74 068-3, Winter Power Meeting, New York.

JONES, K.F. (1993 Sept.). The Effect o Horizontal and Torsional Coupling on Vertical Galloping. 6th International Workshop on Atmospheric Icing on Structures, Budapest, Hungary, 143-148.

JORDAN, J.B. and SAINT-ARMAND, R. (1976). Electrical Corona at Ice Surface. Proc. Of the 4th International Conference on Gas Discharges, Swansea, 239-243.

KANNUS, K. and VERKKONEN, V. (1993). Effect of Ice Coating on the Dielectric Strength of High-Voltage Insulators. Proceeding of the 4th International Workshop on the Atmospheric Icing of Structures, Paris, France, 296-301.

KAWAI, M. (1970 Nov./Dec.). AC Flashover Test and Project UHV on Ice - Coated Insulators. IEEE Trans., Vol. PAS-89, 1800-1804.

KHALIFA, M.M. and MORRIS, R.M. (1968 June). Performance of Line Insulators under Rime Ice. IEEE Trans., on Power App. & Syst., Vol. PAS-86, 692-698.

KIESSLING, F. and RUHNAU, J. (1993 Sept.). Ice Loads on Overhead Power Lines in Germany and their Impact on Reliability and Design. 6th International Workshop on Atmospheric Icing on Structures, Budapest, Hungary, 127-132.

KUFFEL, E. and ZAENGL W.S. (1984). High-Voltage Engineering Fundamentals, Pergamon Press.

KUROIWA, D. (1958). Icing and Snow Accretion. Monograph Series of Research, Institute of Applied Electricity, Japan, 1-30.

KUROIWA, D. (1965). Icing and Snow Accretion on Electric Wires. U.S. Army Cold Regions Research and Engineering Laboratory, Research Report 123, 1-10.

LEE, L.Y., NELLIS, C.L. and BROWN, J.E. (1975). 60 Hz Tests on Ice-covered 500 kV Insulators Strings. IEEE PES Summer Meeting, Paper A75-499-4, San Francisco.

LI, S. (1988). The Mechanism of the Flashover on a Polluted Dielectric Surface under AC Voltage. Dissertation of Ph. D., Tsinghua University.

MATSUDA, H., KOMURO, H.K. and TAKASU, K. (1991 July). Withstand Voltage Characteristics of Insulator Strings Covered with Snow or Ice. IEEE Trans. on Power Delivery, Vol. 6, 1800-1804.

MEIER, A. and NIGGLI, W.M. (1968 Sept.). The influence of Snow and Ice Deposits on Supertentension Transmission Line Insulator Strings with Special Reference to High Altitude Operation. IEEE Conference Publ. 44, London, England, 386-395

MELO, O.T., TAM, Y.T., FARZANEH, M. (1988 Sept.). Freezing Rain and Fog Events in Southern Ontario: Properties and Effect on EHV Transmission

Systems. 4th International Workshop on Atmospheric Icing on Structures, Paris, France, 70-75.

NEUMÄrker, G. (1959). Verschmutzungszustand und Kriechweg, Monatsber. D. Deut. Akad, Wiss., Berlin, Vol. 1, 352-359.

OBENAUS, F. (1958). Fremdschichtüberschlag und Kriechweglänge. Deutsche Elektrotechnik, Vol. 4, 135-136.

OGUCHI, H. et al. (1953). Icing on Electric Wires. Research on Snow and Ice. No. 1, 45-49.

PEYREGNE, G, RAHAL, A.M., HURAUX, C. (1982). Flashover of a Liquid Conducting Film, Part 1: Flashover Voltage and Part 2: Time to Flasover – Mechanisms. IEEE Trans. EI-17, No. 1, February, 1982, 10-19.

PHAN, C.L., ALLAIRE, M.A. and MCCOMBER, P. (1977). Accumulation du verglas et du givre sur les nouveaux isolateurs sous H.T. Canadian Electtrical Engineering Journal, Vol. 2, No. 4, 24-28.

PHAN, C.L., and MATSUO, H. (1983). Minimum Flashover Voltage of Iced Insulators. IEEE Trans. Electrical Insulation, EI-18-6, 605-618.

PHAN, C.L., PIROTTE, P. and TRINH, N.G. (1974). A study of Corona Discharges at Water Drops Over the Freezing Temperature Range. IEEE Trans. on Power App. & Syst., Vol. PAS-93, No.2. 724-734

RAHAL, A.M. (1979 Nov./Dec.). Flashover Mechanism of High Voltage Insulators, IEEE PAS-98, No. 6.

RENNER, P.E., HILL, H.L. and RATZ, O. (1971 June). Effects of Icing on DC Insulation Strength. IEEE Trans. on Power App. & Syst., Vol. PAS-90, 1201-1206.

RIZK, F.A.M. (1970). Application of Dimensional Analysis to Flashover Characteristics of Polluted Insulators, Proc. IEE, Vol. 117, 2257-2231.

RIZK, F.A.M. (1971 Jan./Feb.). Analysis of Dielectric Recovery with Reference to Dry-Zone Arc on Polluted Insulators, IEEE Conf. Paper No. 71 C 134 PWR, Winter Power Meeting, New York.

RIZK, Farouk A.M. (1981). Mathematical Models for Pollution Flashover. Electra, Vol. 78, 71-103.

RUMELI, A. (1976). Flashover Along a Water Column. IEEE Trans. EI-11, No.4, December 1976, 115-120.

SAGAWARA, N., HOKARI, K., ANDO, H., YOSHIDA, K., HIROTA. M. and TATOKORO, Y. (1993 Sept.). Insulation Properties of Atmospheric Iced Insulators Installed in High Mountains. 6th International Workshop on Atmospheric Icing on Structures, Budapest, Hungary, 237-242.

SAGAWARA, N., HOKARI, K., NOSAKA, T., TATOKORO, Y. and MIZUMURA, M. (1990 Oct./Nov.). Insulation Resistance of Transmission Line Insulators Depending on the Accretion of Ice. 5th International Workshop on Atmospheric Icing on Structures, Tokyo, Paper B 4-9, 1-6.

SATO, M., SAITO, H., KAGA A. and AKAGAMI H. (1989). Fundamental Characteristics of AC Flashover on Contaminated Insulators Covered with Ice. Japanese Journal of Applied Physics, Vol. 28, No.5 889-896.

SCHNEIDER, H.M. (1975). Artificial Ice Tests on Transmission Line Insulators-A Progress Report. IEEE PES Summer Meeting, Paper A75-491-1, San Francisco.

SHU, L., SUN , C., ZHANG, J. and GU, L. (1991 Aug.). AC Flashover Performance of Iced and Polluted Insulators for High Altitude Regions. Proceedings of 7th I.S.H., Vol. 4, 303-306.

SU, F. and JIA, Y. (1993). Icing on Insulator String of HV Transmission Lines and the Harmfulness. Proceedings of 3rd International Offshore and Polar Engineering Conference, 655-662.

SUN, C., ZHANG, J., XIE, J., SHU, L., GU, L. AND CHENG M. (1989). Influence of Pressure, Rain, Pollution and Ice on DC Flashover Performance of Line Insulators. Chinese Society of Electric Eng., Vol. 10, No 5, 1-8.

SUNDARARAJAN, R. and GORUR, R.S. (1991 July). Dynamic Modeling of Flashover on Dielectric Surfaces. Proceedings of the 3th International Conference on Properties and Applications of Dielectric Materials, Tokyo, Japan, No.13.

VUCKVIC, Z. and ZDRAVKOVIC, Z. (1990 Oct.). Effect of Polluted Snow and Ice Accretions on High-Voltage Transmission Line Insulators. 5th International Workshop on Atmospheric Icing of Structures, Tokyo.

WATANABE, Y. (1977). Flashover Tests of Insulators Covered with Ice or Snow. IEEE PES Summer Meeting, Paper F-77-507-5.

WILKINS, R. (1969). Flashover Voltage of High-Voltage Insulators with Uniform Surface-Pollution Films. Proc. IEE, Vol. 116, No. 3, 457-465.

ZHANG, J. and FARZANEH, M. (1998). Computation of AC Critical Flashover Voltage of Insulators Covered with Ice. POWERCON ' 98, Beijing, China.

ZHANG, J. and FARZANEH, M. (1998). Propagation of DC Arc on Ice Surfaces. 8th International Offshore and Polar Engineering Conference (ISOPE-98), Montreal, Canada.

ZHANG, J., FARZANEH, M. and CHEN, X. (1995 Aug.). Characteristics of AC Arc on Ice Surfaces. Proceedings of the 9th International Symposium on High Voltage Engineering, Graz, Austria, Paper No. 3177.

ANNEXE I: MATHCAD PROGRAM

Positive Voltage Flashover

Arc Constants:

$A := 213$

$n := 0.53$

$K1 := 1.67$

$Ue := 735$

Narrow Ice Strip:

Arcing Distance (cm): $L := 94$

Ice Width (cm): $w := 38.956$

Freezing Water Conductivity (μS/cm): $\sigma := 80$

Equivalent Ice Surface Conductivity:

$\gamma e := (0.063 \cdot \sigma + 5.75) \cdot 10^{-6}$

$\gamma e = 1.079 \cdot 10^{-5}$

Initial Values:

$x := 50$

$I := 0.2$

Given

$$n \cdot A \cdot x \cdot I^{n-1} - \frac{1}{\pi \cdot \gamma e} \cdot \ln\left(\frac{2 \cdot L}{\frac{\pi \cdot I}{K1}}\right) - \ln\left(\tan\left(\frac{\pi \cdot x}{2 \cdot L}\right)\right) - \frac{1}{2 \cdot \pi \cdot \gamma e} = 0$$

$$A \cdot I^{n} - \frac{I}{\gamma e \cdot 2 \cdot L \cdot \sin\left(\pi \cdot \frac{x}{2 \cdot L}\right) \cdot \cos\left(\pi \cdot \frac{x}{2 \cdot L}\right)} = 0$$

$$\begin{matrix} xc \\ Ic \end{matrix} := \text{Find}(x, I)$$

$xc = 81.782$

$Ic = 0.201$

$$x2 := \begin{cases} L & \text{if } xc > L \\ xc & \text{otherwise} \end{cases}$$

$x2 = 81.782$

$$Uc := A \cdot x2 \cdot Ic^{n} - \frac{Ic}{\pi \cdot \gamma e} \cdot \ln\left(\frac{2 \cdot L}{\pi \cdot \frac{Ic}{K1 \cdot \pi}}\right) \cdot \ln\left(\tan\left(\frac{\pi \cdot x2}{2 \cdot L}\right)\right) - Ue$$

$Uc = 6.61 \cdot 10^{-4}$

$$r0 := \sqrt{\frac{Ic}{K1 \cdot \pi}}$$

$r0 = 0.196$

Arc Constants:

$A := 213$

$n := 0.53$

$K1 := 1.67$

$Ue := 735$

Wide Ice Strip:

Arcing Distance (cm): $L := 30$

Ice Width (cm): $w := 38.95$

Freezing Water Conductivity (μS/cm): $\sigma := 80$

Equivalent Ice Surface Conductivity:

$\gamma e := (0.063\sigma + 5.75)\cdot 10^{-6}$

$\gamma e = 1.079\cdot 10^{-5}$

Initial Values:

$x := 10$

$I := 0.2$

Given

$$n\cdot A\cdot x\cdot I^{n-1} - \frac{1}{\pi\cdot\gamma e}\cdot\frac{\pi\cdot(L-x)}{w} - \ln\left(\frac{w}{2\cdot\pi\cdot\frac{I}{K1\cdot\pi}}\right) - \frac{1}{2\cdot\pi\cdot\gamma e} = 0$$

$$A\cdot I^{n} - \frac{I}{\gamma e\cdot w} = 0$$

$$\begin{matrix} xc \\ Ic \end{matrix} := \text{Find}(x, I)$$

$xc = 43.451$

$Ic = 0.207$

$$x2 := \begin{cases} L & \text{if } xc > L \\ xc & \text{otherwise} \end{cases}$$

$x2 = 30$

$$Uc := A \cdot x2 \cdot Ic^{-n} + \frac{Ic}{\pi \cdot \gamma e} \cdot \left[\frac{\pi \cdot (L - x2)}{w} + \ln\left[\left[\frac{w}{2 \cdot \pi \cdot \sqrt{\frac{Ic}{K1 \cdot \pi}}} \right] \right] \right] + Ue$$

$Uc = 3.645 \cdot 10^{4}$

$$r0 := \sqrt{\frac{Ic}{K1 \cdot \pi}}$$

$r0 = 0.198$

Negative Voltage Flashover

Arc Constants:

$A := 169$

$n := 0.58$

$K1 := 1.75$

$Ue := 608$

Narrow Ice Strip:

Arcing Distance (cm): $L := 94$

Ice Width (cm): $w := 38.95$

Freezing Water Conductivity (μS/cm): $\sigma := 80$

Equivalent Ice Surface Conductivity:

$$\gamma e := (0.061 \cdot \sigma + 5.59) \cdot 10^{-6}$$

$$\gamma e = 1.047 \cdot 10^{-5}$$

Initial Values:

$x := 50$

$I := 0.2$

Given

$$n \cdot A \cdot x \cdot I^{n-1} - \frac{1}{\pi \cdot \gamma e} \cdot \ln\left(\frac{2 \cdot L}{\pi \cdot I \cdot K1}\right) \cdot \ln\left(\tan\left(\frac{\pi \cdot x}{2 \cdot L}\right)\right) - \frac{1}{2 \cdot \pi \cdot \gamma e} = 0$$

$$A \cdot I^{n} - \frac{I}{\gamma e \cdot 2 \cdot L \cdot \sin\left(\pi \cdot \frac{x}{2 \cdot L}\right) \cdot \cos\left(\pi \cdot \frac{x}{2 \cdot L}\right)} = 0$$

$$\begin{pmatrix} xc \\ Ic \end{pmatrix} := \text{Find}(x, I)$$

$xc = 81.119$

$Ic = 0.185$

$x2 := \begin{cases} L & \text{if } xc > L \\ xc & \text{otherwise} \end{cases}$

$x2 = 81.119$

$$Uc := A \cdot x2 \cdot Ic^{-n} + \frac{Ic}{\pi \cdot \gamma e} \cdot \left[\ln\left[\frac{2 \cdot L}{\pi \cdot \sqrt{\frac{Ic}{K1 \cdot \pi}}} \right] - \ln\left(\tan\left(\frac{\pi \cdot x2}{2 \cdot L} \right) \right) \right] + Ue$$

$Uc = 6.109 \cdot 10^{3}$

$$r0 := \sqrt{\frac{Ic}{K1 \cdot \pi}}$$

$r0 = 0.183$

Arc Constants:

$A := 169$

$n := 0.58$

$K1 := 1.75$

$Ue := 608$

Wide Ice Strip:

Arcing Distance (cm): $L := 30$

Ice Width (cm): $w := 38.956$

Freezing Water Conductivity (μS/cm): $\sigma := 80$

Equivalent Ice Surface Conductivity:

$\gamma e := (0.061 \cdot \sigma + 5.59) \cdot 10^{-6}$

$\gamma e = 1.047 \cdot 10^{-5}$

Initial Values:

$x := 10$

$I := 0.2$

Given

$$n \cdot A \cdot x \cdot I^{n-1} - \frac{1}{\pi \cdot \gamma e} \cdot \frac{\pi \cdot (L - x)}{w} - \ln\left(\frac{w}{2 \cdot \pi \cdot \sqrt{\frac{I}{K1 \cdot \pi}}}\right) \cdot \frac{1}{2 \cdot \pi \cdot \gamma e} = 0$$

$$A \cdot I^{n} - \frac{I}{\gamma e \cdot w} = 0$$

$$\begin{matrix} xc \\ Ic \end{matrix} := \text{Find}(x, I)$$

$xc = 42.713$

$Ic = 0.184$

$$x2 := \begin{cases} L & \text{if } xc > L \\ xc & \text{otherwise} \end{cases}$$

$x2 = 30$

$$Uc := A \cdot x2 \cdot Ic^{n} - \frac{Ic}{\pi \cdot \gamma e} \cdot \frac{\pi \cdot (L - x2)}{w} - \ln\left(\frac{w}{2 \cdot \pi \cdot \sqrt{\frac{Ic}{K1 \cdot \pi}}}\right) - Ue$$

$Uc = 3.385 \cdot 10^{-4}$

$$r0 := \sqrt{\frac{Ic}{K1 \cdot \pi}}$$

$r0 = 0.183$

Alternative Voltage Flashover

Arc Constants:

$A := 185$

$n := 0.63$

$K1 := 2.04$

$Ue := 953$

$k := 1258$

$b := 0.53$

Narrow Ice Strip:

Arcing Distance (cm): $L := 490$

Ice Width (cm): $w := 46.2$

Freezing Water Conductivity (μS/cm): $\sigma := 80$

Equivalent Ice Surface Conductivity:

$\gamma e := (0.067 \cdot \sigma + 5.58) \cdot 10^{-6}$

$\gamma e = 1.094 \cdot 10^{-5}$

$Um := 20000$

$x := 40$

Given

$$A \cdot k^{\frac{n}{b}} \cdot \left(1 - \frac{n}{b}\right) \cdot x^{\frac{n}{b}} \cdot Um^{\frac{n}{b}} - \frac{k^{\frac{1}{b}}}{(\pi \cdot \gamma e)} \cdot \frac{\pi \cdot \frac{L - x}{w} - \ln\left(\frac{w}{2 \cdot \pi \cdot 0.395}\right)}{b} \cdot x^{\frac{1}{b} - 1} \cdot Um^{\frac{1}{b}} - k^{\frac{1}{b}} \cdot x^{\frac{1}{b}} \cdot \frac{Um^{\frac{1}{b}}}{\gamma e \cdot w} = 0$$

$$Um := A \cdot x \cdot \left(k \cdot \frac{x}{Um}\right)^{\frac{n}{b}} - Ue - \frac{k \cdot \left(\frac{x}{Um}\right)^{\frac{1}{b}}}{\pi \cdot \gamma e} \cdot \frac{\pi \cdot (L - x)}{w} - \ln\left(\frac{w}{2 \cdot \pi \cdot 0.395}\right)$$

$$\begin{matrix} Uc \\ xc \end{matrix} := Find(Um, x)$$

$Uc = 4.351 \cdot 10^5$

$xc = 346.256$

$$Ueff := \frac{Uc}{2}$$

$Ueff = 3.077 \cdot 10^5$

$\frac{xc}{L} = 0.707$

$$Ec := \frac{Ueff}{L}$$

$$Im := \left(k \cdot \frac{xc}{Uc}\right)^{\frac{1}{b}}$$

$Im = 1.002$

$Ec = 627.933$

$$r0 := \sqrt{\frac{Im}{K1 \cdot \pi}}$$

$r0 = 0.395$

Arc Constants:

$A := 185$

$n := 0.63$

$K1 := 2.04$

$Ue := 953$

$k := 1258$

$b := 0.53$

Wide Ice Strip:

Arcing Distance (cm): $L := 37$

Ice Width (cm): $w := 46.2$

Freezing Water Conductivity (μS/cm): $\sigma := 80$

Equivalent Ice Surface Conductivity:

$\gamma e := (0.067 \cdot \sigma + 5.58) \cdot 10^{-6}$

$\gamma e = 1.094 \cdot 10^{-5}$

$Um := 20$

$x := 10$

Given

$$A \cdot k^{\frac{n}{b}} \cdot \left(1 - \frac{n}{b}\right) \cdot x^{\frac{n}{b}} \cdot Um^{n} - \frac{k^{\frac{1}{b}}}{(\pi \cdot \gamma e)} \cdot \frac{\ln\left(\frac{2 \cdot L}{\pi \cdot 0.285}\right) - \ln\left(\tan\left(\pi \cdot \frac{x}{2 \cdot L}\right)\right)}{b} \cdot x^{\frac{1}{b}-1} \cdot Um^{\frac{1}{b}} - k^{\frac{1}{b}} \cdot x^{\frac{1}{b}} \cdot \frac{Um^{\frac{1}{b}}}{\gamma e \cdot 2 \cdot L \cdot \sin\left(\frac{\pi \cdot x}{2 \cdot L}\right) \cdot \cos\left(\frac{\pi \cdot x}{2 \cdot L}\right)} = 0$$

$$Um(x) := A\cdot x\cdot k\cdot\left(\frac{x}{Um}\right)^{\frac{n}{b}} - Ue\cdot\left(\frac{k\cdot\left(\frac{x}{Um}\right)^{\frac{1}{b}}}{\pi\cdot\gamma e}\right)\cdot\ln\left(\frac{2\cdot L}{\pi\cdot 0.285}\right)\ln\left(\tan\left(\frac{\pi\cdot x}{2\cdot L}\right)\right)$$

$$\begin{pmatrix} Uc \\ xc \end{pmatrix} := Find(Um, x)$$

$Uc = 5.553\cdot 10^{4}$

$xc = 31.209$

$Ueff := \frac{Uc}{2}$

$Ueff = 3.927\cdot 10^{4}$

$\frac{xc}{L} = 0.843$

$Ec := \frac{Ueff}{L}$

$Im := \left(k\cdot\frac{xc}{Uc}\right)^{\frac{1}{b}}$

$Im = 0.52$

$Ec = 1.061\cdot 10^{3}$

$r0 := \frac{Im}{K1\cdot\pi}$

$r0 = 0.285$